Summer 7-15-2019

Ecological and morphological response of rodents to environmental change over the late Quaternary

Catalina Tome
University of New Mexico - Main Campus

Catalina Tomé

Candidate

Biology

Department

This dissertation is approved, and it is acceptable in quality and form for publication:

Approved by the Dissertation Committee:

Felisa A. Smith , Chairperson

Seth D. Newsome

Sherry Nelson

S. Kathleen Lyons

ECOLOGICAL AND MORPHOLOGICAL RESPONSE OF RODENTS TO ENVIRONMENTAL CHANGE OVER THE LATE QUATERNARY

by

CATALINA TOMÉ

B.S., Biology, University of California Santa Cruz, 2011

M.S., Biology, University of New Mexico, 2015

DISSERTATION

Submitted in Partial Fulfillment of the
Requirements for the Degree of

Doctor of Philosophy

Biology

The University of New Mexico
Albuquerque, New Mexico

July 2019

ACKNOWLEDGEMENTS

I would to thank my advisor, Dr. Felisa Smith, whose mentorship and support not only made this dissertation possible, but a joy. I am also grateful to the members of my committee, Dr. Seth Newsome, Dr. Kate Lyons, and Dr. Sherry Nelson, for their feedback and guidance and the amazing example they set as scientists. Thank you to my collaborators, Emma Elliott Smith, Dr. Tom Stafford and Fred Whiteman Jennings, for their work and the many discussions that helped build these projects.

Thank you to Dr. Ara Winter and Dr. Jocie Colella for their help, as well as all the wonderful members of the Smith lab, and the amazing people at the Center for Stable Isotopes. I would also like to acknowledge and thank the careful and detailed work of Dr. Rickard Toomey, whose work at Hall's Cave helped make this research possible.

I would like to thank Texas Memorial Museum, the Museum of Southwestern Biology, the Smithsonian National Museum of Natural History and the James F. Bell Museum of Natural History for access to their collections. In particular, I thank Chris Sagebiel (Texas Memorial Museum Collections Manager), Dr. Ernie Lundelius, and Dr. Jon Dunnum (Museum of Southwestern Biology Senior Collection Manager of Mammals), for their help with specimen and site information.

Funding for this research was provided by the National Science Foundation (NSF-DEB 1555525 and 1744223), the 2008 Smithsonian Institution Fellowship Program, the Graduate Research Allocations Committee from the Biology Graduate Student Association, and the UNM Biology Department donors and grants.

Finally, I thank my parents and sister for their love and support and giving me some perspective when I most needed it, and to all my friends.

ECOLOGICAL AND MORPHOLOGICAL RESPONSES OF RODENTS TO ENVIRONMENTAL CHANGE OVER THE LATE QUATERNARY

by

Catalina Tomé

B.A., Biology, University of California Santa Cruz

M.S., Biology, University of New Mexico

Ph.D., Biology, University of New Mexico

ABSTRACT

The rapid progression of modern climate change is already altering ecosystems worldwide. By employing the fossil record, we can investigate how animals responded to past climatic changes and biodiversity loss, and help inform conservation efforts for the future. The paleontological record of the late Quaternary (past ~22000 years) encompasses a period of considerable environmental change in North America. Rising temperatures and climatic fluctuations are coupled with the extinction of the majority of large bodied mammals on the landscape. The combination of climate change and extinction events led to changes in vegetation and community structure which likely affected the resources available and interactions between the remaining mammals within communities. To contend with changing biotic interactions, animals may have adapted by changing certain ecological and morphological traits, such as dental morphology, body size or diet. Here, we investigate the

impacts to the rodents *Neotoma* and *Sigmodon.* Our study finds varying responses across these small bodied mammals, suggesting that each is adapting to different stressors between climate and community changes, but that both are impacted by small and large scale biotic and abiotic changes.

TABLE OF CONTENTS

LIST OF FIGURES

LIST OF TABLES

Chapter 1

The relationship between molar morphology and ecology in *Neotoma*

Catalina P. Tomé[1], Winifred Whiteman Jennings[2], Felisa A. Smith[1]

[1]Department of Biology, University of New Mexico, Albuquerque, NM
[2]Department of Math, Science and Engineering, Central New Mexico Community College, Albuquerque, NM

Abstract

The extensive diversity in dental form across mammals and its strong correlation with function provides insights into the diet, habitat and behavior of both extant and extinct taxa. Understanding the extent of variation in dental morphology across species allows for more accurate identification of fossils as well as a better ability to infer relationships between form and function. Here we examined the amount of variation in the size and shape of the first upper molar for the genus *Neotoma*. We employed elliptic Fourier analysis to consider differences in the shape of 2D outlines for 23 populations and 6 species of *Neotoma*, varying in body size and habitat preferences. As expected, molar length is a strong predictor of body size; significantly and negatively correlated with temperature, particularly in species whose ranges span large latitudinal gradients. We found significant differences across the molar shape of all species, with no evidence of a phylogenetic signal. While outline analysis could not robustly classify molars to the species level, we did find a greater degree of folding and more acute angling of molar lophs in *N. cinerea* and *N. mexicana*, who have highly generalized diets. In contrast, wider lophs with shallower enamel infolding was characteristic of species specializing on softer, more succulent resources (i.e., *N. albigula* and *N. micropus*). *N. floridana* were inaccurately classified to species in the majority of cases, but

were the only molars correctly identified to locality 100% of the time, suggesting that dietary specializations at a local level may drive morphological changes within the species as well as across the genus.

Introduction

Mammals demonstrate an incredible diversity in dental form and function that mirrors a broad range of ecological niches and diets. The evolution of teeth in mammals has been widely studied, with characteristics of tooth size, shape and masticatory mechanisms of the jaw correlating with diet (Gould 1975, Janis and Fortelius 1988, Ungar and Williamson 2000, Schmidt-Kittler 2002, Evans and Sanson 2003, Samuels 2009, Ungar 2010, Ungar and Sponheimer 2011). The cheek teeth of herbivores, for example, are generally high crowned with increased folding along their enamel. This allows for a greater grinding capacity at the occlusal surface to help deal with high quantities of abrasive plant matter and/or grit intake and increased wear rates generally associated with open, grassland habitats (Janis and Fortelius 1988, Janis 1995, Williams and Kay 2001, Jardine et al. 2012, Lucas et al. 2014, Samuels and Hopkins 2017). The morphology of carnivoran teeth, on the other hand, is better suited for shearing and slicing, with a higher degree of shearing surfaces, either due to size or crests, associated with groups consuming higher proportions of vertebrates compared to invertebrates or fruits (Van Valkenburgh 1989, Strait 1993a, 1993b, Meiri et al. 2005). Enamel is also durable; thus, teeth are well preserved in the fossil record (Van Valkenburgh 1994). Consequently, variation in dental morphology provides a means of identification for both fossil and modern mammal taxa (Carrasco 2000, Hillson 2005, Ungar 2010), as well as insights into their ecology (Van Valkenburgh 1994, Thomason 1997). While the use of dental

form to study adaptations and diet is extremely useful, it is important to account for factors that may constrain the precision of identifications and inferences.

The evolution and life history of a mammal influences the morphological variation in dental form. Genetic and developmental constraints may limit the adaptation of form to dietary function (Evans and Sanson 2003, Evans et al. 2007, Ledevin et al. 2010, Rodriguez et al. 2013). Tooth characteristics of an individual can also be altered throughout their lifetime. Wear can play an important role in changing the shape of the occlusal (chewing) surface, sometimes in an uneven manner (Harris 1984, Guérécheau et al. 2010, Ledevin et al. 2010). A study on bank voles, for example, found that wear (age) was the primary source of variation across the occlusal surface of the third upper molar, while intra-specific variation was tied to the presence/absence of an additional posterior structure due to developmental constraints on size of the molar (Ledevin et al. 2010) Characterizing the dental variation within a genus thus improves accuracy of identification of materials and the interpretation of the relationships between tooth form and ecology across space and time.

Here we focus on the genus *Neotoma.* We first investigate whether the first upper molar accurately distinguishes between species varying in size and ecology. Second, we investigate the relationship between tooth morphology and locality due to differences in climate and vegetation. *Neotoma* or woodrats, are found across most of North America (Figure 1.1), extending from the Northwestern Territories of Canada to the Nicaragua in Central America (Hall 1981, Betancourt et al. 1990). The genus includes animals of 80-500^{+}g, occupying a diverse array of habitats and subsisting on a wide variety of resources (Wiley 1980, Cornely and Baker 1986, Macêdo and Mares 1988, Jones and Hildreth 1989, Carraway and Verts 1991, Smith, 1997, Verts and Carraway 2002). We focus on *Neotoma*, or

woodrats, because the genus played an important role in late Pleistocene paleoecological studies due the detailed plant and animal records preserved within their middens (e.g. Betancourt et al. 1990, Smith et al. 1995, 2009, Smith and Betancourt 2003, 2006). However, *Neotoma* skeletal remains are difficult to identify to species, with identifications generally relying on single or loose molars (Harris 1984).

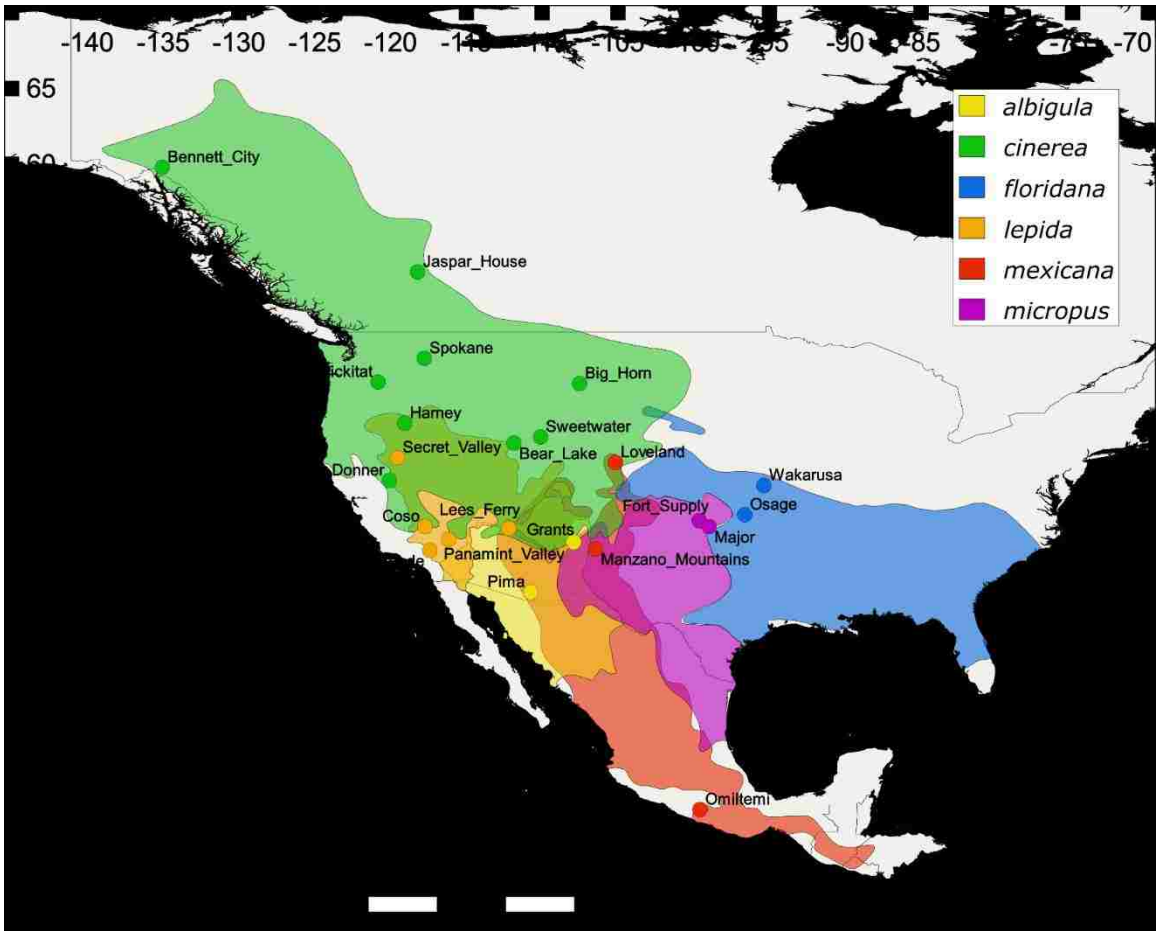

Figure 1.1. Selected *Neotoma* species distributions across North America. Distributions and localities (labelled dots) of *Neotoma* used in study shown for species: *N. albigula* (yellow), *N. cinerea* (green), *N. floridana* (blue), *N. lepida* (orange), *N. mexicana* (red), and *N. micropus* (purple). Map was produced in QGIS Desktop 3.03, using species distributions from IUCN (2018).

Neotoma have high-crowned, rooted molars, with three confluent or offset lophs (Zakrzewski 1993) (Figure 1.2A-F). *N. cinerea* (Figure 1.2B) and *N. mexicana* (Figure 1.2E) exhibit sharply prismatic lophs and deeper fold patterns between the lophs, while *N. albigula* (Figure 1.2A) and *N. lepida* (Figure 1.2D) tend to have more rounded lophs with shallower enamel folding patterns (Van Devender et al. 1977). *N. cinerea N. goldmani*, *N. lepida, N. mexicana,* and *N. stephensi* can be distinguished from *N. albigula, N. floridana* and *N. micropus* by the presence of a lateral dentine tract within the first lower molar (Harris 1984). Locality specific studies have had varying success separating fossil *Neotoma* using characteristics such as toothrow width, breadth of the second first molar loph, the rootward extent of the anteromedial groove and the presence/absence of pits at the base of enamel reentrants, among others (Dalquest et al. 1969, Zakrzewski 1993, Repenning 2004). While genus identification is possible for all three molars, isolated second and third molars are not identifiable to species and thus first molars are commonly used (Repenning 2004). However, it is not clear how robust these patterns are because this work did not include the substantial variation within each species.

The first upper molar (UM1) of *Neotoma* is particularly interesting because of variation in an anterolingual fold on the anteroloph across the different species (Figure 1.2). The anterolingual fold is generally shallow or lacking in *N. stephensi* and *N. lepida*, more developed in *N. cinerea, N. mexicana* and *N. micropus*, and is considered highly variable in *N. floridana* (Zakrzewski 1993, Repenning 2004). Variation in the fold has been reported in coastal and desert populations of *N. lepida* in California and Mexico (Patton et al. 2007). Thus, this feature may provide an additional metric for identification. Furthermore, geographic variation in morphology between and within species may be related to

environmental variables (Travis 1994), and may be related to different degrees of herbivory (Grayson, *pers. comm*). We hypothesize there to be a phylogenetic species level effect on dentition, but with similarities between species to exist for populations found in similar environments (potentially due to dietary overlap).

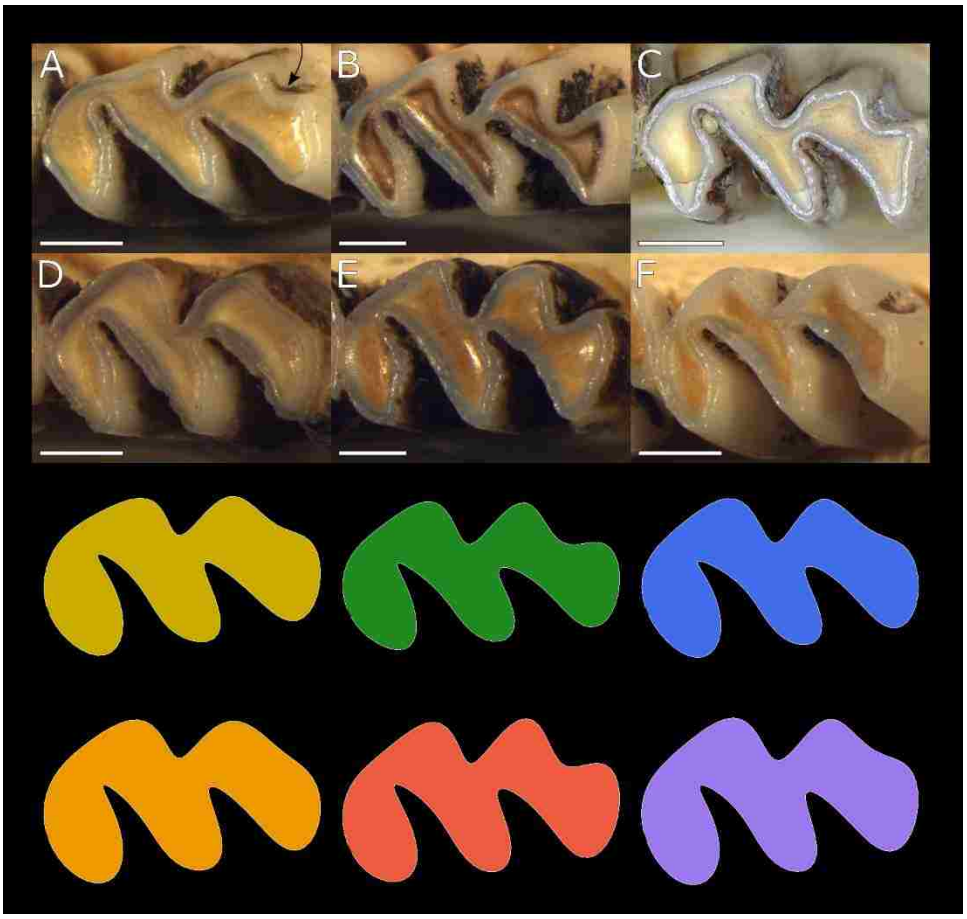

Figure 1.2. Photographs and mean shape of *Neotoma* molars. Photographs of the first upper left molars of 6 species of *Neotoma*: A) *N. albigula*, B) *N. cinerea*, C) *N. floridana*, D) *N. lepida*, E) *N. mexicana*, and F) *N. micropus*. Scale bar displays 1mm of length. Mean shape of the first upper molar of G) *N. albigula*, H) *N. cinerea*, I) *N. floridana*, J) *N. lepida*, K) *N. mexicana*, and L) *N. micropus* produced from elliptical Fourier coefficients.

Here, we use geometric morphometrics to quantify the variation across several species of the genus *Neotoma*, using an elliptical Fourier analysis of first upper molar outlines to

determine variation in shape across species. Geometric morphometrics is the quantification of variation across similar morphological features by considering the form or shape of an object independently of size or orientation (Claude 2008, Zelditch et al. 2012). Physical features are recorded using different shape coordinate systems (commonly landmarks or outlines) to compare deviations of morphological features across specimens. Landmarks use discrete, homologous anatomical points to test for variations across similar structures. In contrast, 2D outlines mark the entire perimeter of a shape to take into account curves and total shape of each specimen; this can then be to determine similarities and differences in shape across specimens (Bookstein 1997, Adams 1999, Adams et al. 2004). Previous studies using outline analysis have employed elliptical Fourier analysis, in which closed outlines (made up of x, y coordinates) are transformed into a set of harmonic ellipses with 4 coefficients each. The elliptical Fourier analysis is used to produce a matrix of coefficients that describe each shape in the data set, which can be used to run multivariate analyses (Kuhl and Giardina 1982, Bonhomme et al. 2014). Applications of outline analysis include considering morphological variation in mammal molars (Renaud et al. 1996 Michelle 2016), rodent mandibles (Renaud & Millen 2001), human cranial deformation (Frieß and Baylac 2003), leaf shape (Adebowale et al. 2012), and pollen grains (Bonhomme et al. 2013), among others.

Materials and Methods

Species Examined

We focused on 6 species in the genus Neotoma.---We examined 230 *Neotoma* specimens comprising 6 species (*N. albigula* (20), *N. cinerea* (90), *N. floridana* (20), *N.*

lepida (50), *N. mexicana* (30), and *N. micropus* (20)) from 23 localities in this study (Table 1.1, Figure 1.1). Specimens came from the Smithsonian National Museum of Natural History (USNM) in Washington D.C., and the James F. Bell Museum of Natural History (MMNH) at the University of Minnesota (St. Paul, MN) (Appendix 1 Table 1).

Table 1.1. Eigenvalues, proportional and cumulative contribution for the first 9 (of 40) principle components, explaining a total of 94% variation in molar outline shape across *Neotoma* species. Principle components 10-40 each had less than 1% of an effect on shape variation.

Principle Component	Eigenvalues	Proportion (%)	Cumulative Proportion (%)
1	5.13E-01	51.3	51.3
2	1.50E-01	15	66.3
3	9.96E-02	10	76.3
4	5.80E-02	5.8	82.1
5	4.58E-02	4.5	86.7
6	2.49E-02	2.5	89.1
7	2.04E-02	2	91.2
8	1.72E-02	1.7	92.9
9	1.13E-02	1.1	94

Neotoma albigula (White-throated woodrat) is primarily found in arid regions across the southwestern United States and into central Mexico (Figure 1.1) (Hall 1981, Macêdo and Mares 1988). *N. albigula* is typically associated with cactus. In the Sonoran Desert, for example, up to 4-45% of the white-throated woodrats' diet can be made up of *Opuntia*, which is thought to serve as both a food and water source (Vorhies and Taylor 1940, Olsen 1976, Orr et al. 2015). Populations in Colorado and across the Great Basin also consume large quantities of *Juniperus*; as much as 35% of the diet, in the absence of *Opuntia* and *Yucca* (Finley 1958, Dial 1988).

Neotoma cinerea (Bushy-tailed woodrat) has a geographic range from the Yukon and Northwest Territory of Canada to the southwestern United States, spanning the Pacific shore to the Great Plains (Figure 1.1) (Hall 1981, Smith 1997). The range covers ~30 degrees of latitude, and a wide variety of habitats and climatic conditions. *N. cinerea* are predominantly rock-dwellers, but can be found across vastly different habitats, such as desertic pinyon-juniper forests, coastal deciduous-coniferous forests, and mountainous pine, Douglas fir and aspen forests as long as rock shelter is available (Finley 1958, Brown 1968, Hickling 1987, Smith 1997). The bushy-tailed woodrat is considered to have a highly generalized diet, tending to eat abundant leafy vegetation, with preferences varying between different subspecies and populations (Finley 1958, Smith 1997). Populations in Colorado, for example, specialize on aspen, Douglas-fir, juniper, prickly-pear, hackberry, among a variety of different plants (Finley 1958). Coastal *N. cinerea* eat higher quantities of Douglas-fir, spruce and hemlock, along with a variety of other vegetation and berries (Carey 1991).

Neotoma floridana (Eastern woodrat) occupies both arid and subtropical areas, ranging across the eastern United States, from the Atlantic coast (from Florida to North Carolina) to the Great Plains (northern Colorado to southern Texas) (Figure 1.1) (Wiley 1980, Hall 1981). In Colorado, *floridana* makes use of cactus, as well as skunkbush, greasewood and *Yucca*, but it has also been found to specialize on acorns, osage orange and oak berries across its range, among other green vegetation, fruits and seeds (Murphy 1952, Rainey 1956, Finley 1958, Wiley 1980).

Neotoma lepida (Desert woodrat) is found in arid habitats in the western United States from southern Oregon and Idaho through the Baja California peninsula of Mexico (Figure 1.1) (Hall 1981, Verts and Carraway 2002). *N. lepida* make use of various xeric

adapted plants, and tends to specialize on a few resources at a population level. Different populations in California have been shown to focus on creosote, sage, oak, juniper and *Yucca*, while consuming more juniper in Utah, shadscale and prickly-pear in Idaho and Colorado (Finley 1958, Cameron and Rainey 1972, Meserve 1974, Verts and Carraway 2002).

Neotoma mexicana (Mexican woodrat) ranges across ~20 degrees of latitude, from the southwestern United States (northern Colorado) to western Honduras (Figure 1.1) (Hall 1981, Cornely and Baker 1986). *N. mexicana* is considered to have a relatively generalized diet, typically consuming foliage over other plant parts, and eating relatively little cactus or grass (Finley 1958). Taking advantage of abundant resources, *N. mexicana* eats a variety of plants, generally shrubs and forbs. The Mexican woodrat makes greater use of conifer needles, scrub oak, and juniper in Colorado where it is found most commonly among oak and piñon-juniper, and acorns and juniper berries in New Mexico and Texas, among other green vegetation, seeds and nuts (Finley 1958, Cornley and Baker 1986, Schmidly and Bradley 2016).

Neotoma micropus (Southern Plains woodrat) is generally found in semiarid regions in the southern Great Plains of the United States and northeastern Mexico (Figure 1.1) (Hall 1981, Braun and Mares 1989). *N. micropus* heavily utilizes cactus across its range. *Opuntia* is a primary food source for *micropus* in both Colorado (as tree cactus) and Texas (as prickly-pear) (Finley 1958, Schmidly and Bradley 2016). An absence of tree cactus will also lead to a greater use of prickly pear and *Yucca* (Finley 1958). Across the species ranges, *N. micropus* will eat mixed quantities of other green vegetation, fruits and seeds (Finley 1958, Braun and Mares 1989).

Specimen Selection and Preparation

We selected localities along the latitudinal and/or longitudinal gradients of each species range to select for varying climatic conditions and potential differences in dietary preferences. Specimens were included in localities using latitude, longitude or specific locality from museum tag information. The majority of specimens included in each locality were collected within a 3-5 year range, with the exceptions of Bear Lake, Harney and Omiltemi whose years spanned approximately 50, 20 and 60 years, respectively. Specimens selected were adults or sub-adults based on an assigned wear index and localities with fewer than 10 individuals were removed from analyses.

Teeth were assigned a wear index from 1-5 using the following criteria: 1) Little to no wear present, with enamel of the first molar not worn flat; 2) enamel of first molar flat but little wear present; 3) molar worn but no rounding of enamel border is present; 4) molar worn with slight rounding of enamel borders; 5) molar heavily worn and rounding of enamel edges obscures outlines. Because tooth wear can cause changes to the occlusal surface in *Neotoma* (Repenning 2004), molars that were assigned wear indexes of 1 or 5 were not used in producing outlines of molars. Thus, populations were composed of specimens with wear indices 2-4.

The occlusal surface of the upper first molars (UM1) was photographed using either an Olympus Scope DP12, or a Canon EOS 70D with a Canon EF 50mm f/1.8 STM lens. Photographs were digitized into two-dimensional outlines of the left UM1. Right UM1s were used for specimens whose left molar was missing or broken, with images being flipped horizontally to mirror the orientation of a left molar. Outlines followed the outer edge of enamel at the crown of the molar and were saved as x, y coordinates using the polygon tool

in ImageJ 1.50i. Outlines had an average of 178 points (± 56 coordinates). Molar area was measured using the polygon tool and length was measured using the straight line tool in ImageJ 1.50i. Each specimen was measured twice to minimize measurement error; all length measurements had a standard error below 0.05. The final data set consisted of 230 molars, with outlines, areas and lengths. All analyses employed R 3.3.3 (R Core Team 2016) and were performed in RStudio 1.0.136 (RStudio Team 2016).

Climate and Vegetation

To examine the interactions between climate, vegetation and molar morphology, we obtained locality specific variables using ClimateWNA, PRISM and NASA EOSDIS MODIS data. ClimateWNA provides scale free historical (1901-2014) climate data throughout North America by locally downscaling historical PRISM and ANUSPLIN data (Wang et al. 2016). Climate data for specimens collected between 1985-1900 was downloaded from the PRISM (Daly et al. 2008), that has historical data modelled using 30-year normals from North American station data for localities across the United States. We used mean annual temperature (MAT), maximum annual temperature (MxAT), minimum annual temperature (MnAT), mean annual precipitation (MAP), using locality latitude and longitude for the year the specimen was collected. Specimens collected prior to 1985 or without locality modelled climate data (N=45, including all specimens from localities: Jasper House (*N. cinerea*), Coso (*N. lepida*) and Panamint Valley (*N. lepida*), were excluded and climate analyses were performed on the remaining 185 specimens.

Precise vegetation indices by year could not be acquired for our specimens as they were collected between 1880-1970. Therefore, in order to include an index for potential differences in vegetation presence across our localities we used the Normalized Difference Vegetation Index (NDVI) of the Moderate Resolution Imaging Spectroradiometer (MODIS) data from NASA's Earth Observing System Data and Information System (EOSDIS) (https://earthdata.nasa.gov/about). We used the MODIS/Terra Vegetation Indices Monthly L3 Global 0.05 Deg CMG V006 (MOD13C2.006) data set, which has a 0.5° spatial and monthly temporal resolution of NDVI from February of 2000 to the present (Didan 2015). NDVI is a calculated ratio using near-infrared radiation (NIR) to red reflectance (Red): NDVI = (NIR – Red) / (NIR + Red). This normalized transform gives values between -1 and 1, with 1 indicating the largest proportion of green leaves present and 0 indicating the absence of vegetation (Didan 2015). NDVI was obtained from raster files from the MOD13C2.006 February 2000 data using QGIS Desktop 3.03 and locality latitude and longitude and analyses included all 230 specimens.

Data Analysis

We examined variation in molar size (length and area) between and across species localities of *Neotoma* using analysis of variance (ANOVA) and Tukey multiple comparisons of the means tests. Kruskal -Wallis and Wilcoxon rank sum tests were used for localities where the assumptions for parametric analyses were not met (across *N. lepida* and *N. mexicana*). We used multiple linear regressions with AIC to investigate whether molar size correlated with climate (MAP, MAT, MxAT or MnAT) or vegetation (NDVI). Furthermore, because cheek teeth have been shown to scale isometrically with body size (Fortelius 1985),

linear regressions were used to evaluate the relationship of molar length and area with body size using specimens body length (total length minus tail length) information.

Outlines (x, y coordinates) were imported into R and a general Procrustes analysis (GPA) was run to superimpose outlines prior to running an Elliptic Fourier analysis (EFA). The GPA was performed to account for any differences in the starting point, size, orientation and location of outlines, which can affect the EFA (Rohlf 1990). Ten configuration landmarks were placed at homologous points along the molar outlines for use in reorientation. The GPA uses an average molar shape to center and normalize the orientation and size of all outlines by minimizing the difference between the sum squared distances of each outline to the centroid size of the mean shape. The configuration landmarks are used to calculate rotation parameters for each outline per iteration (Rohlf and Slice 1990, Frieß and Baylac 2003, Claude 2008, Zelditch et al. 2012). An Elliptical Fourier analysis was then performed on the outlines. EFA can be used to turn the x, y coordinates for each closed outline into a harmonic ellipse. Each harmonic is described by four coefficients (two for each x and y coordinate) which define the shape of the original outline (Kuhl and Giardina 1982, Bonhomme et al. 2014). Here, we chose to use 10 harmonics, accounting for 99% of the total harmonic power, such that the shape of each molar was approximated using 40 EF coefficients.

Principal component analysis (PCA) was performed on the elliptic Fourier coefficients to characterize variation in the shape of UM1 across *Neotoma.* PCA reduced the number of EF coefficients into independent principal components (PCs) that describe the primary components of variation in molar shape (Table 1.1). We plotted the PCs against each other to visualize UM1 shape relationships across our *Neotoma* species. An inverse Fourier

transform was used to visualize the effect of each PC on the shape of the molar outline on the PC scatterplots. A multivariate analyses of variance (MANOVA) was performed on the first 9 resulting PC scores, retaining 94% of explained variation (Table 1.1), to test for differences in molar outlines of species across the genus and across localities at the species level. Further differences between species and across species localities was considered using a jackknife validation within a canonical variate analysis (CVA). CVA uses linear combinations of input variables to test group discrimination by considering differences among group means using within-group variation to scale the axes of the CV coordinate system (Zelditch et al. 2012). A CVA was run on the first 9 principle components to test whether specimen molars could be reliably assigned to species. We ran multiple linear regressions with AIC on the first 3 PC scores to examine whether shape of the upper first molar was associated with regional climate or vegetation. Outline analyses were run using the packages Momocs 1.3.0 (Bonhomme et al. 2012) and Morpho 2.6 (Schlager 2016).

Phylogeny

We tested for a phylogenetic signal on molar shape by considering the mean molar shape of each species, as produced by the elliptical Fourier coefficients, against the estimated *Neotoma* phylogeny from Matocq et al. (2006). To reproduce the general *Neotoma* tree topology from Matocq et al. (2006), we downloaded all sequenced loci (4 mitochondrial: *12S, 16S, COII, cytb*; 4 nuclear: *MLR, MYH6, EN2, FGB*) for a representative from each species (*N. albigula*, NK50148; *N. cinerea*, BYU17790; *N. floridana*, TK52109; *N. lepida*, MVZ197379; *N. mexicana*, TK78350; *N. micropus*, TK54559) from GenBank. Sequences were aligned using MUSCLE v3.8 (Edgar 2004). We generated a maximum-likelihood

phylogeny in RaxML v. 8.2 (Stamatakis 2014) with 10,000 iterations and a 25% burn-in under a GTR model of evolution. The resulting newick tree was imported into R and analyzed using Geomorph 3.0.6 (Adams et al. 2018). We tested for phylogenetic signal ("physignal", 10,000 iterations) against morphology data comprised of 120 mean molar shape coordinates per species. The function "plotGMPhyloMorphoSpace" was used to produce the plot of the phylogeny across principal dimension of tangent space based on the Procrustes-aligned 230 elliptical coordinates.

Results

Teeth Size and Body Mass

The size of the first upper molar was significantly different in both length (ANOVA: F-value = 77.22, df = 5/224, $p < 0.001$) and area (ANOVA: F-value = 8.33, df = 5/224, $p < 0.001$) across *Neotoma* species (Table 1.2, Figure 1.3). Furthermore, both the area and length of the UM1 were significantly correlated with each other (linear model: F = 186, adjusted $r^2 = 0.45$, df = 228, p-value < 0.001) and total body length. Molar length, however, acts as a better proxy for body size (linear model: F = 274.9, adjusted $r^2 = 0.58$, df = 197, p-value < 0.001) than molar area (F = 119.4, adjusted $r^2 = 0.37$, df = 197, p-value < 0.001). Significant differences in molar length and area therefore reflect differences in body size across *Neotoma. Neotoma cinerea* and *Neotoma lepida* had significantly different molar lengths to all other species and each other, while *N. floridana*, *N. mexicana* and *N. micropus* were indistinguishable (Table 1.2, Figure 1.3). Differences in molar area were found only between *Neotoma lepida* compared to *N. cinerea* and *N. micropus* (Table 1.2). With the exception of

Neotoma albigula and *Neotoma micropus*, UM1 length and area, and therefore body size, were also found to be significantly different across various populations within the same species (Table 1.2).

Table 1.2. Results of the Tukey multiple comparisons of the means tests for ANOVAs run on the molar area and molar length across *Neotoma* species and localities. Kruskal-Wallis and Wilcoxon rank sum tests are reported for molar area of *N. lepida* and *N. mexicana.* Significant differences are denoted as follows: p-value < 0.05 (*), p-value < 0.01 (**) and p-value < 0.001 (***). Only species or localities with significant differences shown.

Across Species	**UM1 Length**	**UM1 Area**	**Across Localities**		**UM1 Length**	**UM1 Area**
N. albigula - N. cinerea	***		*N. cinerea*			
N. albigula - N. floridana				Bear Lake - Jasper House	***	
N. albigula - N. lepida	***			Big Horn - Sweetwater	*	
N. albigula - N. mexicana				Donner - Jasper House	***	
N. albigula - N. micropus	*			Harney - Jasper House	*	
N. cinerea - N. floridana	***			Jasper House - Spokane	**	
N. cinerea - N. lepida	***	***		Jasper House - Sweetwater	***	
N. cinerea - N. mexicana	***			Klickitat - Sweetwater	*	
N. cinerea - N. micropus	**		*N. floridana*			
N. floridana - N. lepida	***			Osage - Wakarusa		*
N. floridana - N. mexicana			*N. lepida*			
N. floridana - N. micropus				Coso - Oro Grande	**	***
N. lepida - N. mexicana	***			Coso - Panamint Valley		*
N. lepida - N. micropus	***	***		Coso - Secret Valley		*
N. mexicana - N. micropus				Lees Ferry - Oro Grande		*
				Oro Grande - Panamint Valley		***
				Oro Grande - Secret Valley	*	
				Panamint Valley - Oro Grande		**
			N. mexicana			
				Loveland - Manzano Mountains		**
				Loveland - Omiltemi	**	***
				Manzano Mountains - Omiltemi	**	

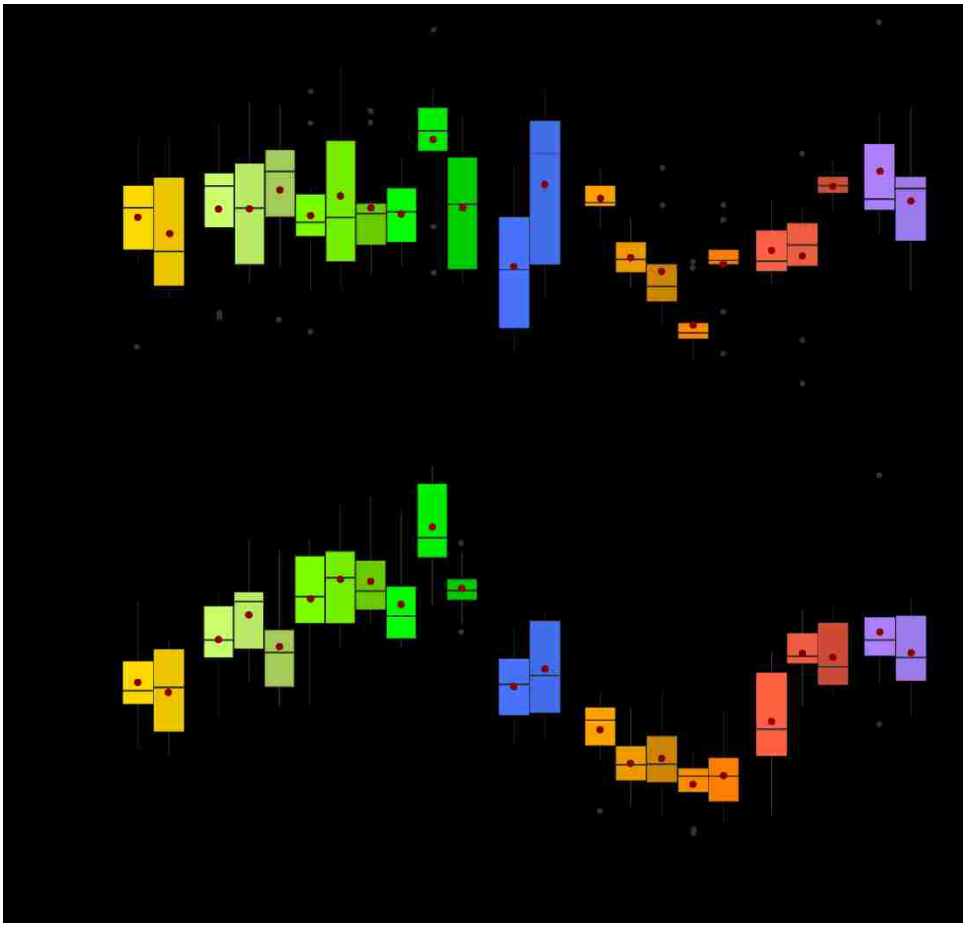

Figure 1.3. Molar length and area across *Neotoma* localities. Distribution of upper first molar A) area (mm^2) and B) length (mm) across species of *Neotoma* with localities ranked from lowest to highest latitude (left to right).

Molar Shape

The shape of the first upper molar varied significantly among species of *Neotoma* (MANOVA, HL = 3.88, df = 5, p-value < 0.001). The results of the pairwise MANOVA showed significant differences in shape between all species (all pairs: p-value < 0.01). PCA of the EF coefficients found the first 9 PCs to explain about 94% of the variance in molar shape (Table 1.1). The elliptic Fourier analysis (Figure 1.4) found three general "morpho" groups across *Neotoma.* The two groups with the most variation in molar shape separate *N.*

cinerea and *N. mexicana* from *N. albigula* and *N. lepida*. However, *N. floridana* and *N. micropus* are less differentiable from the four other species and from each other. Ellipses representing 50% confidence ranges for species molar morphology, show a large degree of overlap across *N. floridana* and *N. mircopus* with the four other species across PC1-3 (Figure 1.4A-C). Comparisons of the first 3 PCs (Figure 1.4A-C), which account for ~76.3% of molar shape variation separate species into 3 general morpho-groups: Group A (*N. cinerea* and *N. mexicana*), Group B (*N. albigula* and *N. lepida*) and Group C (*N. floridana* and *N. micropus*). PC1, accounting for 51.3% of outline variation in shape (Table 1.1), describes the degree of folding along the reentrant on the lingual side of the molar (Figure 1.4D). Specimens with lower PC1 values have deeper grooves between the lophs of the UM1 and a clear presence of the anterolingual fold. Higher PC1 values correspond to molars with a shallower groove along the lingual side of the tooth and absence of the anterolingual fold. PC2, characterizing 15% of molar shape variation (Table 1.1), describes molar width and angle of the lophs in relation to the lingual-bucco plane. Higher PC2 values represent wider molars, with the lophs arranged more parallel to one another from anteroposteriorly (Figure 1.4D). Thinner molars whose lophs have great anteroposterior angling have lower PC2 values. PC3 describes variation in the width and spacing of the 3 lophs, with higher values corresponding to wider lophs and lower PC3 values corresponding to thinner, generally more separated lophs (Figure 1.4D).

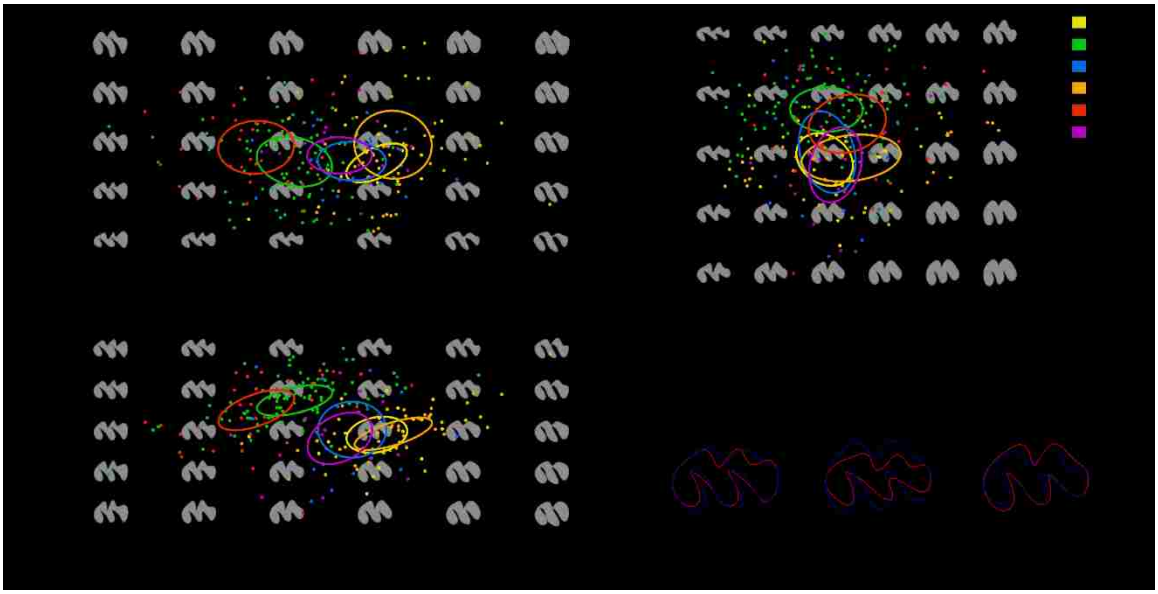

Figure 1.4. Principle Components of *Neotoma* molar shape. First 3 principle components plotted against one another for all 230 specimens. Ellipses represent 50% confidence range for species UM1 outline shape. Together, PC1-3 explain 76.3% of variance in shape, with differences being represented by molar shape projections (grey) for A) PC1 vs PC2, B) PC1 vs PC3, and C) PC2 vs PC3. D) +2SD (blue) and – 2SD (red) from mean molar shape shows the variance explained by PC1-3.

Overall, outline analysis could not consistently assign molars to the correct species. Indeed, jackknife validation of the CVA on the first 9 PC scores (encompassing 94% of shape variation) outlines into the correct species only 68.3% of the time. However, classification of some species was much more robust. For example, *N. cinerea* had the highest percent of correct classification (91.1%), followed by *N. mexicana* (76.7%). After which only *N. lepida* was classified correctly more than 50% of the time (68%, Table 1.3). The medium sized species were classified correctly just under half the time, *N. albigula* (45%) and *N. micropus* (40%). *N. floridana* was misclassified the most, with only 5% of molars belonging to the species being placed within the appropriate group. *Neotoma cinerea* and *mexicana* were most commonly misclassified as each other (4.4% and 20%,

Table 1.3. Percent of *Neotoma* UM1 outlines correctly classified to species from canonical variate analysis jackknife cross-validation. Bold values indicate outlines that were correctly assigned to their species over 50% of the time.

		% Classification:					
		N. albigula	*N. cinerea*	*N. floridana*	*N. lepida*	*N. mexicana*	*N. micropus*
Known Group:	*N. albigula*	45.0	5.0	0.0	20.0	10.0	20.0
	N. cinerea	0.0	**91.1**	2.2	2.2	4.4	0.0
	N. floridana	10.0	25.0	5.0	40.0	0.0	20.0
	N. lepida	10.0	4.0	16.0	**68.0**	0.0	2.0
	N. mexicana	0.0	20.0	0.0	0.0	**76.7**	3.3
	N. micropus	10.0	5.0	10.0	25.0	10.0	40.0

respectively), and are rarely misclassified with other species (Table 1.3). In contrast, over half of the *N. albigula* and *N. micropus* were misclassified, most commonly as *N. lepida* and *N. floridana*, respectively. *N. floridana* was misclassified as *N. lepida* more often (40%) than as any other species (Table 1.3). Comparisons of the first 3 CV scores (Figure 1.5, A-C) are shown to highlight species variation in UM1 outline shape across *Neotoma*, with explained proportions of within-group variation being CV1 64.8%, CV2 27.2% and CV3 5%. Jackknife validation testing for how accurately individuals could be classified to locality within species found somewhat opposite results. Species that were more distinguishable by molar shape across the genus tended to have lower accurate assignments to locality, and vice versa. Every individual of *N. floridana*, for example, was correctly assigned to locality, while *N. cinerea* could only be correctly assigned to locality about 26% of the time. Of the remaining species, *N. micropus* and *N. mexicana* individuals were correctly sorted to locality over half the time (75% and 60%, respectively), while over half of *N. lepida* (46%) and *N. albigula* (35%) were misplaced.

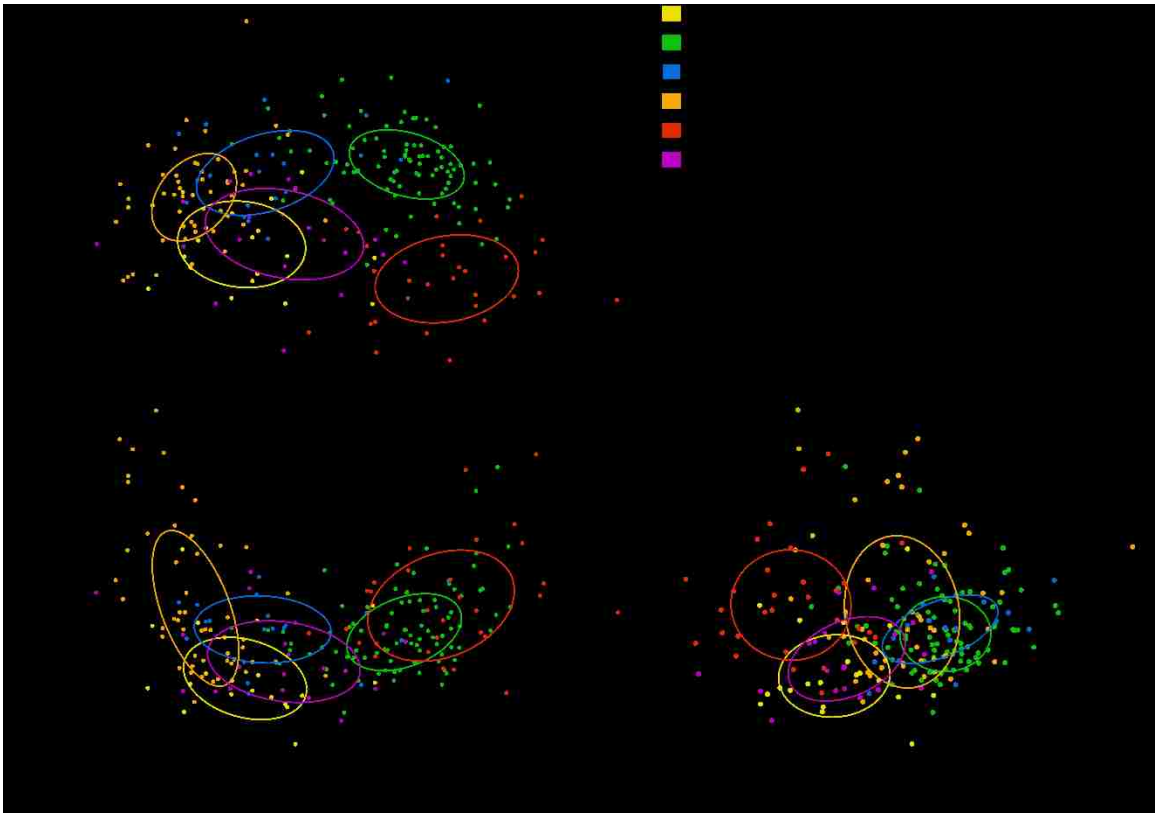

Figure 1.5. Canonical Variate Scores of *Neotoma* molar shape. Comparison plots of first 3 canonical variate scores calculated from the first 9 PC scores. Ellipses represent 50% confidence ranges for correct classification to species. CV1 explains 64.8% of within-group variation, CV2 27.2% and CV3 5%.

Climate and Vegetation

We found significant correlations between size and shape and climatic variables and vegetation index. Mean annual precipitation (MAP), mean annual temperature (MAT) and minimum annual temperature (MnAT) gave the highest quality model for UM1 length (multiple regression model: AIC = -530.9, adjusted $r^2 = 0.21$, df = 181, p-value < 0.001, Table 1.4), with a negative relation between temperature and length. Shape variation as characterized by PCs 1-3 were significantly correlated with both climate and vegetation, with maximum annual temperature (MxAT) consistently present in all significant models (Table

1.4) and associated with shallower folding patterns, wider molars and wider, more closely situated lophs. Climate was significantly correlated with molar area in *N. floridana* (MAT), *N. lepida* (MAP, MAT, MnAT) and *N. mexicana* (MAT, MxAT), but no correlation was found between molar area and vegetation (Table 1.4). Maximum temperature was significantly and negatively correlated with *N. mexicana* (Table 1.4), while MAP, MAT, MnAT, NDVI were correlated with molar length in *N. cinerea* and *N. lepida.* PC1 (degree of lingual folding) was not found to be significantly correlated with climate between populations of *Neotoma* species (Table 1.4). Mean annual temperature was important in the majority of significant models. Minimum annual temperature was important to significant size and shape correlations in *N. cinerea, N. lepida, N. micropus*, while maximum annual temperature was most present in correlations across *N. mexicana.* The vegetation index was not found to be significantly correlated to shape variation between *Neotoma* species populations.

Table 1.4. Multiple regression model results of climate and vegetation index to UM1 length and area across species (Spp.). Models included climate and vegetation variables: mean annual precipitation (MAP), mean annual temperature (MAT), maximum annual temperature (MxAT) and minimum annual temperature (MnAT), normalized difference vegetation index (NDVI) from ClimateWNA (Wang et al. 2016), PRISM (Daly et al. 2008) and NASA EOSDIS Land Processes DAAC (Didan 2015). Significance (Sig.) of models are denoted as follows: not significant (*ns*), $p < 0.05$ (*), $p < 0.01$ (**) and $p < 0.001$ (***).

Spp.	Size Variable	Best Model	Variable Sign	AIC	*F*	Adj. r^2	df	Sig.
all species	UM1 Area	MxAT + NDVI	+, -	-76.7	2.97	0.02	182	*ns*
	UM1 Length	MAP + MAT + MnAT	+, -, -	-530.9	17.63	0.21	181	***
	PC1	MAP + MxAT + NDVI	-, +, -	-1143.6	14.35	0.18	181	***
	PC2	MAP + MAT + MxAT + MnAT + NDVI	-, -, +, +, -	-1351.2	4.92	0.1	179	***
	PC3	MxAT	-	-1419.4	18.62	0.09	183	***
	PC1 + PC2 + PC3	MAP + MxAT	-, +	-1045.8	11.86	0.11	182	***

Spp.	Size Variable	Best Model	Variable Sign	AIC	*F*	Adj. r^2	df	Sig.
albigula	UM1 Area	MAP + MAT	-, +	-8.2	1.58	0.06	17	*ns*
	UM1 Length	MAP + MAT + MxAT	-, +, -	-71	1.84	0.12	16	*ns*
	PC1	MAT	+	-137.4	2.12	0.06	18	*ns*
	PC2	MAT	+	-154.1	0.92	0	18	*ns*
	PC3	MAP + MxAT	+, -	-157.7	1.71	0.07	17	*ns*
	PC1 + PC2 + PC3	MAT	+	-118.8	2.06	0.05	18	*ns*
cinerea	UM1 Area	MAP	+	-28.7	0.88	0	65	*ns*
	UM1 Length	MAP + MAT + MnAT + NDVI	+, + -, +	-232.9	3.71	0.14	62	**
	PC1	MAT + MnAT	+, -	-437.4	2.09	0.03	64	*ns*
	PC2	MAT + MxAT + MnAT + NDVI	-, +, +, -	-488.9	2.52	0.08	62	*ns*
	PC3	MAT + NDVI	+, +	-560.2	4.09	0.09	64	*
	PC1 + PC2 + PC3	MxAT	+	-399	1.42	0.01	65	*ns*
floridana	UM1 Area	MAT	-	0.3	5.87	0.26	18	*
	UM1 Length	MAT	-	-69.9	0.79	-0.01	18	*ns*
	PC1	MAT	-	-131.6	1.03	0	18	*ns*
	PC2	MAP	+	-153.2	0.2	-0.04	18	*ns*
	PC3	MAT	+	-165.2	50.79	0.72	18	***
	PC1 + PC2 + PC3	MxAT	+	-122.4	3.03	0.1	18	*ns*
lepida	UM1 Area	MAP + MAT + MnAT	-, +, -	-38.5	8.97	0.47	24	***
	UM1 Length	MAP + MAT + MnAT + NDVI	-, +, -, -	-109.8	2.87	0.22	23	*
	PC1	MxAT	-	-182.7	3.94	0.1	26	*ns*
	PC2	MAT + MxAT + MnAT	+, -, -	-206	7.53	0.42	24	**
	PC3	MnAT	-	-232.1	0.19	-0.03	26	*ns*
	PC1 + PC2 + PC3	MAP	-	-157.4	1.3	0.01	26	*ns*
mexicana	UM1 Area	MAT + MxAT	+, -	-34.4	8.71	0.35	27	**
	UM1 Length	MxAT	-	-110.9	18.19	0.37	28	***
	PC1	MxAT	+	-192	1.04	0	28	*ns*
	PC2	MAT + MxAT	+, -	-227.4	10.28	0.39	27	***
	PC3	MAP + MAT + MxAT	-, -, +	-235.7	3.77	0.22	26	*
	PC1 + PC2 + PC3	MAT	-	-163.3	0.58	-0.01	28	*ns*
micropus	UM1 Area	MAT	+	-6.3	0.69	-0.02	18	*ns*
	UM1 Length	MxAT	-	-62.6	1.62	0.03	18	*ns*
	PC1	MAT	-	-132.8	0.22	-0.04	18	*ns*
	PC2	MAT + MxAT + MnAT	+, -, -	-161.3	3.25	0.26	16	*
	PC3	MAP	-	-142.6	0.76	-0.01	18	*ns*
	PC1 + PC2 + PC3	MAP	-	-115.4	2.35	0.07	18	*ns*

Phylogeny

Our maximum-likelihood tree topology matched that of Matocq et al. (2006) (Figure 1.6). Molar outline shape did not exhibit a significant phylogenetic signal ($K = 0.7075$, p-value > 0.05), suggesting that more closely related *Neotoma* species did not have strong similarities in molar outline. Projection of the phylogenetic tree onto shape space (Figure 1.6), shows a series of overlapping branches and lack of clustering among sister species; phylogeny does not drive the overall patterns in molar shape.

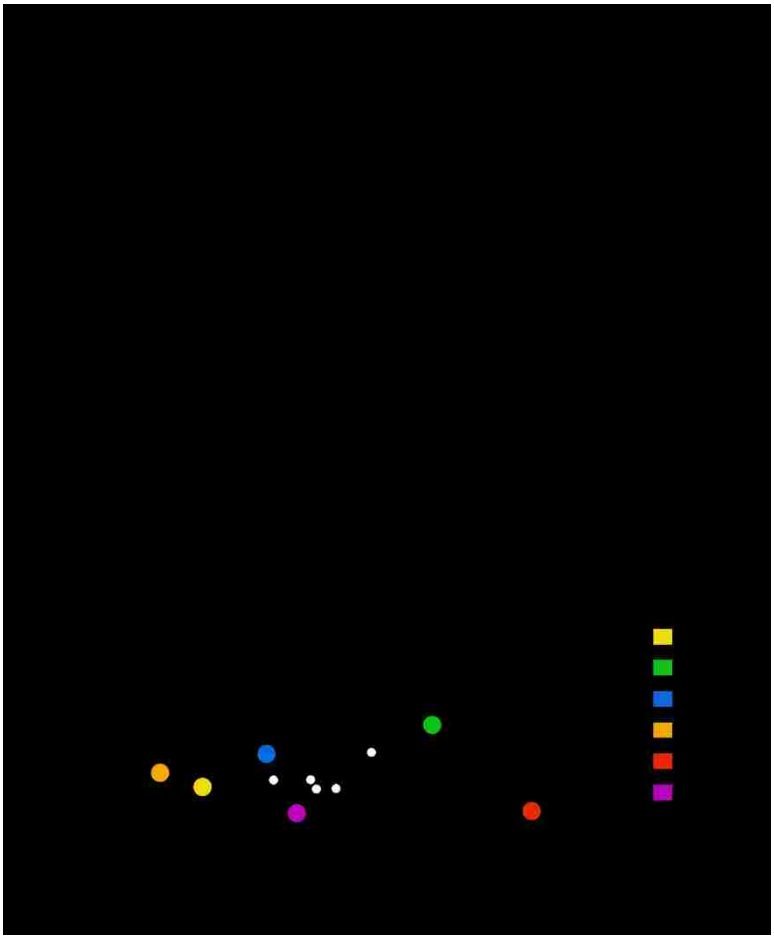

Figure 1.6. Neotoma Cladogram and Phylogeny in Shape Space. A) Maximum-likelihood tree topology of *Neotoma* reconstructed from Matocq et al. (2006). B) Phylogenetic tree of *Neotoma* as projected in morphospace for PC1 and 2.

Discussion

We find that both the size and shape of the first upper molar of *Neotoma* varies significantly both between and within species. The significant relationship between molar size and body length, coupled with the known correlations between body size and temperature suggests molar size likely reflects ambient temperatures (Brown and Lee 1969, Smith et al. 1995, 1998, Smith and Betancourt 1998, 2003). An overall lack of phylogenetic signal in the evolution of molar outline shape for species may suggest that variations are not solely driven by lineage, but may reflect dietary ecology.

Differences in molar length reflect previously observed patterns in body size of *Neotoma. Neotoma* whose species' ranges have wide latitudinal gradients, such as *N. cinerea* and *N. mexicana*, exhibit a north to south body size gradient (Cornely and Baker 1986, Smith 1997, Smith and Betancourt 2003). *Neotoma lepida* is an exception to this pattern and southern populations are generally larger than northern ones (Verts and Carraway 2002). However, it should be noted that the temperature gradient across the range of *N. lepida* is east to west, with eastern, desert populations being typically smaller than western, coastal populations (Brown and Lee 1969). We found both of these patterns reflected in our data (Figure 1.3). Furthermore, because we found body length to be significantly correlated with molar length, we suspect these patterns reflect local population adaptations of body size to temperature. Past work on *Neotoma* demonstrated a strong response of woodrats to environmental temperature across both space and time; increased temperature led to decreased body size (Brown and Lee 1969, Smith et al. 1995, 1998, Smith and Betancourt 1998, 2003). Indeed, woodrats are the poster child for Bergmann's Rule, which states that within a genus, species that are found further north at colder latitudes tend to be larger than

those found further south at warmer latitudes (Bergmann 1847, Mayr 1956). When considering all species together, we found mean and minimum annual temperature be negatively correlated to UM1 length (Table 1.4). Furthermore, molar length had a negative correlation with minimum annual temperature in *N. cinerea*, and maximum annual temperature in *N. mexicana*. Because these species are at the northern and southern most latitudes of the genus range, respectively, it would make sense that the lowest and highest temperatures would negatively affect body length, as *N. cinerea* would increase body size with decreasing temperatures, while *N. mexicana* would decrease body size with increasing temperatures.

The complexity of the molars generally supports previously described molar shape variations within the genus. *N. mexicana* and *N. cinerea* have the lowest PC1 values, exhibiting a greater folding of the anterior lophs, with more a prominent anterolingual fold (Figure 1.2H, K, Figure 1.4A, B). In contrast, *N. albigula* and *N. lepida* have wider lophs with shallower folds between them, and minimal to no development of the anterolingual fold (Figure 1.2G, J, Figure 1.4A-C). The mean UM1 shape of *N. floridana* and *N. micropus* (Figure 1.2I, L) do not have as wide or shallow lophs as *N. albigula* and *N. lepida*, but also do not have as deep of an anterolingual fold as *N. cinerea* and *N. mexicana.* Thus, the greatest degree of UM1 shape difference is between *N. cinerea* and *N. mexicana* versus *N. albigula* and *N. lepida*. These results support those described by Van Devender et al. (1977), and align generally well with Zakrzewski (1993) and Repenning (2004), though we did not find ridge folding to be as prominent within our *N. micropus* specimens. While these general patterns may assist in identifications into 3 morpho-group classifications the results of the jackknife cross-validation (Table 1.3) suggest that precise classification to the species level

using outline shape alone is not reliable for distinguishing across these 6 species of *Neotoma*. Interestingly, the greater similarity between species in morphospace does not reflect phylogenetic relations across the genus (Figure 1.5).

The lack of phylogenetic signal coupled with the grouping of species into 3 general morpho-groups may indicate an important relationship with diet. Matocq and Murphy (2007) similarly found that craniodental morphology diverged in overlapping populations of *N. fuscipes* and *N. macrotis.* Within the six species of *Neotoma* discussed here, *N. cinerea* and *N. mexicana* are the two species consuming the least amount of succulent plants (Finley 1958, Cornley and Baker 1986). *Neotoma albigula* and *N. micropus* share similar dietary habits (large quantities of *Opuntia*) compared to the *N. cinerea* and *N. mexicana,* while neither *N. lepida* nor *N. floridana* are as dependent on cactus as *N. albigula* and *N. micropus* (Finley 1958, Vorhies and Taylor 1940). Species subsisting on softer, more succulent foods (e.g. cacti) have a lower degree of folding along the lophs of their molars. In contrast, species such as *N. cinerea* that are larger in body size may be making larger use of a wider amount of tougher or fibrous foods (e.g., juniper oak, fruits, seeds, etc.) (Finley 1958, Cornley and Baker, 1986, Smith 1995a, 1997, Wang et al. 2003) and exhibit molars whose lophs tend to be more tightly angled. Because increased folding patterns may provide more efficient grinding across the occlusal surface of the teeth (Kay and Hiiemae 1974, Ungar 2010), selection pressure maybe drive the greater anterolingual folding (represented by PC1, Figure 1.4A, B and D) in *N. cinerea* and *N. mexicana* whose populations generally make use of a larger variation of resources across their species ranges.

We were only able to robustly classify 2 species based on their molars. In particular, cross-validation was effective for *Neotoma cinerea* and *N. mexicana* (90% and 75%,

respectively, Table 1.3, Figure 1.5A-B) followed by *N. lepida* (68%, Table 1.3, Figure 1.5A-B). *N. cinerea* and *N. mexicana* are the two species that most clearly separated from other groups by PC1 and PC3, which together explain about 60% of molar outline variation in shape (Table 1.2, Figure 1.4B). While efforts were made to select for specimens within a certain age range, the degree of wear along a molar can cause large variations in the occlusal surface of teeth (Harris 1984, Ledevin 2010, Guérécheau et al. 2010, Mitchell 2016), the effects of which may be playing an important role in species classification.

The relationship between differences in shape (PC1-3) and climate is not as clear. Species that are more related in morphospace do not share the same correlations with temperature and precipitation (Table 1.4). The first 3 PC scores (~76% of explained outline variation) are significantly correlated to mean annual precipitation and maximum annual temperature across *Neotoma*, with PC1 and PC2 also being correlated to vegetation index (Table 1.4). The relationship between shape and climate across all species would suggest that individuals experiencing less precipitation, hotter temperatures or in areas with less green vegetation should generally have lophs that are wider with smaller in-folding angles between lophs. The first PC, or about half of explained shape variation (Table 1.1), was not significantly correlated with climate at the species level (Table 1.4).

Intraspecific variation in molar size was found across different localities of *N. cinerea*, *N. floridana, N. lepida*, and *N. mexicana* (Table 1.2). Significant differences in molar length, and thus correlated body size, of *N. cinerea*, *N. lepida* and *N. mexicana* were found across each species latitudinal range, with size patterns for *N. cinerea* and *N. mexicana* conforming to Bergmann's rule. Indeed, molar length at Jasper House, the second most northern locality of *N. cinerea*, was found to be significantly larger from 5 of 8 other

southern localities (Table 1.2, Figure 1.2). *N. mexicana's* Omiltemi population at the extreme south of the range (Figure 1.1) was significantly smaller compared to both northern populations (Table 1.2, Figure 1.2). As such, *N. cinerea* and *N. mexicana* tend to increase in body size from southern, warmer localities to northern, colder localities.

Interestingly, cross-validation of localities by outline shape found that *N. floridana* and *N. micropus* were correctly classified 100% and 75% of the time, respectively, despite these 2 species having the lowest correct classifications when looking across all 6 species. Furthermore, molar area was significantly different between the 2 populations of *N. floridana* considered. *Neotoma floridana* and *N. micropus* were found to have intermediate folding and loph patterns (Figure 1.4-1.5), between Morpho-Group A (*N. cinerea: N. mexicana*) and Morpho-Group B (*N. albigula: N. lepida*). The 100% correct classification of members of *N. floridana* into their proper localities may suggest a correlation with different local diets. While *N. floridana* makes use of an array of resources across its range, the species, as with most *Neotoma*, will specialize on the most abundant resources between localities (Murphy 1952, Rainey 1956, Finley 1968, Wiley 1980). Different selective pressures across populations may then be driving morphological changes in the molar form of *N. floridana* such that variation between localities is greater. In contrast, *N. cinerea*, which has the most identifiable morphology between species (Table 1.3), is only correctly identified about 25% of the time at the locality level. The inability to classify *N. cinerea* at the local level may be due to the wide range of resources across its extensive species range (Finley 1968). The differences in inter- and intraspecific classifications may also be an artifact of the higher representation of *N. cinerea* compared to *N. floridana* or *N. micropus* in our data set, as well as a larger geographic range, encompassing a broader set of habitats (Figure 1.1).

Overall, the six species of *Neotoma* examined in this study show varying degrees of differences in the size and shape of the first upper molar. Strong correlations of molar and body length compliment previously described patterns of latitudinal and temperature gradients, both between and within species. While elliptical Fourier analysis of molar outline did not provide a general tool for discriminating between all species, it was useful for some, and moreover, suggested a potential link between dental morphology and dietary generalization/specialization both at the species and local level. A combined use of size measurements and shape analysis may further increase precision of molar classifications. Species within Morpho-Group B, for example, would likely become better resolved when accounting for the fact that *N. lepida* is typically smaller than *N. albigula.* Here we used dietary preference as described in the literature to explain certain morphological patterns. A study comparing variation in shape for individuals using exact resource use or stable isotope analysis to characterize isotopic niche space would provide greater insight into the role of diet with variation in dental morphology across the genus. The abundance of *Neotoma* in the fossil record of North America, particularly through the extensive use of the animal and plant remains of their paleomiddens would further improve our understanding of what these records show, not only for the genus of *Neotoma,* but the ecosystem with which they coexisted.

Chapter 2

The response of a small herbivorous mammal (*Sigmodon hispidus,* hispid cotton rat) to the Late Pleistocene megafauna extinction

Catalina P. Tomé[1], Emma A. Elliott Smith[1], S. Kathleen Lyons[2], Thomas W. Stafford Jr[3], Seth D. Newsome[1], and Felisa A. Smith[1]

[1]Department of Biology, University of New Mexico, Albuquerque, NM
[2]School of Biological Sciences, University of Nebraska-Lincoln, Lincoln, NE
[3]Stafford Research, 200 Acadia Avenue, Lafayette, CO

Abstract

The catastrophic loss of large-bodied mammals during the terminal Pleistocene likely led to cascading effects within communities. While the extinction of the top consumers probably expanded the resources available to survivors of all body sizes, little work has focused on the responses of the smallest mammals. Here, we use a detailed fossil record from the southwestern United States to examine the response of the hispid cotton rat (*Sigmodon hispidus*) to biodiversity loss and climatic change over the late Quaternary. In particular, we focus on potential changes in diet and body size. We characterize diet through carbon ($\delta^{13}C$) and nitrogen ($\delta^{15}N$) isotope analysis of bone collagen in fossil jaws and body size through measurement of fossil teeth; the abundance of material allows us to examine population level responses at millennial scale for the past 16ka. *Sigmodon* was not present at the cave during the full glacial; first appearing at ~16ka after ice sheets are in retreat. It remained relatively rare until ~12ka when warming Holocene temperatures allowed it to expand its species range northward. We find changes in both diet and body size of *Sigmodon hispidus* over time: the

average body size of the population varied by ~20% (90-110g) and mean $\delta^{13}C$ and $\delta^{15}N$ values ranged between -13.5 to -16.5‰ and 5.5 to 7.4‰ respectively. Employment of a state-space model suggested changes in mass were influenced by diet, maximum temperature and community structure, while the modest changes in diet were most influenced by community structure. Overall, *Sigmodon* exhibited a high level of ecological plasticity, maintaining a fairly similar dietary niche over time despite contemporaneous changes in climate and herbivore community composition that followed the megafauna extinction. Broadly, our results suggest that small mammals may be as sensitive to small-scale biotic interactions within their ecosystem as they are to large-scale changes.

Introduction

Large-bodied mammals play a critical role within communities and ecosystems. Either directly or indirectly, they influence soil and vegetation structure and composition, nutrient cycling and other biogeochemical processes, and especially, the distribution and abundance of other mammals (Ripple et al. 2015, Malhi et al. 2016, Smith et al. 2016a). The loss of apex consumers can lead to cascading effects, changing community structure and species (Estes et al. 1998, 2011, Schmitz et al. 2000, Shurin et al. 2002, Dirzo et al. 2014, Ripple et al. 2014). For example, experimental removal of large-bodied mammals from plots across a variety of ecosystems has led to increased rodent abundance, likely because of alterations of vegetation abundance and composition (Keesing 1998, Parsons et al. 2013, Galetti et al. 2015). While empirical studies demonstrate rapid responses by the small-bodied mammal community, the ultimate consequences remain unclear, since direct and indirect effects may take decades or longer to be fully realized (Brown and Munger 1985, Smith et al. 1997, Ernest et al. 2000,

Brown et al. 2001). Thus, longer-term perspectives are essential for investigating the influence of biodiversity loss and predicting how such events may change the interactions and dynamics within an ecosystem over evolutionarily relevant time scales (Smith et al. 2010, Blois et al. 2013). Moreover, given the precarious state of most megafauna today (Davidson et al. 2009, Ripple et al. 2015, Smith et al. 2016a), such studies are crucial for effective management.

The late Pleistocene megafaunal extinction led to the loss of more than 70 species in North America, including all mammals weighing > 600 kg (Martin and Klein 1989, Lyons et al. 2004). The high degree of size-selective extinction was unprecedented in the Cenozoic mammalian record (Alroy 1999, Smith et al. 2018), and likely had significant impacts on the community structure and function of surviving animals (Smith et al. 2018). For example, extinct species had significantly more ecological associations than do modern species today, suggesting a more tightly organized web of species interactions (Smith et al. 2016b). Thus, loss of megafauna at the terminal Pleistocene is a good proxy for examining the consequences of modern losses in biodiversity, which preferentially target Earth's remaining large-bodied mammals (Davidson et al. 2009, Smith et al. 2018). Here, we are particularly interested in the influence of biodiversity loss on surviving smaller-bodied mammals within the community.

Confounding the loss of biodiversity at the end Pleistocene was a rapidly changing climate associated with the termination of Pleistocene glaciations. While temperatures in the Northern Hemisphere increased from the late Pleistocene to the Holocene, this millennial-scale climate warming was punctuated by several significant temperature fluctuations (IPCC 2014). These included the Younger Dryas (12.8-11.5 ka) – a cooling and warming event which terminated in a particularly abrupt 7°C temperature increase over as little as several decades, the 8.2 ka cold event – a sudden ~3C decrease in global temperature that persisted for several

centuries, and the mid-Holocene Warm Period or Climatic Optimum (~7-5 ka), which appears to have been concentrated in the Northern Hemisphere (Alley 2000, Rohling and Pälike 2005, Li et al. 2012). These and other climatic changes led to substantial shifts in the composition and distribution of flora and fauna across North America at both regional and continental scales (Prentice et al. 1991, Graham et al. 1996, Whitlock and Bartlein 1997, Lyons 2003, 2005, Blois et al. 2010, Gottfried et al. 2012, Cotton et al. 2016).

Fluctuations in environmental temperature are known to influence the morphology and ecology of species (Bergmann 1847, Brown 1968, Andrewartha and Birch 1984, Gylnn 1993, Smith et al. 1995, Ashton et al. 2000, Stenseth et al. 2002, Walther et al. 2002, Millien et al. 2006). Indeed, the ecogeographic relationship between population and/or species body mass and temperature gradients is so well-characterized it is termed Bergmann's rule; the principle that within a genus, larger species are found in colder climates and smaller species in warmer ones (Bergmann 1847, Mayr 1956). Bergmann's rule is well-supported for most mammals both across time and space, suggesting environmental temperatures have a strong impact on body size evolution (Brown and Lee 1969, Smith et al. 1995, Ashton et al. 2000, Gillooly et al. 2001, Freckleton et al. 2003, Millien et al. 2006, Smith 2008); but see: McNab 1971 and Blackburn et al. 1999. Moreover, changes in body size have consequences because of the allometric scaling of many life history and physiological processes such as metabolism, growth, reproduction, locomotion, home range size, and even the degree of consumption of plant fiber (McNab 1980, Peters 1983, Calder 1984, Justice and Smith 1992, Smith 1995a). Thus, selection for a larger (or smaller) body size changes how animals interact with and/or are impacted by their ecosystem (Damuth 1981, Peters 1983, Calder 1984). This coupling of

climatic change at the late Quaternary with the terminal Pleistocene megafauna extinction likely led to substantial ecosystem alterations for surviving mammals.

We assessed the relative importance of changes in climate, resources and community structure on both diet and body size of *Sigmodon hispidus*, a medium sized herbivorous rodent, over the past 16,000 years. We employ stable isotope analysis and measurements of fossil molars. We focused on an exceptionally well-stratified and radiocarbon dated fossil record in the Edwards Plateau, Great Plains of Texas. In the Pleistocene, *S. hispidus* lived there with a diverse assemblage of megaherbivores, including mammoths, giant ground sloths, mastodons, camels, and multiple species of horses and pronghorn. Because today *Sigmodon hispidus* is generally most abundant in grass dominated habitats where it primarily consumes green grass stems (Kincaid and Cameron 1982, Randolph et al. 1991), we hypothesized its degree of niche specialization would lead to greater pressure from ecosystem changes at the late Quaternary.

Stable isotope analysis has become a common proxy for characterizing shifts in diet through space and time (Koch 2007), and can provide unique insights into foraging ecology on different time scales depending on the tissues analyzed (Martinez del Rio et al. 2009). Isotope analysis has been used in both paleontological and archaeological contexts to quantify ecological shifts, including the relative use of different plant functional types by consumers, trophic structure (e.g., food-chain length), and niche partitioning that are otherwise difficult to interpret using traditional paleontological approaches (Koch 2007, Koch et al. 2009). Here, we were fortunate that collagen was well-preserved in the fossil bones, allowing measurement of both $\delta^{13}C$ and $\delta^{15}N$ values for fossils spanning the late Pleistocene to Holocene transition.

Earlier studies suggested *Sigmodon hispidus* follows Bergmann's rule (Ashton et al. 2000, Meiri and Dayan 2003); thus, we hypothesized that increased Holocene temperatures likely led to decreased body size (Figure 2.1a, path C). Shifts in climate and in the composition of the herbivore community, however, may have had indirect effects through changes in vegetation composition and/or resource availability; these could have led to selection for larger or smaller body size (Figure 2.1a, paths AE, AG, DE, DG). Community reorganization might also have directly influenced competitive interactions for resources (Figure 2.1a, paths F, H). Because studies of modern megafauna suggest their absence leads to an increased resource base in smaller animals (Keesing 1998, Okullo et al. 2013), we suspected a similar expansion might have occurred in the terminal Pleistocene after the extinction of megafauna. Modern exclusion studies are limited temporal scope extending from years to decades (Owen-Smith 1998, Okullo et al. 2013) and it is not clear how the absence of megafauna influences vegetation over long time periods.

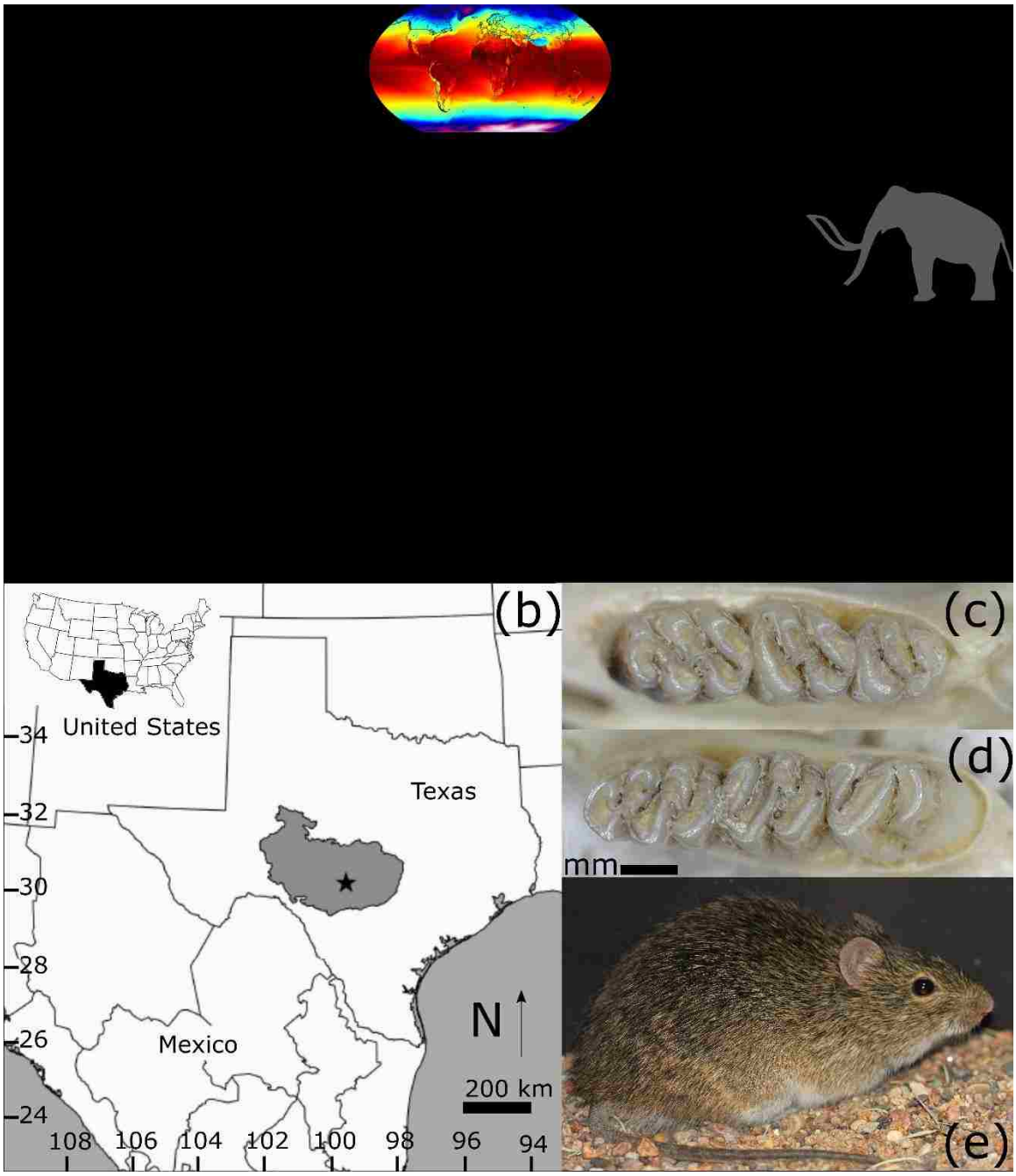

Figure 2.1. Conceptual diagram, site attributes and study organism. a) Conceptual diagram of potential abiotic and biotic interactions affecting *Sigmodon hispidus* populations at Hall's Cave over the past 16,000 years. Both extinct (grey) and extant (black) animals occur within the community. b) Location of Hall's Cave on the Edwards Plateau in Texas. c) Upper and d) lower tooth rows of *Sigmodon hispidus* at 50x magnification. e) Picture of *S. hispidus* (J.N. Stuart, https://www.flickr.com/photos/stuartwildlife/5727265600).

We note that our study is the first to characterize both population body size and dietary shifts for a single species in a single locality at such fine-grained level for ~16ka. While studies using *Neotoma* paleomiddens and sites such as Porcupine Cave or Lamar Cave have previously yielded insights into body size and biodiversity shifts with climate change at the species and/or community level (Smith et al. 1995, Smith and Betancourt 1998, 2003, Hadly 1996, Barnosky 2004), they have not combined these data with isotope-based analysis of diet shifts over time. The substantial amount of fossil material, and the robust and detailed age model provide a unique opportunity to reconstruct the ecology (diet and body size) of the vast majority of a mammalian community in a period marked by intense shifts in both biodiversity and climate.

Material and Methods

I. *Study Site and Data Sources*

A. *Site, Temporal Record, and Natural History*

Our study employs a high temporal resolution fossil record from the southwestern United States. Hall's Cave is located on the Edwards Plateau in Kerrville County, Texas (Figure 2.1b). Today, vegetation in the region consists mostly of savanna, shrub and woodland characterized by juniper, mesquite and oak, with both tall and short grasses (Toomey 1993, Joines 2011). Paleontological studies began in the 1960s and have continued to the present, with most excavations of specimens by Toomey and his colleagues (1993). The collection, including unprocessed bulk matrix is housed at the Vertebrate Paleontology Lab of the Texas Memorial Museum (TMM), University of Texas, Austin.

Hall's Cave has a uniquely well-resolved stratigraphic sequence dating back about 22,000 cal BP and a particularly abundant small- and medium-sized mammal record. Past excavations of the site have yielded thousands of mammal and other vertebrate animal specimens across a range of body sizes and trophic guilds, many of which have already been identified (Toomey 1993). Previous work from the site include reconstructions of both soil erosion (Cooke et al. 2003) and climate using faunal remains (Toomey 1993, Toomey et al. 1993, Joines 2011), magnetic susceptibility of the cave sediments (Ellwood and Gose 2006, Bourne et al. 2016), and the phytolith record of the cave (Joines 2011). Most recently, the community assemblage and species interactions of the Edwards Plateau were characterized across the past 22 thousand years (Smith et al. 2016b).

We developed an age model based on 62 radiocarbon dates of bone collagen from Hall's Cave (Appendix 2 Figure 1, Table 2). A linear regression of the calibrated radiocarbon ages (cal BP) and Stratigraphic Depth (cm) yielded a robust predictive equation ($Y = -14.57 + 0.015 X$; df=61, $P<0.001$, $R^2=0.934$). Because elements were originally collected in 5 to 15cm intervals, the midpoint of the stratigraphic depth was employed in the regression.

Sigmodon hispidus is a medium sized rodent (80-150g) that currently ranges across the southern United States and Mexico. It is a generalist primary consumer usually found in grass dominated habitats, where it supplements a primary diet of green grass stems of intermediate nutritive value with more nutritious dicot leaves and fruit (Martin 1986, Randolph et al. 1991). Cotton rats in Texas tend to occupy tall grass (i.e., cordgrass, bluestem, beardgrass) or shrub habitats, used both as protective cover and a food resource (Cameron and Spencer 1981, Kincaid and Cameron 1985, Schmidly and Bradley 2016). Interspecific interactions of *Sigmodon* with other Texas rodents include aggressive displacement of *Baiomys taylori*

(pygmy mouse) and competitive exclusion of *Reithrodontomys fulvescens* (harvest mouse) (Raun and Wilks 1964, Cameron 1977).

All *Sigmodon* have highly diagnostic 'S' shaped molars (Figure 2.1c & d) readily allowing discrimination from other rodents in the fossil matrix. Here, we follow Toomey (1993) and refer all material to *Sigmodon hispidus* based on geographic and elevational range attributes (Baker and Shump 1978, Cameron and Spencer 1981, Toomey 1993). In addition to specimens previously identified by Toomey (1993), we identified and accessioned 1030 additional individuals from either presorted elements or bulk materials from the fossil matrix. Our final dataset consisted of 1332 individual maxillary or mandibular first molars and jaw elements spanning the past 16,000 years.

Sigmodon materials are not uniformly present throughout time. *Sigmodon* were not present from 22-16ka cal BP and were comparatively rare from 16-12ka cal BP (50 specimens). *S. hispidus* became common in the early-Holocene (852 specimens), and decreased during the mid- (307 specimens) and late-Holocene (123). Thus, to maintain sufficient sample size we binned data into 14 temporal time intervals over the last 16,000 cal BP (Table 2.1) which were chosen to incorporate important climatic and faunal events whilst maintaining sufficient sample size. This allowed us to conduct population level analyses using the paleontological record.

Table 2.1: Summary by time level bin divisions. Age Range is the calendar years before present (1950 AD) comprising each interval. N Mass and N Isotopes show sample sizes for molar measurements and $\delta^{13}C$ or $\delta^{15}N$. Only $\delta^{15}N$ was found to change significantly over time (ANOVA $P<0.01$, df=13/306, details in results). Temperature and precipitation data from the CCSM3 (Lorenz et al. 2016a, 2016b) are averaged for each time bin. Sorenson to Modern represents similarity in community composition relative to the 0-1500 (cal BP) age range.

Age Range (cal BP)	N Mass	N Isotopes	Mean Mass (g) (± Std dev)	Maximum Mass (g)	Mean $\delta^{13}C$ (‰) (± Std dev)	Mean $\delta^{15}N$ (‰) (± Std dev)	Mean Temperature (°C) (± Std dev)	Mean Precipitation (mm) (± CV)	Species Richness	Sorenson to Modern
0 – 1500	14	12	100.5 ± 21.4	149.9	-15.8 ± 2.7	5.7 ± 1.4	18.7 ± 7.3	545.4 ± 0.4	34	1.00
1500 – 3100	18	22	109.1 ± 22.5	144.5	-16.5 ± 1.8	5.5 ± 0.8	18.7 ± 7.4	537.2 ± 0.4	36	0.89
3100 – 5400	13	15	96.1 ± 16	130.6	-15.7 ± 2.7	6.5 ± 1.1	18.6 ± 7.7	554.4 ± 0.4	35	0.81
5400 – 6100	13	21	89.8 ± 11.2	104.1	-14.9 ± 2.8	5.7 ± 0.8	18.6 ± 8.0	549.8 ± 0.4	31	0.77
6100 – 6400	13	26	99.5 ± 20.5	146.3	-14.9 ± 2.4	5.9 ± 0.7	18.7 ± 8.1	536.3 ± 0.4	32	0.79
6400 – 6700	19	9	95.9 ± 19.3	135.7	-15.7 ± 3.6	6 ± 0.4	18.7 ± 8.2	526.8 ± 0.4	33	0.78
6700 – 7700	16	21	89.5 ± 16.8	120.9	-15.2 ± 2.9	6.2 ± 0.9	18.5 ± 8.5	534.3 ± 0.4	33	0.78
7700 – 8400	25	21	96.3 ± 22.9	157.4	-13.5 ± 2.5	7.4 ± 1.4	18.4 ± 8.8	532.3 ± 0.4	36	0.71
8400 – 9000	34	29	90.8 ± 17.6	134.0	-14.7 ± 3.2	7.0 ± 1.3	18.3 ± 8.9	536.1 ± 0.4	35	0.70
9000 – 9400	15	13	96.6 ± 21.1	130.6	-15.0 ± 2.4	6.7 ± 0.8	18.4 ± 9.0	552.5 ± 0.3	35	0.70
9400 – 10000	26	16	89.9 ± 18.6	151.8	-14.5 ± 3.0	6.8 ± 1.4	18.3 ± 9.0	561.6 ± 0.3	39	0.69
10000 – 11000	45	23	94.6 ± 16.6	122.5	-15.6 ± 3.5	6.9 ± 1.1	17.7 ± 8.9	592.5 ± 0.3	35	0.67
11000 – 12700	7	7	100.1 ± 27.3	146.3	-14.1 ± 3.9	7.3 ± 0.8	16.9 ± 9.3	626.6 ± 0.3	53	0.62
12700 – 15800	12	31	96.5 ± 12.9	120.9	-14.5 ± 3.0	6.7 ± 1.0	15.5 ± 10.1	636.6 ± 0.4	74	0.52

B. *Community Data*

Data on community composition were extracted from a compilation by Smith et al (2016b) based largely on Toomey (1993) and the Neotoma Paleoecology Database (2015). Since 2016, updates in the understanding of the evolutionary history of horses in North America have led to the synonomization of two horse species (Winans 1989, Hay et al. 2010, Barron-Ortiz and Theodor 2011, Kefena et al. 2012), necessitating changes in our fossil identifications; ongoing fossil identifications of bulk matrix have also expanded the temporal duration of several species (e.g. *Baiomys taylori* and *Onychomys leucogaster*). Species were assigned to a trophic guild following Smith et al. (2016b). Using this revised species list, we re-calculated α-diversity (richness), β-diversity (Sorenson index) and percent of each trophic guild within the community for each time interval.

C. *Climatic Data*

We employed the Community Climate System Model (CCSM3) climate data. This unified dataset of climate simulations for North America extends to 21,000 cal BP in 500-year intervals (Lorenz et al. 2016a, b). The CCSM3 data have 0.5° spatial resolution such that we extracted data for the region surrounding Hall's Cave. Because the CCSM3 combines simulations and interpolates data for all of North America, it represents larger scale climatic events from the terminal Pleistocene onwards. Data obtained from the CCSM3 included mean daily maximum temperature, mean daily minimum temperature, and total monthly precipitation. These variables were extracted in 500-year intervals and averaged following the 14-age intervals used for the community data (Table 2.1).

II. *Analyses*

A. *Body Size*

Of the 1332 fossil *Sigmodon* elements, we obtained body size estimates for 399 using the length of the first upper or lower molar (UM1, LM1), which is a reliable indicator of mass (Damuth and MacFadden 1990) (Figure 2.1c & d); the remainder lacked a quantifiable M1. Measurements were taken using Mitutoyo Digital Calipers Series 500 under a Nikon 10x dissecting microscope. Each tooth was measured three times (~1200 measurements total); samples whose means yielded > 5% standard error were discarded. These were generally cracked or broken teeth and thus difficult to accurately measure.

Fossil elements employed in our work consisted of loose left or right mandibles and maxillae, generally with only partial toothrows. Because an individual could potentially be represented 4 times (ULM1, URM1, LLM1 and LRM1), we established a set of criteria to reduce duplicate individuals and calculated the minimum number of individuals (MNI). First, we quantified the amount of natural variation between left *versus* right, and upper *versus* lower molars in modern *Sigmodon hispidus.* Using a reference collection of museum specimens from the Museum of Southwestern Biology, we measured uppers and lowers and right and left molars for 20 individuals ranging in mass from 44 to 206g (Appendix 2 Table 3). We found that across the 20 specimens examined, modern animals were bilaterally symmetrical; there was less than a 1% difference between left and right molars. However, upper and lower molars varied; upper molars were on average 10% smaller than lower molars (Linear Model, $P<0.0001$, df=19, adjusted $r^2=0.68$, Appendix 2 Figure 2).

Because elements (LLM1s, LRM1s, ULM1s, and URM1s) were not uniformly found across stratigraphic levels (Appendix 2 Table 1), we employed the LM1 preferably; when

upper molar measurements were used, we standardized by adding 10% to the length. To mitigate the likelihood of a single individual being represented twice in a stratigraphic level, we only used a single element unless the standardized measurements were > 1% different in size from all other elements in that time bin. Thus, for each unique stratum, we selected the LLM1s and then all LRM1s whose lengths were at least 1% different from those LLM1s. Next, we compared the ULM1s to all LM1s, followed by the URM1s to all other molars already selected for that stratum. A difference > 1% was chosen because the variation between left and right molars of either upper or lower elements of modern individuals was below 1% (Appendix 2 Table 3).

Because measurements of first molars were taken on fully erupted molars, no juveniles were included. However, without full toothrows we could not fully assess the ontogenetical development of some animals. Thus, analyses were conducted both with and without putative subadults. Subadults were identified as animals whose estimated body size was lower than 1.5 standard deviations from the mean, as is commonly done in modern studies (Birney et al. 1975, Swihart and Slade 1984).

Our final data set included 270 animals after the removal of potential duplicates and subadults. Body size was computed for lower first molar lengths using the allometric equation (Martin 1990): Log mass (g) = 3.310*(Log M1 length) + 0.611 (r^2=0.96, %PE=15.58, df=32). We conducted a number of sensitivity analyses to examine the influence of our data manipulations; our analyses were robust regardless of methodology employed (Appendix 2).

B. *Stable Isotope Analysis*

We analyzed stable carbon ($\delta^{13}C$) and nitrogen ($\delta^{15}N$) isotopes from 319 *Sigmodon* maxillary and mandible bones to investigate potential shifts in diet. Carbon isotope values provide insight into what vegetation herbivores are consuming within a system (DeNiro and Epstein 1978). Global average $\delta^{13}C$ values for C_3 and C_4 plants are -26.5‰ and -12.5‰ (Bender 1971, Cerling et al. 1997), respectively, and previous studies have shown that these plant functional groups have similar isotope values in the Great Plains (Derner et al. 2006). $\delta^{13}C$ and $\delta^{15}N$ values of primary consumers like *Sigmodon* mirror that of their diet, but are positively offset due to physiologically mediated processes that discriminate again the light isotope (^{12}C or ^{14}N) during the nutrient assimilation and tissue synthesis; such offsets are often referred to as trophic discrimination factors and for consumer bone collagen are ~2-4‰ for both $\delta^{13}C$ and $\delta^{15}N$ (Koch 2007). Because carbon and nitrogen isotope values vary depending on relative consumption of C_3 and C_4 vegetation and trophic level, $\delta^{13}C$ versus $\delta^{15}N$ isotopic niche space can serve as a proxy for dietary niche space (Newsome et al. 2007). Given the relatively long isotopic incorporation rate for bone collagen (Hobson and Clark 1992, Koch et al. 2009), the short lifespan of most rodents, which ranges on average around 6 months to 1 year in wild *Sigmodon* (Rose and Salamone 2017), assures that isotope measurements represent diet integrated across most of an individual's lifetime.

We subsampled ~150-250 mg of bone from each fossil mandible/maxillary fragment using a low speed Dremel tool. Following sampling, we extracted the organic collagen matrix from the bone by demineralizing with 0.25N HCl at 3-4°C for 24-48 hours depending on initial sample density. Following demineralization, samples were lipid extracted via soaking in 2:1 chloroform/methanol for 72 hours, changing the solution every 24-hours. Samples were then

washed 5-7 times with distilled water and lyophilized. Approximately 0.9-1.0mg of each dried collagen sample was weighed on a microbalance and packaged into 0.35 mm tin capsules and submitted to the University of New Mexico Center for Stable Isotopes for analysis. $\delta^{13}C$ and $\delta^{15}N$ values of all samples were analyzed using a Costech elemental analyzer (Valencia, CA) interfaced with a Thermo Scientific Delta V Plus isotope ratio mass spectrometer (Bremen, Germany) at the University of New Mexico Center for Stable Isotopes (Albuquerque, NM). Isotope values are reported as δ values, where $\delta = 1000[(R_{sample}/R_{standard})-1]$ and R_{samp} and R_{std} are the $^{13}C:^{12}C$ or $^{15}N:^{14}N$ ratios of the sample and standard, respectively; units are in parts per thousand, or per mil (‰). The internationally accepted reference standards are Vienna Pee Dee Belemnite (VPDB) for carbon and atmospheric N_2 for nitrogen (Fry 2006, Sharp 2017). The standard deviation of organic references within a run was $\leq$0.2‰ for both $\delta^{13}C$ and $\delta^{15}N$ values. In addition, as a control for the quality of our ancient collagen samples, we measured [C]:[N] ratios. The theoretical weight percent [C]:[N] ratios of unaltered bone collagen falls between 2.8-3.5 (Ambrose 1990). Any samples with [C]:[N] ratios >3.5 we considered too diagenetically altered to provide reliable isotope data and were excluded from all analyses.

After removal of potential duplicates and subadults, our final dataset consisted of 384 animals. Of these 266 had isotopes, 270 had mass measurements and 152 had both (Table 2.1). These sample sizes allowed us to examine changes over time at the population level, largely unprecedented for a paleoecological study where sample size is almost always an issue.

C. *Statistics*

Analyses were conducted at two temporal scales using both parametric and non-parametric tests. The first set of analyses sorted body size and isotope data into pre- (12700-

15800 cal BP) versus post- (0-12700 cal BP) extinction bins to investigate the impact of the megafauna loss on *Sigmodon*. The second set of analyses were more finely resolved, and employed 14-time intervals over the last ~16,000 years (Table 2.1).

Sample sizes between the pre- and post-extinction intervals were uneven because *S. hispidus* was less abundant in the older strata. We analyzed body size and isotope variation in the two populations (pre- and post-) using the F-test and Levene's test for homogeneity of variances. Differences in the means and distributions were evaluated using a series of parametric and non-parametric tests to account for non-normal distributions of mass and $\delta^{13}C$ within the post-extinction time bin.

We determined changes in *Sigmodon's* mass and isotopic niche space using ANOVAs, Spearman's rank test, and Bayesian ellipse area models. Inconsistences in normal distributions across time bins led us to consider median, first quartile and maximum mass changes within the general population against diet and climate variables using linear models. Here, maximum mass is the mass of the largest individual within a time bin. Isotopic niche space was characterized using Bayesian based standard ellipse areas (SEA_B) of $\delta^{13}C$ and $\delta^{15}N$ using the SIBER based method in the R based SIAR package (Jackson et al. 2011, Parnell and Jackson 2013, R Core Team 2016). SEA_B were calculated using the posterior estimates for each group (here based on 10,000 draws), with ellipses plotted using 50% coverage in JMP Pro 13 (version 13.1) to show shifts in the isotopic niche space of *Sigmodon hispidus* through time. All statistical analyses were performed using R software version R.3.3.2 (R Core Team 2016) and RStudio 1.0.136 (RStudio Team 2016).

A state-space model was run to consider whether shifts in mass or diet seen in *Sigmodon* are driven more strongly by each other, by climatic variables (temperature or

precipitation) or community changes (α-diversity, β-diversity, or changes within the trophic guilds). A state-space model in its simplest form can be thought of as a linear model where each data point gets its own slope and dataset at each time bin. Here, each point has a state of known and unknown components and that state at time t+1 is a function of that point's state at time t. As such, points will be more similar the closer they are to each other in time. This allows for potential changes in the importance of independent variables on the response variable to be considered at each time bin in order to determine the magnitude of their overall influence. State-space models are therefore useful for data that have variation in the distribution of residuals and the potential for the non-independence of variables to change across a time series (Commandeur and Koopman 2007). State-space models have been employed in ecology to consider changes in population dynamics and biodiversity in a variety of vertebrates (Flowerdew et al. 2017, Leung et al. 2017, Rogers et al. 2017), as well as in economics (Harvey 1990, Kim and Nelson 1999, Durbin and Koopman 2001). We used a stochastic local level and slope model allowing the importance of each explanatory variable to vary at each time point, to account for the fact that each variable may be having larger or smaller effects on the response due to the range and grouping of data values within our time bins. For example, whether climatic variables or community variables are impacting a response in *S. hispidus* more or less may vary in response to a period of higher community turn-over (such as the megafauna extinction event) or greater fluxes in temperature and precipitation (e.g., the Younger-Dryas event).

We created separate models to analyze our mass and isotopic variables ($\delta^{13}C$ and $\delta^{15}N$). Our model consisted of a trend constant (μ), and an unknown regression weight (β) for each explanatory variable. A $\mu>0$ indicates a positive correlation to our response and a $\mu<0$ indicates

a negative correlation to our response. While β represents the relative strength of each explanatory variable on the response. If we consider our mass model for example, a $\mu>0$ corresponds to increasing body size, with the β of single explanatory variable giving the relative amount of increase associate with that variable. We ran each model a total of 4000 times, using a Markov Chain Monte Carlo (MCMC) algorithm with 4 chains and 1000 iterations each using the rstan package (Stan Development Team 2018) in the program R. Modelled values fall within the 50% uncertainty interval of the Bayesian framework, such that half of the 50% intervals (2000 of the total 4000 iterations) will contain values falling within the observed values of the data. Our variables and their associated β's are as follow: body size (BS, β_1), $\delta^{13}C$ (dC, β_2), $\delta^{15}N$ (dN, β_3), mean precipitation (mP, β_4), maximum temperature (mxT, β_5), minimum temperature (mnT, β_6), α-diversity (aDiv, β_7), β-diversity (bDiv, β_8), % browsers (perB, β_9), % carnivores (perC, β_{10}), % frugivores/granivores (perF, β_{11}), % grazers (perG, β_{12}), % insectivores (perI, β_{13}), % omnivores (perO, β_{14}). Model structures are given below with graphs of modelled to raw values for each model available in Appendix 2 (Figure 3, Table 6):

$$Y_{mass} = \mu_t + \beta_2(dC) + \beta_3(dN) + \beta_4(mP) + \beta_5(mxT) + \beta_6(mnT) + \beta_7(aDiv) + \beta_8(bDiv) + \beta_9(perB) + \beta_{10}(perC) + \beta_{11}(perF) + \beta_{12}(perG) + \beta_{13}(perI) + \beta_{14}(perO)$$

$$Y_{carbon} = \mu_t + \beta_1(BS) + \beta_3(dN) + \beta_4(mP) + \beta_5(mxT) + \beta_6(mnT) + \beta_7(aDiv) + \beta_8(bDiv) + \beta_9(perB) + \beta_{10}(perC) + \beta_{11}(perF) + \beta_{12}(perG) + \beta_{13}(perI) + \beta_{14}(perO)$$

$$Y_{nitrogen} = \mu_t + \beta_1(BS) + \beta_2(dC) + \beta_4(mP) + \beta_5(mxT) + \beta_6(mnT) + \beta_7(aDiv) + \beta_8(bDiv) + \beta_9(perB) + \beta_{10}(perC) + \beta_{11}(perF) + \beta_{12}(perG) + \beta_{13}(perI) + \beta_{14}(perO)$$

Results

Analyses of body mass for pre- and post-extinction time intervals (Figure 2.2a) showed no significant change in either variation (F test $P>0.1$, df=11/257; Levene test $P>0.1$, df=1/268) or distribution (Two sample t-test $P>0.1$, df=268; Wilcoxon rank sum test $P>0.1$) of body size. Furthermore, mass did not change significantly between individual time bins (ANOVA $P>0.1$ df = 13/368, Kruskal-Wallis rank sum test $P>0.1$, df=13). Mean mass ranged from approximately 90-110g. Maximum mass ranged between about 120-160g, with the largest individuals occurring 7.7-8.4ka (Table 2.1; Figure 2.2f).

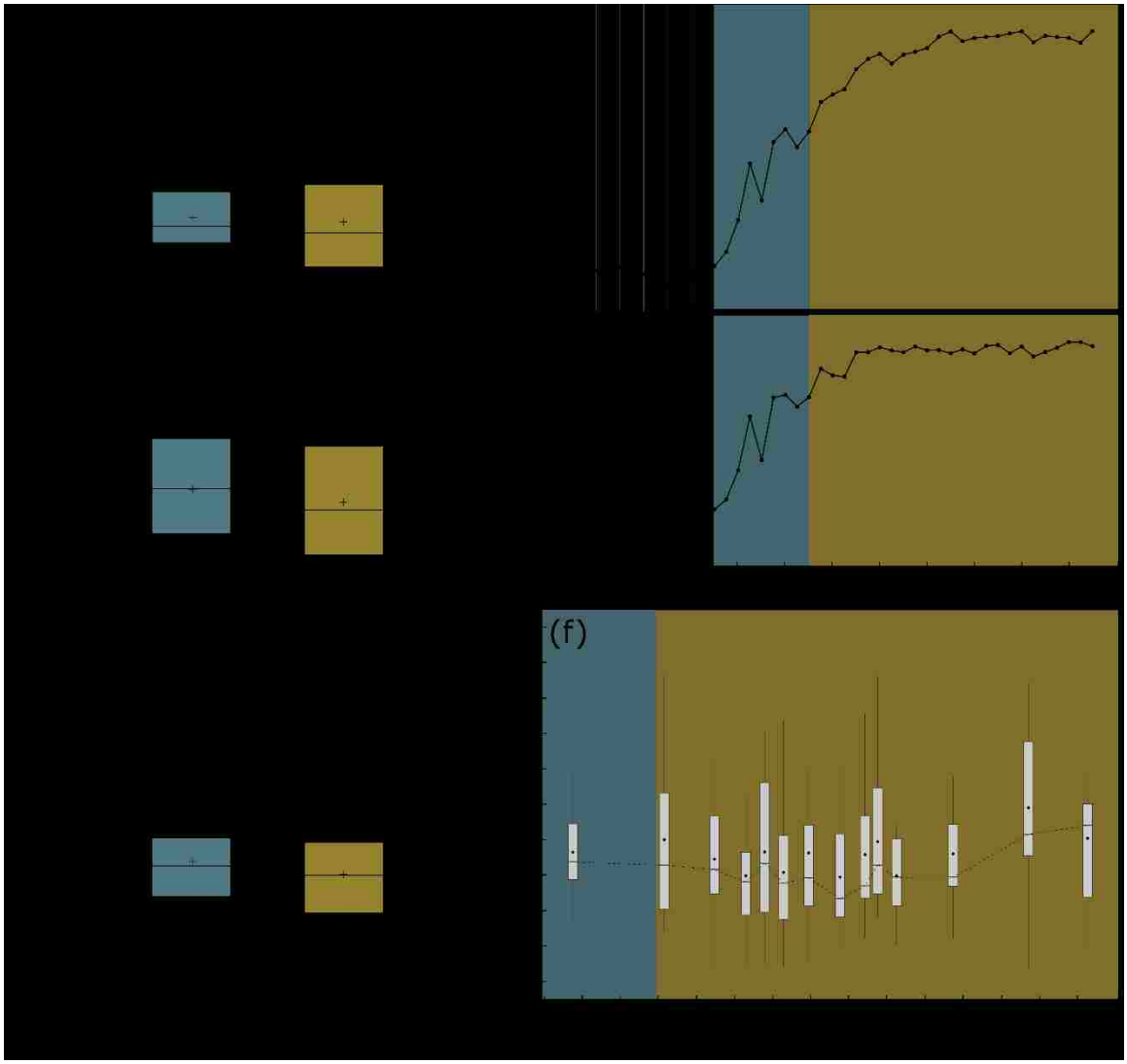

Figure 2.2. Changes in *Sigmodon hispidus* before and after the megafauna extinction, and in mass over the past 16ka. Boxplots representing median and interquartile ranges, with means marked by + for a) Mass, b) $\delta^{13}C$ and c) $\delta^{15}N$ distributions of the cotton rat. Pre- and post-extinction intervals are between 12700-15800 cal BP and 0-12700 cal BP, respectively. Changes in d) maximum and e) minimum temperature (^{o}C) across the past 23 thousand years for the Hall's Cave community. *Sigmodon* appears in the Hall's Cave fossil record at ~16ka (blue) and become abundant in the record at ~12ka (yellow). Temperature data from the CCSM3 (Lorenz et al. 2016a, 2016b) is downloaded at 500-year intervals. Changes in f) body size are plotted as medians (connected lines), means (diamonds) and interquartile ranges.

No significant differences were found in the variation (F test $P>0.1$, df=30/234; Levene test $P>0.1$, df=1/264) or distribution (Two sample t-test $P>0.1$, df=264; Wilcoxon rank sum test $P>0.1$) of *Sigmodon* $\delta^{13}C$ or $\delta^{15}N$ values from before and after the extinction event (Figure 2.2b & c). Mean $\delta^{13}C$ and $\delta^{15}N$ values and associated standard deviations for each time interval are reported in Table 2.1 and Figure 2.3. Mean $\delta^{13}C$ values did not significantly change across individual time bins (ANOVA $P>0.1$, df=13/306, Kruskal-Wallis rank sum test $P>0.1$, df=13), but $\delta^{15}N$ values significantly decreased (ANOVA $P<0.01$, df=13/306, Kruskal-Wallis rank sum test $P<0.01$, df=13, Appendix 2 Table 4 for details). $\delta^{13}C$ and $\delta^{15}N$ values were positively and significantly correlated across several time intervals (Figure 2.3, Appendix 2 Table 5). Bayesian standard ellipse areas showed a trend for a slightly expanded isotopic niche space from about 7700 to 15800 cal BP, with the exception of the most modern time interval (~0-1500 cal BP), and ranged from about 4.7 to 11.1‰[2] (Figure 2.3).

Results from our state-space model (Table 2.2) reflect the slight increase in mass from the oldest (12700-15800 cal BP) to the most recent (0-1500 cal BP) time interval (Table 2.1, Figure 2.2f). Higher $\delta^{13}C$, $\delta^{15}N$ values and maximum temperature corresponded to larger body size ($\beta_2 = 1.7$, $\beta_3 = 1.0$, $\beta_5 = 0.9$; ~30%, ~17% and 16%, respectively, of positive β values for mass, Table 2.2). Minimum temperature and the proportion of omnivores in the community also were also associated with increasing body size, but to a smaller degree ($\beta_6 = 0.6$, $\beta_{14} = 0.7$, about 11% and 12%, respectively). Overall, community variables were associated with decreased body mass, with the percent of grazers having the largest impact ($\beta_{12} = -0.9$, ~41% of total negative β values for mass), followed by the percent of insectivores ($\beta_{13} = -0.6$, ~25%), percent browsers ($\beta_{12} = -0.4$, ~19%), and α-diversity ($\beta_{12} = -0.3$, ~14%).

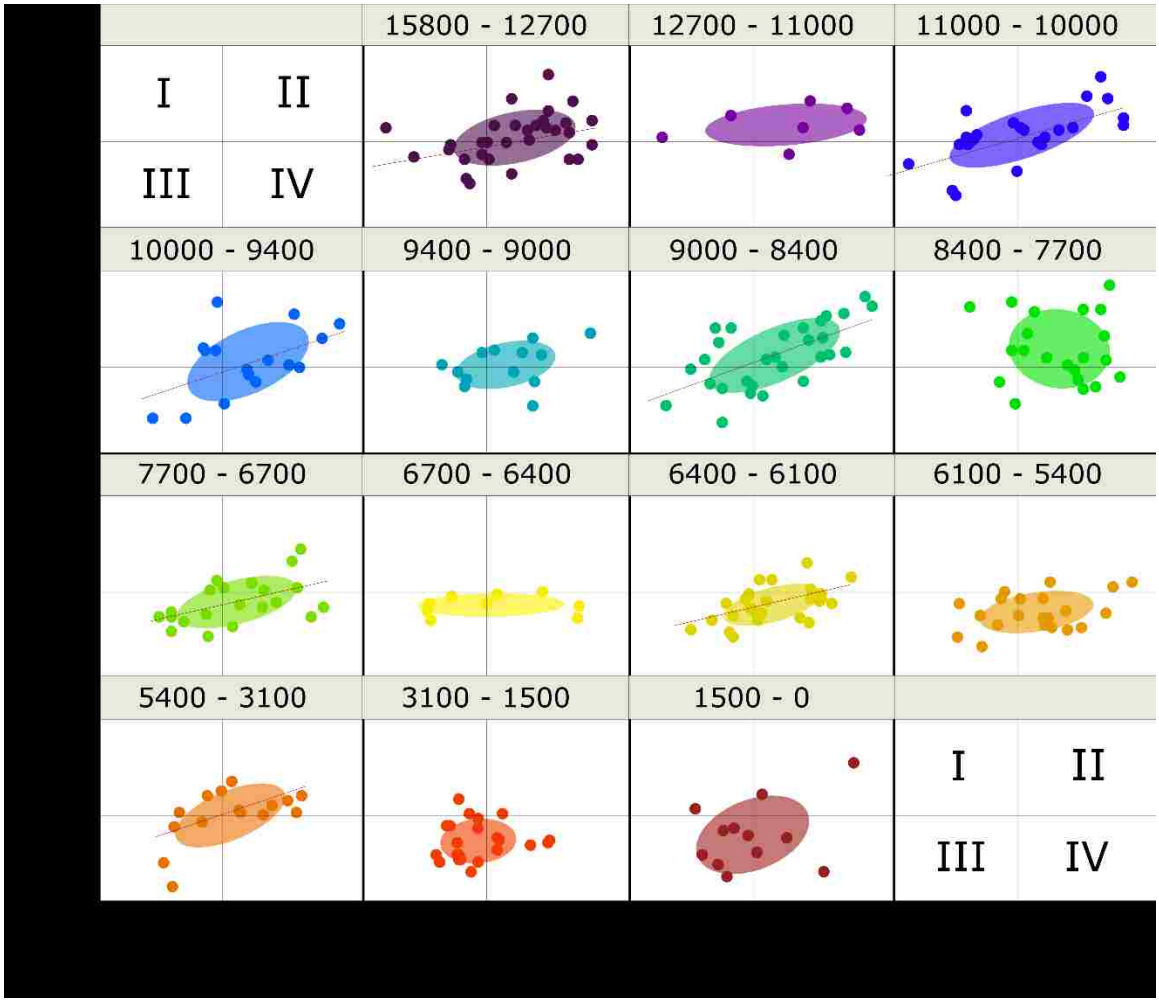

Figure 2.3. Isotopic niche space of *Sigmodon hispidus* over time. Standard ellipse areas (SEAs) representing where *Sigmodon* populations lie in $\delta^{13}C$ and $\delta^{15}N$ space with 50% coverage of data. Cross (+) within each panel divides isotopic space into 4 quadrants (I-IV) to help illustrate movement in SEAs over time, with the lines intersecting at $\delta^{13}C$ = -16‰ and $\delta^{15}N$ = 6.5‰. Red lines indicate a significant relation between $\delta^{13}C$ and $\delta^{15}N$ (Linear Fit P<0.05, see Appendix 2 Table 5 for details).

Sigmodon hispidus bone collagen $\delta^{13}C$ values were most positively associated with $\delta^{15}N$ (β_3 = 1.2 of total 2.9 positive influence on $\delta^{13}C$, or about 40%), in agreement with the correlation of higher $\delta^{13}C$ values with higher $\delta^{15}N$ reported above. $\delta^{13}C$ become more negative (shift towards C_3 vegetation), occupying less area in quadrants I and IV (Figure 2.3) from 6700-7700 cal BP onwards. This overlaps with the decrease in $\delta^{15}N$, as seen by a shift in the standard

ellipse areas into quadrant III and IV (Figure 2.3). Higher $\delta^{13}C$ in *Sigmodon* were also associated with increases in both the proportion of granivores and grazers in the community (β_{11} = 0.5 and β_{12} = 0.5, ~17% each), followed by β-diversity

Table 2.2: Regression weight (β) values as given for each explanatory variable by the 3 state-space model outputs for mass (Y_{mass}), $\delta^{13}C$ (Y_{carbon}) and $\delta^{15}N$ ($Y_{nitrogen}$). Values in bold have 15% or more of relative positive or negative influence on explanatory variable.

		Y_{mass}	Y_{carbon}	$Y_{nitrogen}$
Main Variables				
body size	β_1	~	0.0	0.0
$\delta^{13}C$	β_2	**1.7**	~	0.2
$\delta^{15}N$	β_3	**1.0**	**1.2**	~
Climate Variables				
mean precipitation	β_4	0.0	0.0	0.0
maximum temperature	β_5	**0.9**	-0.1	**-0.8**
minimum temperature	β_6	0.6	0.2	**0.6**
Community Variables				
α-diversity	β_7	-0.3	**-0.3**	0.0
β-diversity	β_8	0.1	0.4	**-0.6**
% browsers	β_9	**-0.4**	0.2	0.0
% carnivores	β_{10}	0.3	-0.2	0.0
% frugivores/granivores	β_{11}	0.4	**0.5**	**-0.4**
% grazers	β_{12}	**-0.9**	**0.5**	-0.1
% insectivores	β_{13}	**-0.6**	**-0.8**	**0.3**
% omnivores	β_{14}	0.7	**-0.3**	**0.2**

(β_{13} = 0.4, ~12%, Table 2.2). Lower $\delta^{13}C$ values were associated to a greater proportion of insectivores in the community (β_{13} = -0.8 of total 1.8 negative β values for $\delta^{13}C$, or about 46%), suggesting lower $\delta^{13}C$ values indicative of greater use of C_3 resources when more mammalian insectivores are on the landscape (Table 2.2). Lower $\delta^{13}C$ values in *Sigmodon* were also

associated with α-diversity (β_{12} = -0.3, ~18%) and the percent of omnivores in the mammalian community (β_{14} = -0.3, ~18%).

Sigmodon hispidus bone collagen $\delta^{15}N$ values were negatively correlated with maximum temperature (β_5 = -0.8 of total 1.9 negative β values for $\delta^{15}N$, or ~41%), β-diversity (β_{13} = -0.6, ~34%) and the proportion of granivores present in the mammalian community (β_{11} = -0.4, ~19%, Table 2.2). Higher $\delta^{15}N$ values in *Sigmodon* were associated with minimum temperature (β_6 = 0.6 of overall 1.4 positive β values for $\delta^{15}N$, or about 47%), and the proportion of insectivores and omnivores in the community (β_{13} = 0.3 and β_{13} = 0.2, about 21% and 18%, respectively). Overall, our results suggest that *S. hispidus* is being influenced by both climatic and community variables over time, likely through a combination of direct and indirect effects, but that the combination of these effects is not driving a strong shift in body size and/or diet.

Discussion

The combination of climate change and biodiversity loss at the terminal Pleistocene did influence the ecology of *Sigmodon hispidus* in the Edwards Plateau ecosystem. *Sigmodon* were not present in the Hall's Cave record from ~22–16 ka, likely because temperatures in the region were too low. *Sigmodon* remained relatively rare until ~12 ka when rising temperatures at the end of the Pleistocene (Figure 2.2d & e) allowed the species to expand its range northward (Dunaway and Kaye 1961, Fleharty et al. 1972, Cameron and Spencer 1981, Slade et al. 1984, Sauer 1985, Graham et al. 1996, Eifler and Slade 1998). While the late Pleistocene megafaunal extinction did not mark a simple binary shift in *Sigmodon* body size and diet,

changes due to the community restructuring that occurred throughout the Holocene as a consequence of the extinction (Smith et al. 2016b) had varying effects on *Sigmodon's* ecology.

We find substantial variation in both body mass and the isotopic niche space of *Sigmodon* at Hall's Cave over time. Overall, body mass fluctuated by more than 20% over the past 16ka, with substantial variation over time (SD: 11.2-27.3 g, Table 1.1, Figure 2.2f). By far the most important factor influencing body mass was diet. Relative consumption of more C_4 resources led to larger body mass (Table 2.2, Figure 2.4a, path I); $\delta^{13}C$ values were two times more important than any other climatic or community variable in our state space model (Table 2.2, Figure 2.4a). Interestingly, warmer temperatures had a positive influence on mass (Table 2.2, Figure 2.4a, path C) contrary to our expectation based on Bergmann's rule. This suggests that body size changes are more strongly influenced by shifts in available resources than by temperature directly.

Larger body size in *Sigmodon* may have provided access to different resources due to varying metabolic rate or digestive abilities (McNab 1980, Hammond and Wunder 1991, Nagy 2005). Greater consumption of lower quality resources, such as grasses, require larger and/or more complex digestive systems (i.e. greater gut capacity) to account for the faster food passage rates of rodents (Batzli and Cole 1979, Gross et al. 1985, Justice and Smith 1992, Veloso and Bozinovic 1993, Smith 1995b). Thus, larger body size in *Sigmodon* may be associated with a higher consumption of C_4 grass on the Edwards Plateau. Moreover, larger body size may provide *Sigmodon* with a compeitive advantage within the community (Martin 1986, Glass and Slade 1980, Kincaid and Cameron 1982), while alternatively smaller body size and increased numbers of

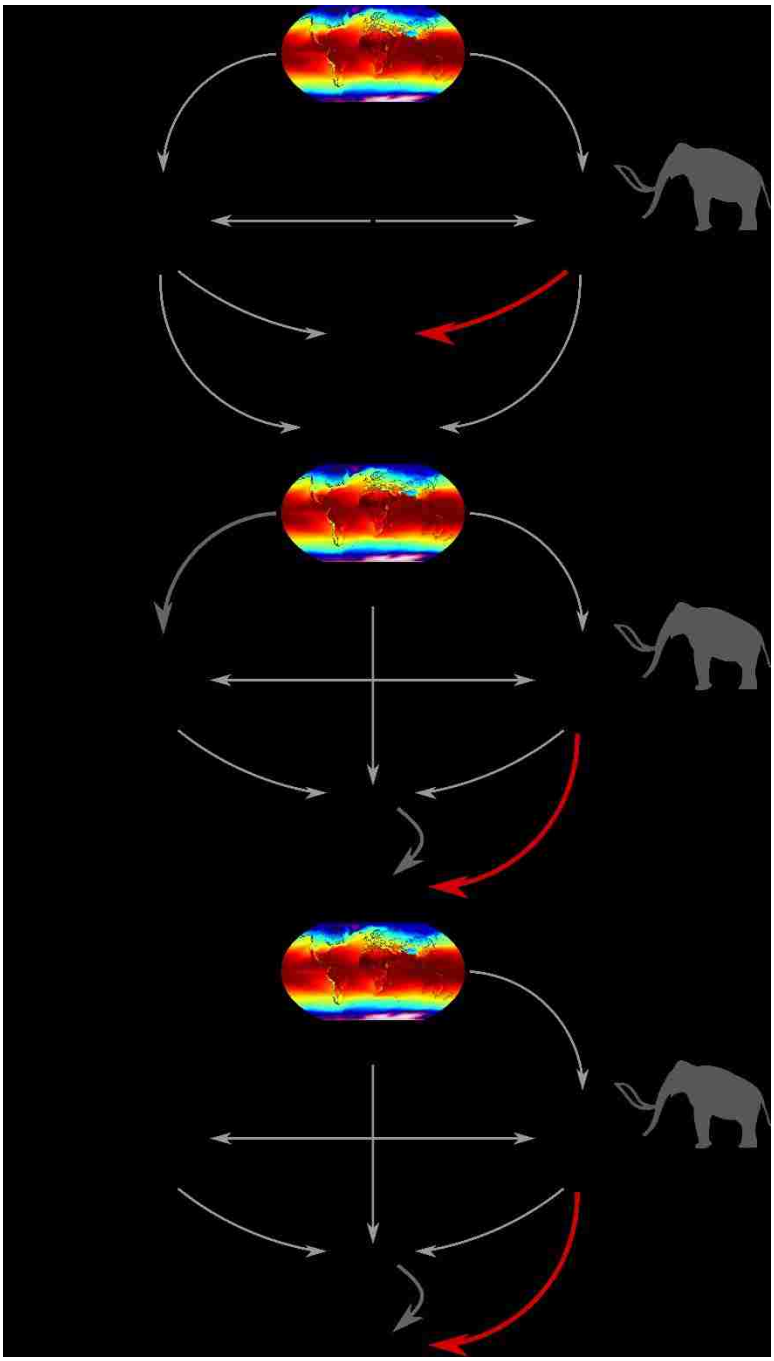

Figure 2.4. Associations of explanatory variables on body size and diet. General representation of explanatory variables on a) body size, b) $\delta^{13}C$, and c) $\delta^{15}N$. Arrows represent positive (black) or negative (red) influences, with line thickness representing the relative strength.

grazer, insectivore, and browser species (Table 2.2) may then have led to changes in the resources available to *S. hispidus* due to competition.

The influence of diet on changes in body size may have been associated with changes in resource availablility. *Sigmodon* showed variation in both $\delta^{13}C$ (SD: 1.8-3.9‰) and to a lesser extent $\delta^{15}N$ (SD: 0.4 to 1.4‰) values (Table 1.1, Figure 2.3) across time. Modern *Sigmodon* are highly selective of grass habitats, and grasses can account for ~80% of their diet, but this species consumes higher quality dicots when they are abundant (Petersen 1973, Kincaid & Cameron 1982, Kincaid et al. 1983, Randolph et al. 1991, Cameron and Eshelman 1996). The observed variation in $\delta^{13}C$ values suggest that *Sigmodon* is a generalist (Figure 2.3), with shifts potentially reflecting changes in the abundance of C_3 versus C_4 resources (Figure 2.4a, path GI) and expansion and/or contraction of its preferred grassland habitat over time (Figure 2.4a, path E). For example, the majority of individuals at 7700-8400 cal BP were within quadrants II and IV (Figure 2.3), and had $\delta^{13}C$ values higher than -13‰ suggesting that C_4 resources dominated their diet. In contrast, the diet of most individuals at 1500-3100 cal BP had $\delta^{13}C$ values lower than -16‰, corresponding to a diet dominated by C_3 resources after accounting for trophic discrimination. Pollen records from the region show a shift in the vegetation of the Edwards Plateau from a more mesic deciduous/coniferous forest during the Post Glacial period to a grassland and oak savanna landscape in the Holocene (Bryant and Holloway 1985, Toomey et al. 1993). Prior to ~12,000 cal BP, most grasses were C_3, but beginning ~11,000 cal BP C_4 grasses become dominant and have remained so (Cordova and Johnson 2019). Interestingly, we do not see greater use of C_3 by *Sigmodon* prior to 11,000 cal BP, suggesting that cotton rats were already foraging on C_4 grasses despite their relative scarceness on the landscape (Figure 2.3). The period from

2,500-5,700 cal BP is marked by fluctuations in the mesic and xeric vegetation on the Edwards Plateau, and higher levels of C_3 grasses around Hall's Cave (Bryant and Holloway 1985, Toomey et al. 1993, Cordova and Johnson 2019). Here, we do observe a decrease in the use of C_4 resources by *Sigmodon*, which may suggest that they are making use of the higher amount of C_3 grasses available (Appendix 2 Figure 4).These observed shifts in *Sigmodon* diet were likely the result of vegetation change across the Holocene due to shifting climate (Nordt et al. 1994, Fox and Koch 2003, Cotton et al. 2016).

As habitat and resources changed over 16ka, competitive interactions with other mammals may have caused *Sigmodon* to adapt to new life history strategies. Changes in vegetation composition and resource availability resulting from the removal of large-bodied herbivores can lead to shifts in the abundance of small mammals, which in turn may affect predator presence, small mammal biodiversity, and associated intraguild competition (Owen-Smith 1988, Keesing 1998, McCauley et al. 2006, Okullo et al. 2013). The influence of community changes on both the body size (Figure 2.4a, path F) and diet of *Sigmodon* (Table 2.2, Figure 2.4b & c, path H) suggests that post-extinction shifts in both resource availability and biotic interactions influenced *Sigmodon's* ecology. Specifically, a higher percentage of grazers and granivores in the herbivore community after the extinction, which are expected to have fallen within quadrants IV and III in isotopic space respectively (Figure 2.3), were associated with higher consumption of C_4 grasses by *Sigmodon*. While a greater proportion of grazers may have resulted in increased competition within quadrant IV, these results likely reflect the importance megaherbivores, 67% of which were grazers (Smith et al. 2016b), played in the ecosystem before the extinction. The presence of large-bodied herbivores can help maintain grassland ecosystems, reduce woody encroachment and maintain grass species

diversity (Laws et al. 1975, Owen-Smith 1988, Bakker et al. 2006, Asner et al. 2009, Smith et al. 2016a). As such, the increased proportion of C_4 grasses in *Sigmodon's* diet when existing in a community with more grazers could have been due to an increased production or diversity of grasses in the region (Figure 2.4a, path DE). In contrast, granivores forage primarily on C_3 resources (Dammhahn et al. 2013, Galetti et al. 2016), and thus a higher proportion of granivores in the system likely increased competition for resources in quadrant III and may have pushed *Sigmodon* into quadrant IV where it utilizes a higher amount of C_4 vegetation (Figure 2.3).

Dietary shifts may have corresponded not only to vegetation changes, but could have been related to increased omnivory as modern *Sigmodon* populations are known to opportunistically consume insects, though consumption of this resource is generally limited to <5% of diet composition (Kincaid and Cameron 1982, Schetter et al. 1998). The significant decrease in $\delta^{15}N$ values over time could be due to either a decrease in trophic level or a baseline shift in plant nitrogen isotope values in response to changing environmental conditions (DeNiro and Epstein 1981, Amundson et al. 2003). Plant $\delta^{15}N$ varies in relation to the source(s) of inorganic nitrogen, the physiological mechanism used to uptake nitrogen, and environmental conditions (precipitation and temperature) that influence soil $\delta^{15}N$ values via a variety of microbially mediated processes like (de)nitrification and nitrogen fixation (Peterson and Fry 1987, Dawson et al. 2002, Amundson et al. 2003, Murphy and Bowman 2006). In general, plants in environments with lower precipitation and higher temperatures tend to have higher $\delta^{15}N$ values relative to more mesic environments (Ambrose 1991, Austin and Vitousek 1998, Amundson et al. 2003). Our state space model, however, does not find evidence for a correlation between *Sigmodon* $\delta^{15}N$ and precipitation,

and $\delta^{15}N$ values actually show a negative relation with increasing maximum temperature in the region (Table 2.2). Thus, further investigation is required to determine whether the observed shifts in $\delta^{15}N$ of *Sigmodon* are driven by shifts in trophic level versus baseline nitrogen isotope composition of plants, such as a comparison of bone collagen $\delta^{15}N$ values among taxa that have similar functional roles (e.g., herbivores) from the Hall's Cave site, or the analysis of $\delta^{15}N$ values in individual amino acids (Schwartz-Narbonne et al. 2015).

A shift in trophic level would suggest that *Sigmodon* competed with different species for resources over time. A higher proportion of insectivores in the mammalian community is associated with lower $\delta^{13}C$ values in *Sigmodon* (Table 2.2), or a decreasing proportion of C_4 in *Sigmodon's* diet. Insectivores in the southern Plains are expected to occupy quadrant II (Fig 3), with higher $\delta^{15}N$ values reflecting higher trophic level, and relatively high $\delta^{13}C$ values corresponding to C_4-based insect herbivores, e.g., grasshoppers, which are one of the most abundant insects in grassland and savannah environments on the Edwards Plateau (DeVisser et al. 2008, Bergstrom 2013). Thus, the negative relationship between *Sigmodon* $\delta^{13}C$ values and the proportion of insectivores in the community may represent competitive exclusion from quadrant II into quadrant III (towards C_3 resources) or quadrant IV (towards a lower trophic level) (Figure 2.3). The significant positive correlations between $\delta^{13}C$ and $\delta^{15}N$ values observed in some time intervals (Figure 2.3, Appendix 2 Table 4) could have resulted from *Sigmodon* consuming more insects, essentially filling the niche of an omnivore or insectivore in quadrant II when fewer insectivorous mammals are present in the community. While the relatively low variation in $\delta^{15}N$ (Table 2.2) suggests *Sigmodon* was primarily herbivorous, its presence in both quadrants II and IV in some time intervals may be the result of shifts in trophic level. Furthermore, the combined interactions of body mass and diet with shifting climate and

community structure suggest tradeoffs in *Sigmodon* to cope with environmental and ecological changes across this time span.

Overall, *Sigmodon* responded to a combination of direct and indirect effects of both climate and mammalian community changes through the Holocene, with no single variable driving a dramatic change in cotton rat morphology or ecology. The influence of mammalian community composition on both mass and diet may suggest a strong effect of the megafauna extinction as which led to a large-scale restructuring of the mammalian community in this region (Smith et al. 2016b). Variation in $\delta^{13}C$ and $\delta^{15}N$ values associated with shifts in C_3 versus C_4 resource use and trophic level, were likely shaped by intraguild competition and changes in vegetation composition that occurred with changing climate conditions and/or the loss of the large herbivores during the extinction (Owen-Smith 1988, Keesing 1998, Okullo et al. 2013). Because climate and community composition were changing together during this period, there may have been tension between potential drivers that result in contrasting effects on *Sigmodon* populations (Blois et al. 2013). The overall stability we see in the body size and diet of *Sigmodon* suggests a high level of adaptability to community and ecosystem restructuring.

Understanding the response of *Sigmodon* to the late Pleistocene megafauna extinction in North America provides useful insights into the potential responses of small mammals to changes in community structure and ongoing environmental perturbations. The current rate of climate change has led to rapidly rising temperatures over the past 100 years (IPCC 2014) with continued warming and anthropogenic pressures predicted to have increasing effects on fauna globally (Barnosky et al. 2003). Studies have already shown distribution shifts (Parmesan and Yohe 2003, Moritz et al. 2008) and local extirpations (Munday 2004) across many plant and

animal taxa. Work towards conserving biodiversity across the world highlights the importance of the conservation not of a single species but of entire assemblages (Grayson 2007). In the wake of the modern loss in biodiversity, specifically large-bodied species, a combination of ancient and modern studies of generalist species such as *Sigmodon hispidus* may provide a better understanding of the consequences of species removals and provide some insights into how future communities may respond to a combination of abiotic and biotic factors.

Chapter 3

The sensitivity of *Neotoma* to climate change and biodiversity loss over the late Quaternary

Catalina P. Tomé[1], S. Kathleen Lyons[2], Thomas W. Stafford Jr. [3], Seth D. Newsome[1], and Felisa A. Smith[1]

[1]Department of Biology, University of New Mexico, Albuquerque, NM
[2]School of Biological Sciences, University of Nebraska-Lincoln, Lincoln, NE
[3]Stafford Research, 200 Acadia Avenue, Lafayette, CO

Abstract

The late Quaternary was at time of considerable environmental change in North America. Not only was climate highly variable, but the megafaunal extinction at the terminal Pleistocene led to considerable loss of biodiversity. These combined perturbations likely had cascading effects across communities and ecosystems in North America. Here, we focus on a highly-detailed fossil record of the Edwards Plateau in central Texas and consider the response of *Neotoma*, a genus of herbivorous rodents, to biodiversity loss and climate change over the late Quaternary. Specifically, we characterize changes in *Neotoma* body mass and diet using digital measurements of fossil teeth and stable isotope analyses of carbon and nitrogen extracted from bone collagen over 15-time intervals spanning the past 20,000 years. The large number of fossils available for each temporal bin allow us to conduct paleoecological analyses at the population level, which is unique for the fossil record. Overall, we find body mass in *Neotoma* to be significantly correlated to both temperature and biodiversity loss: not only did rising temperature select for lower average population body mass, but mass was significantly

and negatively correlated to turnover independently from the effect of temperature. Moreover, while *Neotoma* diet in the Pleistocene was primarily sourced from C_3 resources, it became progressively more C_3-C_4/CAM through the Holocene. The combination of decreasing population body size and higher C_4/CAM consumption was associated with the regional transition from a mesic forest to a xeric savanna grassland, likely driven by both climate change and the lack of large-bodied mammals in the landscape. Our results may also demonstrate changes in the relative abundance of different woodrat species with different climatic and dietary preferences.

Introduction

The terminal Pleistocene (20-11.7 ka cal BP) encompassed a period of substantial restructuring of North American terrestrial ecosystems, linked to the combined effects of changing climate and substantial biodiversity loss. As glaciers retreated to the north after the last glacial maximum at 21 ka cal BP, climate warmed by ~8^{o}C overall, although this warming was interrupted by numerous temperature reversals (Cole and Arundel 2005, IPCC 2014). The most notable of these was the Younger Dryas (12.8-11.5 ka cal BP), a long period of cooling to near glacial conditions, which ended in a particularly abrupt and rapid 5–7^{o}C increase in temperature that occurred within decades (Dansgaard 1989, Alley 2000). These environmental fluctuations influenced the composition and distribution of flora and fauna across North America (Prentice et al. 1991, Graham et al. 1996, Grayson 2000, Lyons 2003, 2005, Blois et al. 2010, Cotton et al. 2016).

The terminal Pleistocene was further punctuated by the loss of virtually all large-bodied mammals from the continent and led to the loss of >150 large-bodied mammals in the

Americas (Martin 1967, Martin and Klein 1989, Martin and Steadman 1999, Lyons et al. 2004). Highly size-selective, this event saw the loss of all mammals weighing >600 kg, including a diverse group of megafauna such as mammoths, mastodons, horses, lions, camels and giant ground sloths (Lyons et al. 2004, Smith et al. 2018). Large-bodied mammals have substantial impacts within modern communities and ecosystems, both through environmental engineering and species interactions (Owen-Smith 1992, Ripple et al. 2015, Mahli et al. 2016, Smith et al. 2016a). For example, extant megaherbivores in Africa help maintain savanna and grassland habitats by suppressing woody growth, modifying fire regimes, and acting as seed dispersers for plants (Owen-Smith 1992, Dublin et al. 1990, Goheen et al. 2010, 2018). Exclusion of these large-bodied mammals can result in shifts in vegetation composition and abundance and alter distribution, abundance, and competition of other mammals such as rodents (Keesing 1998, Goheen et al. 2004, 2018, Parsons et al. 2013, Keesing and Young 2014, Koerner et al. 2014, Galetti et al. 2015). In the Pleistocene, the megafauna are thought to have played a key role in maintaining open habitats and higher species diversity, repressing fire regimes and increasing nutrient availability across ecosystems (Johnson 2009, Rule et al. 2012, Doughty et al. 2013, Ripple et al. 2015, Bakker et al. 2016). In addition to structural changes in vegetation, the extinction likely had cascading effects on community structure and interactions of the surviving mammals (Smith et al. 2016b).

How these wholesale changes in community dynamics and climate influenced surviving species likely depended on whether species were more sensitive to abiotic or biotic interactions. Changes in environmental temperature often lead to shifts in body size and/or diet, either as a direct consequence of thermal physiology or due to shifting vegetation

(Bergmann 1847, Brown, 1968, Andrewartha and Birch 1984, Brown and Heske 1990, Smith et al. 1995, Ashton et al. 2000, Stenseth et al. 2002, Walsh et al. 2016, Millien et al. 2006). Because body size scales with most life history traits and physiological processes including metabolism, ingestion, and thermal regulation (McNab 1980, Peters 1983, Justice and Smith 1992, Smith 1995), size can influence the types and amounts of resources available to consumers, as well inter- and intraspecies interactions among consumers (Damuth 1981, Peters 1983). At a local scale, enhanced competition for habitat and resources will decrease the abundance of species that share similar size and dietary preferences (Brown 1973, M'Closkey 1976, Bowers and Brown 1982, Brown and Nicoletto 1991, Auffray et al. 2009). The relationship between body size and other ecological factors (such as home range or competition), particularly when combined with dietary and environmental information, can then help inform complex ecosystem and community changes recorded in the paleontological record (Damuth 1981).

Here we characterize the response of *Neotoma* (woodrat) to the environmental and community perturbations within the Edwards Plateau (Texas) (Figure 3.1A-B) over the past ~22,000 years. We quantify shifts in body size and diet using digital imaging of fossil molars and stable isotope analysis of associated bone collagen. We focus on a complex of three potential *Neotoma* species: *N. albigula* (white-throated woodrat), *N. floridana* (Eastern woodrat) and *N. micropus* (Southern Plains woodrat), which differ in body size and dietary preferences. All species of *Neotoma* are folivorous and construct large, obvious houses or dens. Dens are typically built within rock crevices and provide woodrats with protection from both predators and extreme temperatures (Finley 1958, Brown 1968, Brown et al. 1972, Smith 1995, Murray and Smith 2012). Past studies of *Neotoma* suggest all species within the

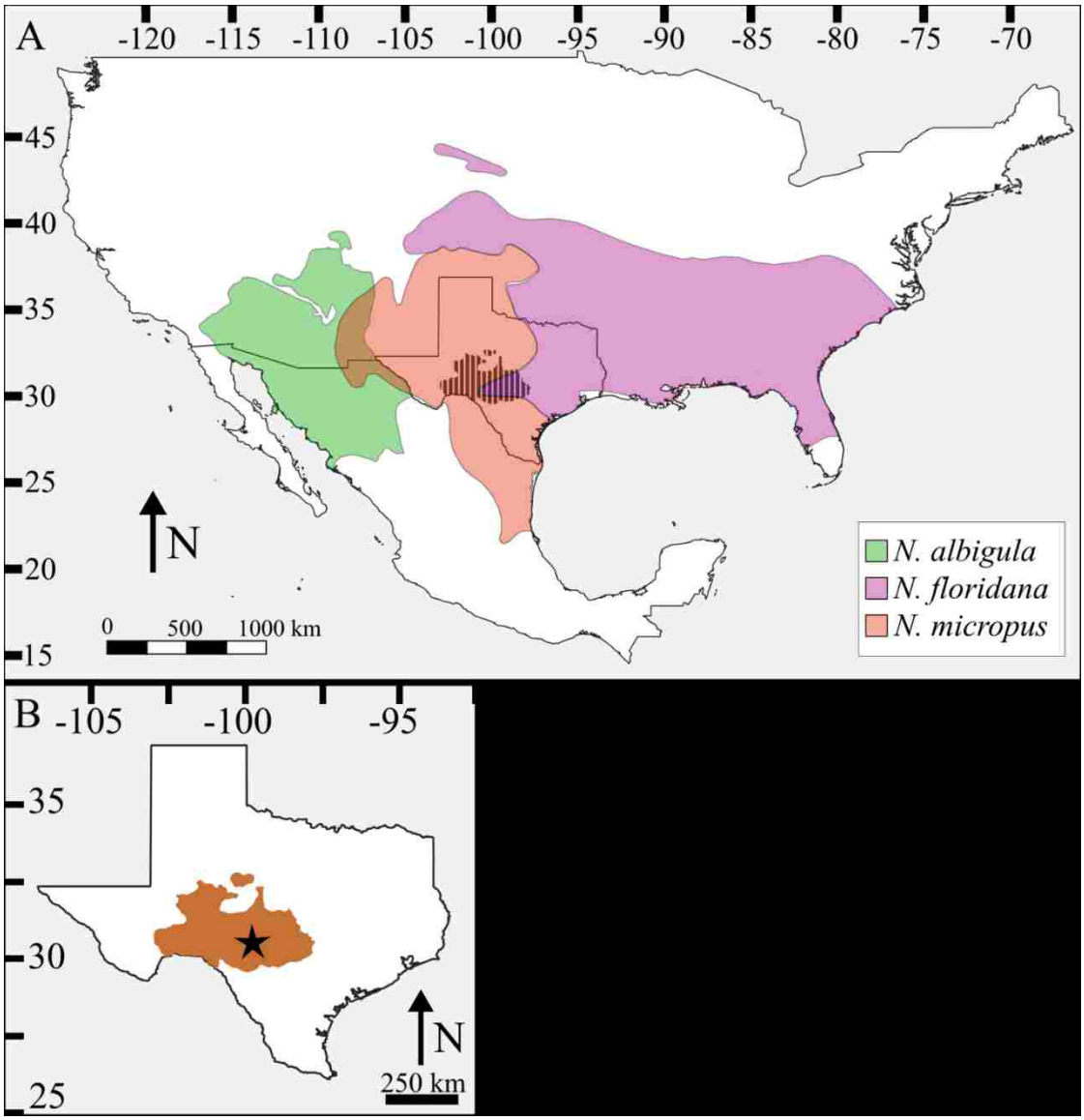

Figure 3.1. Distributions of *Neotoma* species found in Hall's Cave. A) Map of North America with modern distributions of *Neotoma albigula* (green), *N. floridana* (purple), and *N. micropus* (red). Location of the Edwards Plateau in Texas is represented by black, cross hatched area. B) Map of Texas with Edwards Plateau highlighted and location of Hall's Cave marked by the star. C) Age model of Hall's Cave stratigraphy (Tomé et al., *in review*).

genus are highly sensitive to environmental temperature; morphological changes in size are a common response to temperature fluctuations across both space and time (Brown and Lee 1969, Smith et al. 1995, 1998, Smith and Betancourt 1998, 2003). These changes in size are

in accordance with the ecological principle known as Bergmann's Rule; the idea that within a genus, those species inhabiting colder environments will be larger than those in warmer ones (Bergmann 1847, Mayr 1956, Brown and Lee 1969, Ashton et al. 2000, Freckleton et al. 2003, Smith 2008).Thus, we hypothesize that *Neotoma* were strongly influenced by temperature fluctuations in the Edwards Plateau.

Changes in vegetation associated with climate and the terminal Pleistocene megafaunal extinction may have led to shifts in resource availability and competition among consumers, reflected in the response of diet and/or body size in *Neotoma*. Body size is an important component of interspecific interactions for *Neotoma.* When different species of *Neotoma* occur in sympatry, the smaller species may shift their microhabitats or diet (Finley 1958, Cameron 1971, Dial 1988). For example, where they co-occur with larger *N. fuscipes* (~230-300g), *N. lepida* (~120-240g) switch from feeding on oaks (*Quercus turbinella*) to feeding on juniper (*Juniperus californica*); juniper, being higher in toxic compounds, has a higher cost in metabolism and thermoregulation in woodrats (Cameron 1971, Carraway and Verts 1991, Verts and Carraway 2002, McLister et al. 2004, Dearing 2005). Community reorganization following the extinction thus may have influenced dietary responses in *Neotoma* though changes in competition for available resources, or through shifts in the relative abundance of vegetation driven by the absence of megaherbivores.

We assessed dietary changes over time with carbon ($\delta^{13}C$) and nitrogen ($\delta^{15}N$) isotope analysis of bone collagen, which has been used as a proxy for diet composition, trophic level, and niche partitioning across space and time (West. et al. 2006, Koch 2007, Koch et al. 2009). Previous studies have used isotope analysis to quantify the diets of both historical and extinct taxa (Chamberlain et al. 2005, Leonard et al. 2007, Smiley et al. 2016,

Walsh et al. 2016, Ramírez-Pedraza et al. 2019). Changes in diet and body size may also reflect species preferences in terms of environmental conditions and resource availability. The three species of Neotoma potentially present vary in size and habitat affinity. *Neotoma albigula* (~155-250g) and *N. micropus* (~180-320g) both inhabit desert and semi-arid environments and are reliant on cacti, not only for den construction but as a source of food and water (Vorhies and Taylor 1940, Finley 1958, Raun 1966, Olsen 1976, Braun and Mares 1989, Macêdo and Mares 1989, Orr et al. 2015). In contrast, *N. floridana* (~200-380g) typically inhabit more mesic, forested environments and do not have as strong a preference for cacti, typically eating higher proportions of leaves and fruit from available trees and shrubs (Rainey 1956, Finley 1958, Wiley 1980). Regional vegetation changes on the Edwards Plateau may have led to changes in the relative abundance of these 3 species.

Materials and Methods

Study Site

We employ a fossil record from Hall's Cave, which is located in the Edwards Plateau, Texas (Figure 3.1B). During the Full-Glacial (~21 cal BP), the Edwards Plateau was a mix of deciduous forest and conifers, before warming and drying conditions during the Late Glacial period (17-11.6 ka cal BP) led to the transition to a grassland and oak savanna landscape (Bryant and Holloway 1985, Cordova and Johnson 2019). This vegetation remained relatively stable throughout the Post-Glacial period (11.6-0 ka cal BP) and today the region is predominantly a savanna, shrub woodland populated by oak, mesquite and juniper (Bryant and Holloway 1985, Toomey et al. 1993, Joines 2011). Hall's Cave is a fluvial deposit with episodic deposition of sediments and biological materials following heightened periods of

precipitation (Toomey 1993), and is located on a private ranch; the owners have graciously allowed generations of paleontologists to work at the site. The Hall's Cave record extends back to about 20,000 cal BP, with an exceptionally well-dated stratigraphic sequence (Tomé et al., *in review*) (Figure 3.1C). Excavations from Hall's Cave began in the 1960s, and were accelerated in the late 1980s/90s by R. Toomey (1993). To date, the site has yielded thousands of vertebrate specimens, particularly of small and medium body sizes across various trophic guilds (Toomey 1993); our ongoing sorting and identifying of previously collected bulk material is adding to the collection. The vertebrate fossils are housed at the Vertebrate Paleontology Lab of the Texas Memorial Museum (TMM) at the University of Texas, Austin.

Study Organisms

Three *Neotoma* species were hypothesized to be present at Hall's Cave: *N. albigula*, *N. floridana* and *N. micropus* (Toomey 1993); with the latter two extant on the Edward's Plateau today (Figure 3.1A). Unfortunately, the three species cannot be distinguished from one another based solely on molar or lower jaw characteristics (Sagebiel 2010, Tomé et al., *in prep*), which represent the vast majority of our fossil elements. Moreover, the substantial body size overlap precluded using size as an identifier. Thus, we aggregated samples and asked our questions at the level of the genus, which we note is the norm for paleoecological studies. Nonetheless, preliminary ancient DNA work conducted on a sediment column taken from on Hall's Cave suggested a high probability of *Neotoma floridana* being the only woodrat present in the oldest stratigraphic levels (Stafford, *pers. comm.*). In the future, aDNA

of bulk sediments may prove to be a valuable way for differentiating morphologically indistinguishable species.

Neotoma are present in all strata at Hall's Cave, from ~22,000 cal BP to modern (Toomey 1993), but specimen abundance is not uniformly distributed across the time span. To facilitate our analyses of body size and diet of *Neotoma* over time, we aggregated data into 15-time intervals of approximately equal length chosen to include important environmental transitions (Table 3.1). Note however, that the oldest time interval is longer, spanning 16,000-22,000 cal BP; this was because *Neotoma* were relatively rare, with 31 unique elements recovered. Thus, for this time bin, we also included a sample of 14 additional *Neotoma* specimens from a nearby fossil site. Zesch Cave, which is ~75 km away on the Edwards Plateau, and dates from between 16,000-18,000 cal BP (Lundelius Jr 1967, Graham et al. 1987, Sagebiel 2010). The Zesch Cave record shares a similar local taxon to that of Hall's Cave, including the same 3 potential *Neotoma* species. We infer, therefore, it likely had a similar paleoenvironment during the terminal Pleistocene (Sagebiel 2010). All other time bins include only specimens from Hall's Cave and were aggregated across important climatic and faunal events.

Table 3.1. Summary of data for *Neotoma* by time interval. Precipitation, maximum and minimum temperature were extracted from the CCM3 (Lorenz et al. 2016a, b) in 500-year intervals and average each time interval given below.

Age Range (cal BP)	N Mass	N Isotopes	Mean Mass (g) (± Stdev)	Mean $\delta^{13}C$ (± Stdev)	Mean $\delta^{15}N$ (± Stdev)	Maximum Temperature (°C) (± Stdev)	Minimum Temperature (°C) (± Stdev)	Mean Precipitation (mm) (± CV)	Species Richness	Sorenson to Modern
0 - 1500	10	9	170.4 ± 32	-17.8 ± 3.1	5.9 ± 1.3	25.5 ± 7.1	12.1 ± 7.4	554.6 ± 0.4	34	1
1500 - 3100	33	12	181.9 ± 28.1	-19.2 ± 1.9	5.5 ± 1.3	25.5 ± 7.2	11.8 ± 7.6	534.7 ± 0.4	36	0.89
3100 - 5400	63	47	204.2 ± 46.4	-17.9 ± 2.4	5.7 ± 1.1	25.4 ± 7.8	11.8 ± 7.6	558.4 ± 0.4	35	0.81
5400 - 6100	23	19	200.6 ± 41.5	-17.7 ± 2.4	5.5 ± 1.3	25.3 ± 8.0	11.9 ± 7.9	553.1 ± 0.4	31	0.77
6100 - 6400	15	8	200 ± 46.2	-17.5 ± 2.1	5.9 ± 1.1	25.5 ± 8.1	11.8 ± 8.1	536.3 ± 0.4	32	0.79
6400 - 6700	9	10	190 ± 50.7	-18.5 ± 2.1	5.2 ± 1.7	25.5 ± 8.2	11.9 ± 8.2	526.8 ± 0.4	33	0.78
6700 - 7700	35	34	187.9 ± 34.6	-17.1 ± 2.7	6 ± 1.1	25.1 ± 8.7	11.9 ± 8.3	536.7 ± 0.4	33	0.78
7700 - 8400	15	19	203 ± 32.7	-17.5 ± 2	6.4 ± 1.0	25 ± 9.0	11.9 ± 8.4	532 ± 0.4	36	0.71
8400 - 9000	20	18	207 ± 36.1	-17.8 ± 2.1	6.1 ± 1.3	24.8 ± 9.2	11.9 ± 8.6	539.1 ± 0.3	35	0.7
9000 - 9400	11	8	229.3 ± 43.5	-18.3 ± 2.2	6.5 ± 1.5	24.9 ± 9.2	11.9 ± 8.7	552.5 ± 0.3	35	0.7
9400 - 10000	19	19	222.9 ± 45.6	-17.8 ± 2.9	6.1 ± 1.2	24.8 ± 9.3	11.8 ± 8.6	561.5 ± 0.3	39	0.69
10000 - 11000	28	30	203.6 ± 41.4	-19.3 ± 1.2	5.9 ± 1.0	24.3 ± 9.2	11.5 ± 8.7	582.4 ± 0.3	35	0.67
11000 - 12700	45	18	211 ± 44.3	-19.1 ± 1.0	6.1 ± 1.6	22.9 ± 9.7	10.7 ± 9.0	628.1 ± 0.3	53	0.62
12700 - 15800	48	29	212.6 ± 50.2	-18.8 ± 1.6	5 ± 1.5	22.1 ± 10.1	10 ± 9.5	631 ± 0.3	74	0.52
15800 - 22400	22	5	230.1 ± 56.3	-19.5 ± 0.3	4.2 ± 1.1	18.7 ± 10.4	7.1 ± 10.2	685.9 ± 0.4	68	0.45

Morphology

We characterized body size in *Neotoma* using linear measurements of the first upper and lower molars (UM1 and LM1, respectively). These molars were either loose or found in mandibular or maxillary elements, generally with incomplete toothrows. The UM1 and/or LM1 of 671 *Neotoma* were photographed using a calibrated AM4515ZT Dino-Lite Edge digital microscope. The length of each molar was measured twice (~1342 measurements) using the line tool in DinoCapture 2.0. Samples that could not be well-characterized (e.g., whose measurements resulted in a > 5% standard error) were discarded; this led to the loss of 23 specimens. We calculated the minimum number of individuals (MNI) to exclude

potentially replicated individuals (e.g., a single individual could potentially contribute a URM1, ULM1, LRM1, and LLM1).

To help in the estimation of MNI, we determined the 'normal' asymmetry of teeth found among modern woodrats. Measuring the first molars for 20 museum specimens from the Museum of Southwestern Biology (MSB) at the University of New Mexico (Albuquerque, NM) and the James F. Bell Museum of Natural History (MMNH) at the University of Minnesota (St. Paul, MN) (Appendix 3 Table 1) we characterized the upper versus lower, and bilateral symmetry of animals. We found that on average, the difference between the same upper and lower elements (e.g., UM1 and LM1) was less than 5%. Moreover, the bilateral symmetry was very low, with only an average ~0.5% between left and right measurements. These results informed our analysis. First, for each stratigraphic level, we preferentially selected only LLM1s. Second, if our targeted sample size of 20 was not achieved, we then included all LRM1s from that level that were 0.5% greater in size than any measured LLM1s. Third, we included ULM1s from that level that were 0.5% greater in size than any lower molars selected in steps 1 and 2. Lastly, we included URM1s from the same level that were 0.5% greater in size than any previously selected LLm1s, LRM1s and ULM1s.

Tooth measurements were translated into estimates of body mass using an allometric equation for cricetine rodents for the first lower molar length (Martin 1990): Log mass (g) = 3.310*(Log LM1 length) + 0.611 (r^2=0.96, %PE=15.58, df=32). To account for differences between lower and upper molar length in *Neotoma*, upper molar length was standardized by a 5% decrease to measurements prior to calculating body size. After the removal of potential

duplicates, our final dataset included 396 body mass estimates for *Neotoma* across the 15 levels, with between 9-63 mass estimates per time bin (Table 3.1).

Isotope-Based Estimates of Diet Composition and Variation

We employed stable isotope analysis to characterize shifts in diet for *Neotoma* and *Sigmodon* across time. We analyzed stable carbon ($\delta^{13}C$) and nitrogen ($\delta^{15}N$) isotopes from bone collagen extracted from maxillary and mandible bones for 365 *Neotoma.* We attempted to acquire 10 or more samples per time interval to reduce low sample sensitivity in analyses (Jackson et al. 2011). However, sparsity of material led to some intervals containing less than 10 individuals; we excluded a single interval with only 5 individuals (15800-22400 cal BP). Differences in how the photosynthetic pathways of C_3 and C_4 plants fractionate carbon leads to natural variation in $\delta^{13}C$ values across ecosystems that are incorporated into the tissues of consumers (DeNiro and Epstein 1978, Farquhar et al 1989, Cerling et al. 1997). Regional studies within the Great Plains, southern and central Texas have found plant functional groups for C_3 and C_4 plants to have average $\delta^{13}C$ values of about -27‰ and -13‰, respectively (Boutton et al. 1993, 1998; Derner et al. 2006). The nitrogen isotopic composition may reflect trophic position, with increased $\delta^{15}N$ values signifying higher trophic position, or regional variation in $\delta^{15}N$ of the vegetation due to environmental conditions (DeNiro and Epstein 1981, Ambrose 1991, Amundson et al. 2003). The $\delta^{13}C$ and $\delta^{15}N$ values the consumer tissues will differ from that of its diet due to diet-tissue fractionation (Koch 2007). These offsets between diet and tissue are called trophic discrimination factors (TDF). Carbon and nitrogen isotope values thus vary across animals in a community depending upon their trophic level and the relative proportion of C_3 versus C_4

vegetation in their diet, enabling the use of $\delta^{13}C$ versus $\delta^{15}N$ isotopic niche space to act as a proxy for dietary niche space (Newsome et al. 2007).

Following Tomé et al. (*in review*), a subsample of ~150-250 mg of bone was taken from each fossil mandible or maxilla using a Dremel tool. To extract organic collagen matrix from the bone, we demineralized samples with 0.25N HCl at 3-4°C for 24-48 hours. Once demineralization was complete samples were lipid extracted via soaking in 2:1 chloroform/methanol for 72 hours, changing the solution every 24-hours. Each sample was then washed 5-7 times with distilled water and lyophilized. Approximately 0.9-1.0mg of each dried collagen sample was weighed on a microbalance and packaged into 0.35 mm tin capsules. $\delta^{13}C$ and $\delta^{15}N$ values of all samples were analyzed using a Costech elemental analyzer (Valencia, CA) interfaced with a Thermo Scientific Delta V Plus isotope ratio mass spectrometer (Bremen, Germany) at the University of New Mexico Center for Stable Isotopes (Albuquerque, NM). Isotope values are reported as δ values, where $\delta = 1000[(R_{sample}/R_{standard})-1]$ and R_{samp} and R_{std} are the $^{13}C:^{12}C$ or $^{15}N:^{14}N$ ratios of the sample and standard, respectively; units are in parts per thousand, or per mil (‰). Samples were calibrated using international reference standards; Vienna Pee Dee Belemnite (VPDB) for carbon and atmospheric N_2 for nitrogen (Fry 2006, Sharp 2017). The standard deviation of organic references within a run was ≤0.2‰ for both $\delta^{13}C$ and $\delta^{15}N$ values. We excluded any samples whose [C]:[N] ratios were above 3.5 due to diagenetic alteration (Ambrose 1990).

We followed our protocol for MNI as outlined for the mass measurements to ensure that each sample represented a unique individual. Our final dataset for the isotopic analyses consisted of 285 measurements. It is important to note that not all specimens for which we had $\delta^{13}C$ and $\delta^{15}N$ measurements had body measurements, and vice versa. Of the 396

individuals with mass measurements and 285 with isotope measurements, 110 individuals had both. Thus, 185 animals just had $\delta^{13}C$ and $\delta^{15}N$ values and 286 just had body size measurements.

Data

We compared our body size and diet data with measures of the mammal community composition and turnover, climate including temperature and precipitation, and several measures of vegetation composition and change. Community data included α-diversity (richness) and β-diversity (Sorenson Index), extracted from Smith et al. (2016b), updated to reflect current phylogeny, and recalculated to fit within the time intervals we employ here (Table 3.1). The original community data for Hall's Cave was compiled by Toomey (1993) and expanded to encompass the Edwards Plateau using the Neotoma Paleoecology Database (2015) by Smith et al. (2016b).

Climate information came from the Community Climate System Model (CCSM3), which simulates and interpolates 500-year intervals of climate across North America for the past 21,000 years (Lorenz et al. 2016a, b). The CCSM3 data have 0.5^{o} spatial resolution; thus, we were able to obtain regional scale climate events for the Edwards Plateau. Mean daily maximum and minimum monthly temperature and total monthly precipitation data were extracted from the CCSM3 at 500-year intervals. We averaged values to the same temporal resolution/binning used for our fossils (Table 3.1, Figure 3.2A-C).

Vegetation data came from Cordova and Johnson (2019), whom provide pollen and phytolith count information from the Hall's Cave record for the past 18,000 years over 47 stratigraphic depths. We extracted data on the ratio of C_3 to C_4 grasses over time. Increasing

C_4 values generally reflect a shift towards drier conditions and open woodland to grassland environments (Cordova and Johnson 2019). Thus, we used this ratio as a proxy for grassland environments. We also extracted *Opuntia* and Cuppressaceae pollen counts as modern *Neotoma albigula* and *N. micropus* are known to consume larger quantities of prickly pear cacti -up to 45% of diet in *N. albigula* – and moreover, make more use of juniper than *Neotoma floridana* (Vorhies and Taylor 1940, Spencer and Spencer 1941, Finley 1958, Rainey 1956, Wiley 1980, Dial 1988, Braun and Mares 1989, Macêdo and Mares 1988, Schmidly and Bradley 2016). Pollen counts of *Opuntia* and Cuppressaceae and C_3/C_4 grass ratios were fit into our 15-time intervals for analyses (Figure 3.2D).

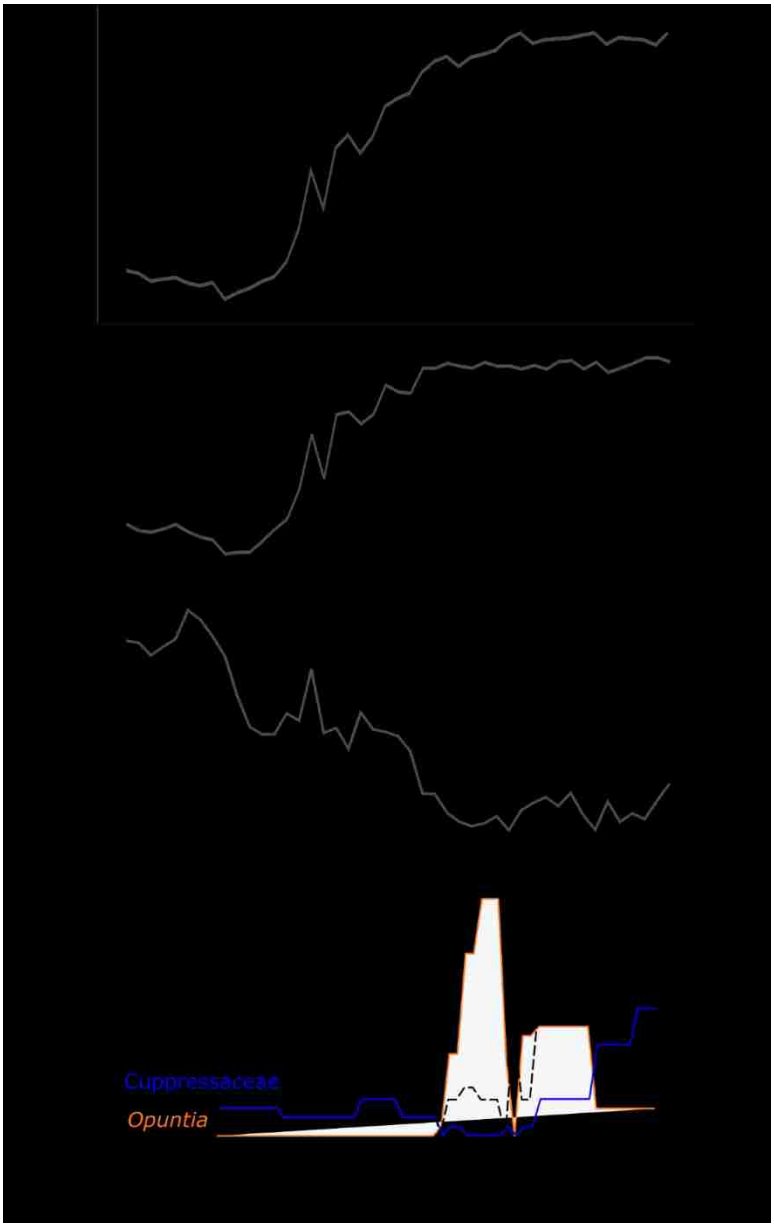

Figure 3.2. Changes in climate and vegetation on the Edwards Plateau over time. Changes in A) maximum, B) minimum temperature and C) precipitation (mm) (Lorenz et al. 2016a, b) over time for the Edwards Plateau. D) Ratio of C_3 versus C_4 grass (%) and pollen counts of Cuppressaceae and *Opuntia* at Hall's Cave over time (Cordova and Johnson 2019).

Statistics

We employed both parametric and non-parametric tests to examine changes in mass and diet over time because in some instance our data violated assumptions of normality. All statistical analyses were performed using R software version R.3.6.0 (R Core Team 2019) and RStudio 1.2.1335 (RStudio Team 2019).

We first analyzed body size and isotope variation before and after the extinction to determine if there was a marked change associated with period of acute biodiversity loss. Here, we employed the F-test and Bartlett's test. To examine changes in mass across the 15-time intervals we used ANOVA and Tukey multiple comparisons. Linear models were also run using maximum (e.g., the largest individual per time interval) and median mass against the mean of the $\delta^{13}C$, $\delta^{15}N$, climate and community variables to evaluate their influence on body mass. When significant correlations were found, we conducted an analysis of covariance (ANCOVA) was run to determine the added effect of each on mass.

We characterized shifts in isotopic niche space using Bayesian based standard ellipse areas (SEA_B) of $\delta^{13}C$ and $\delta^{15}N$ and calculated the overlap of SEAs between adjacent time intervals using the SIAR package for R (Jackson et al. 2011, Parnell and Jackson 2013, R Core Team 2019). Ellipses displaying 50% coverage were plotted using JMP Pro 13 (version 13.1). Changes in isotopic niche space were tested by analyzing $\delta^{13}C$ and $\delta^{15}N$ using ANOVA and Tukey multiple comparisons, across 14-time intervals due to lack of sufficient sample size in the oldest interval. Linear models were run using mean, minimum and maximum $\delta^{13}C$ and $\delta^{15}N$ against maximum and median mass, as well as climate, vegetation and community variables.

The presence of different species of *Neotoma* led us to test for differences in $\delta^{13}C$ across broader mass categories to attempt to partition species level patterns with changes in diet. Because there is a large amount of overlap in size between modern *Neotoma floridana* (200-350g), *N. micropus* (205-310g) and *N. albigula* (190-225g) in Texas (Schmidly and Bradley 2016), mass groups were assigned to try and separate potential species. Mass groups were selected to account for differences in body size of each species across its range compared to Texan populations while maintaining sufficient sample size for analysis. The first group included only individuals with masses less than 180g, which is the lower end of *N. micropus* (~180-320g) across its species range (Braun et al. 1989) such that only *N. albigula* is likely to fall in this category. The second group was between 180-225g, which is likely to include larger *N. albigula* and smaller *N. micropus*, but exclude the majority of *N. floridana*. The third group was between 225-280g, likely excluding *N. albigula* but capturing the largest degree of overlap in size between *N. micropus* and *N. floridana.* The final mass group included all individuals greater than 280g in mass, and likely represent mostly *N. floridana* and potentially a small portion of large *N. micropus.* We tested for differences in diet across mass group using ANOVA and Tukey multiple comparisons.

Results

The *Neotoma* present in the Edwards Plateau community prior to the extinction were significantly larger than after the loss of biodiversity (Table 3.2, Figure 3.3A). Mass of *Neotoma* significantly decreased across time (ANOVA F-value=2.85, df=14/381, $p<0.01$: Kruskal-Wallis chi-squared=38.07, $p<0.001$, Table 3.1, Figure 3.4A). In particular, the mean

Table 3.2. Results for changes in the distributions and variance of *Neotoma* mass and diet ($\delta^{13}C$ and $\delta^{15}N$) for pre- (12700-22400 cal BP) and post-extinction (0-12700 cal BP) time bins. * Welsh Two-Sample T-Test used to account for unequal variances between groups.

	F-Test			Bartlett Test			Two Sample T-Test			Wilcoxon Rank Sum Test	
	F	df	p-value	K-squared	df	p-value	t	df	p-value	W	p-value
Mass	1.54	69/325	0.014	5.86	1	0.016	-2.52	89.2	0.013*	13624	0.011
$\delta^{13}C$	0.45	33/250	0.007	7.60	1	0.006	2.90	55.3	0.005*	3276	0.028
$\delta^{15}N$	1.48	33/250	0.100	2.48	1	0.116	4.40	283	0.000	2290	0.000

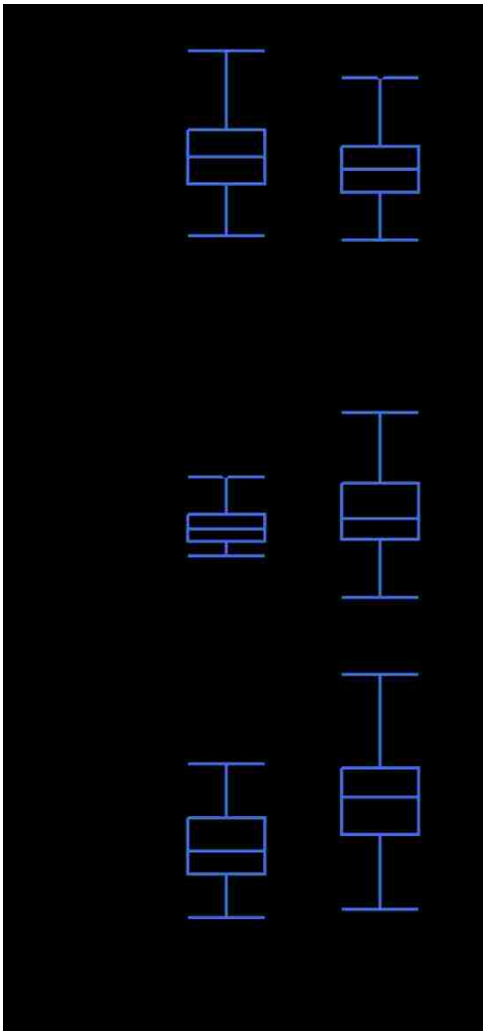

Figure 3.3. Changes in *Neotoma* across the megafaunal extinction event. Boxplots show mean and interquartile ranges for A) mass, B) $\delta^{13}C$ and C) $\delta^{15}N$ distributions of the *Neotoma*, before (pre-) and after (post-) the megafaunal extinction.

body size of *Neotoma* in the oldest time interval (15800-22400 cal BP) was significantly larger than *Neotoma* at 6700-7700 and 0-3100 cal BP (Appendix 3 Table 2 for Tukey comparisons). Decrease in body size also include a 160g size difference between the largest individuals (~230-390g) from the oldest to youngest time intervals. Changes in body size were correlated with both climate and community changes. Decreased maximum mass of *Neotoma* was significantly correlated with increasing maximum temperature and increased turnover in the community (Table 3.3, Figure 3.4B-C). The median body mass of *Neotoma* was significantly and negatively correlated to turnover (Table 3.3). Results of ANCOVA ($F = 1.377$, $p>0.5$) suggest that the temperature is influencing changes in mass independently from turnover. Here, turnover was calculated in terms of similarity to the modern community composition (Table 3.1), such that maximum and median body size decreased with community changes throughout the Holocene towards modern.

Table 3.3. Results of AIC and multiple linear models comparing mass and diet ($\delta^{13}C$ and $\delta^{15}N$) to climate and community metrics. Models were run on maximum and median mass due to the potential for multiple species of *Neotoma.* Precipitation (mm) (Precip), maximum and minimum temperature (^{o}C) (Max_Temp and Min_Temp) were extracted from the CCM3 (Lorenz et al. 2016a,b). Significant p-values are bolded.

Climate Models							
Neotoma	**Best model**		**AIC**	**F-statistic**	**df**	**p-value**	**Adjusted r^2**
Maximum Mass	Max_Temp	*neg.*	100.8	19.26	1/13	**0.001**	0.57
Median Mass	Max_Temp	*neg.*	84.0	3.82	1/13	0.073	0.17
Maximum $\delta^{13}C$	Min_Temp	*pos.*	23.8	8.29	1/13	**0.013**	0.34
Mean $\delta^{13}C$	Precip	*neg.*	-13.9	10.37	1/13	**0.007**	0.40
Minimum $\delta^{13}C$	Max_Temp	*neg.*	-5.5	3.89	1/13	0.070	0.17
Maximum $\delta^{15}N$	Max_Temp + Min_Temp	*neg., pos.*	-7.6	9.13	2/12	**0.004**	0.54
Mean $\delta^{15}N$	Max_Temp + Min_Temp	*neg., pos.*	-31.4	17.36	2/12	**0.000**	0.70
Minimum $\delta^{15}N$	Min_Temp	*pos.*	-19.9	5.72	1/13	**0.033**	0.25
Community Models							
Neotoma	**Best model**		**AIC**	**F-statistic**	**df**	**p-value**	**Adjusted r^2**
Maximum Mass	Sorenson	*neg.*	92.6	42.55	1/13	**0.000**	0.75
Median Mass	Sorenson	*neg.*	74.7	10.56	2/12	**0.002**	0.58
Maximum $\delta^{13}C$	Richness	*neg.*	28.0	3.04	1/13	0.105	0.13
Mean $\delta^{13}C$	Richness	*neg.*	-11.4	6.80	1/13	**0.022**	0.29
Minimum $\delta^{13}C$	Sorenson	*neg.*	-10.7	6.59	2/12	**0.012**	0.44
Maximum $\delta^{15}N$	Sorenson	*pos.*	4.1	0.14	1/13	0.718	-0.07
Mean $\delta^{15}N$	Richness	*neg.*	-20.3	8.14	1/13	**0.014**	0.34
Minimum $\delta^{15}N$	Richness	*neg.*	-19.1	4.73	1/13	0.049	0.21

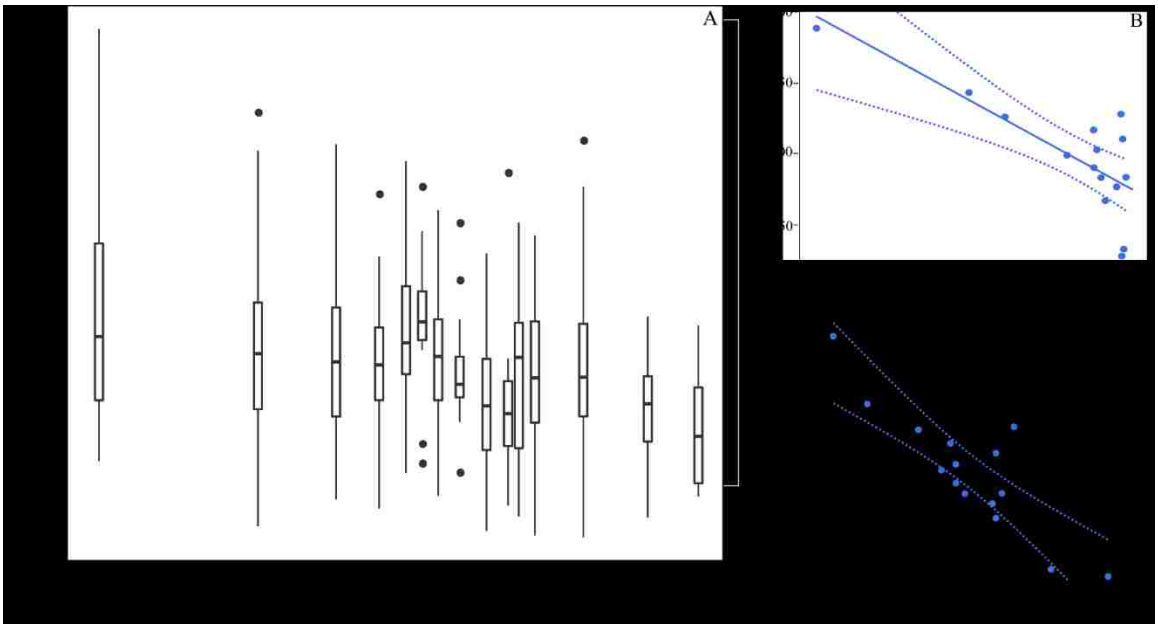

Figure 3.4. Changes mass of *Neotoma* over time. Changes in A) mass of *Neotoma* across 25-time intervals. Linear models of maximum body size (g) versus B) maximum temperature (°C) (Y=715.9-17.2X, df = 1/13, p<0.001, adj. R^2 = 0.57) and C) Sorenson index as similarity of community composition to the youngest time interval (Y=489.9-264.8X, df = 1/13, p<0.001, adj. R^2 = 0.75).

Although body size of *Neotoma* varied significantly across time, these changes did not appear to be related to diet. Linear models found no correlation between either carbon ($\delta^{13}C$) or nitrogen ($\delta^{15}N$) with body size (Table 3.4). Analysis of classified mass groups (<180g, 180-225g, 225-280g and >280g) found a significant difference in the $\delta^{13}C$ values of *Neotoma* (ANOVA F-value=3.27, df=3/106, p<0.05: Kruskal-Wallis chi-squared=9.16, df=3, p<0.05), but multiple comparisons revealed no significantly different pairs (Appendix 3 Table 3) (Figure 3.5).

Table 3.4. Results of linear models comparing mass and diet in *Neotoma*.

Variables Compared	F-statistic	df	p-value	Adjusted r^2
Mass - $\delta^{13}C$	0.15	1/108	0.698	-0.01
Mass - $\delta^{15}N$	0.08	1/108	0.778	-0.01
$\delta^{13}C$ - $\delta^{15}N$	57.66	1/283	**0.000**	0.17

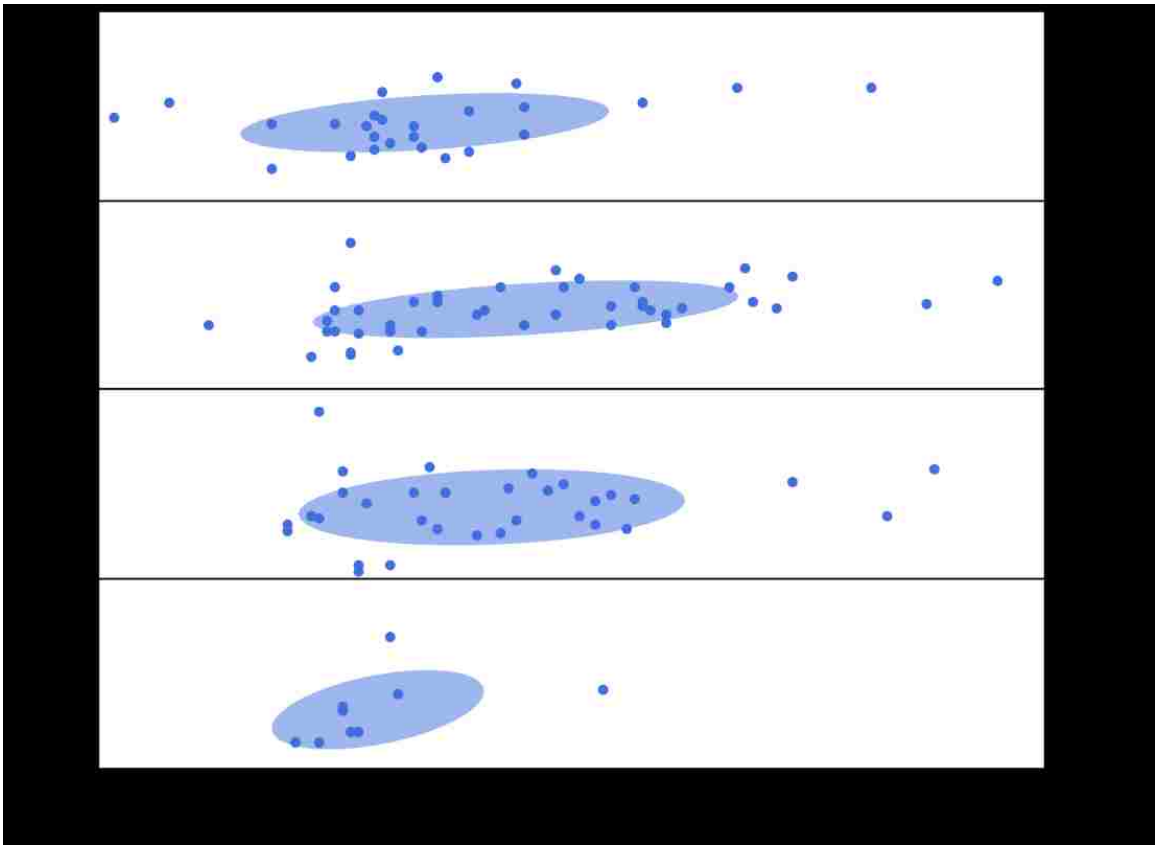

Figure 3.5. Mass groups and diet of *Neotoma*. Isotopic niche space ($\delta^{13}C$ and $\delta^{15}N$) across 4 mass groups (<180g, 180-225g, 225-280g, >280g) of *Neotoma*.

We find differences in the isotopic diet of *Neotoma* before and after the extinction. The genus had significantly lower bone collagen $\delta^{13}C$ and $\delta^{15}N$ values prior the extinction compared with afterwards ($\delta^{13}C$: ANOVA F-value=4.63, df=1/283, $p<0.05$; Kruskal-Wallis chi-squared = 4.82, df = 1, p-value<0.05: $\delta^{15}N$: ANOVA F-value=31.6, df=1/62, p-value<0.001; Kruskal-Wallis chi-squared =19.22, df = 1, $p<0.001$) Table 3.2, Figure 3.3B). While variance in carbon isotope space increased after the extinction, that of the nitrogen isotope space did not (Table 3.2, Figure 3.3C). Analysis of the individual time intervals found only a single significant difference across time. *Neotoma* consumed a significantly greater proportion of C_4/CAM at 6700-7700 cal BP than 10000-11000 cal BP (ANOVA F-value=2.37,

df=14/270, p<0.01, Kruskal-Wallis chi-squared=32.92, df=1, p<0.01, Appendix 3 Table 2). $\delta^{15}N$ values of *Neotoma* were significantly higher at 7700-8400 cal BP than at 12700-15800 cal BP (ANOVA F-value=2.49, df=14/270, p<0.01, Kruskal-Wallis chi-squared=33.75, df=14, p<0.01, Appendix 3 Table 2).

The isotopic niche space (SEA_B) of *Neotoma* increased over time (Figure 3.6A-C, 7). The $\delta^{13}C$ and $\delta^{15}N$ values of *Neotoma* were significantly and positively correlated, with increasing $\delta^{15}N$ values being associated with a proportion of C_4/CAM consumed (Table 3.4). *Neotoma* used more C_3 resources during periods of higher precipitation and α-diversity. Bone collagen $\delta^{13}C$ values were significantly and negatively correlated to precipitation and richness (Table 3.3, Figure 3.6D-E), such that *Neotoma* was consuming more C_3 resources under more mesic conditions and when more α diversity was present, both of which are highest prior to the extinction event. $\delta^{15}N$ values were significantly and negatively correlated with maximum temperature and positively with minimum temperatures, and negatively correlated with α-diversity (Table 3.3). Overlap in dietary niche space was highest between about 0-3100, 3100-6100, and 9000-10000 cal BP (Figure 3.6C, Figure 3.7).

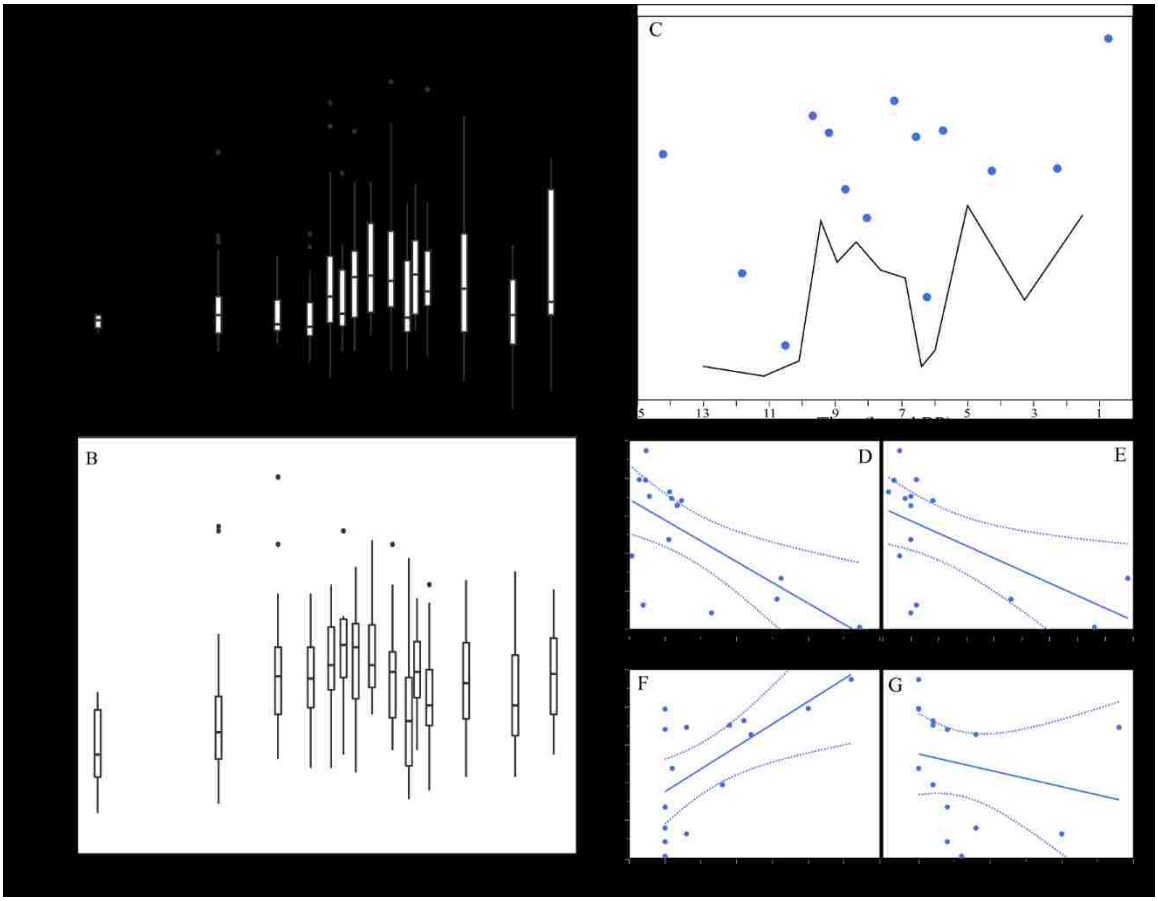

Figure 3.6. Changes in bone collagen $\delta^{13}C$ and $\delta^{15}N$ of *Neotoma* over time. A) Changes in the $\delta^{13}C$ values and B) Changes in the $\delta^{15}N$ values of *Neotoma* through time. C) Standard ellipse areas (SEA)(‰) and overlap of adjacent SEAs (solid line) through time. Linear relationships between D) precipitation (Y=-12.0-0.01X, df=1/13, $p<0.01$, adj. $R^2 = 0.29$), E) species richness (Y=-16.9-0.03X, df=/13, $p<0.05$, adj. $R^2 = 0.29$), F) pollen counts of *Opuntia* (Y=-18.6-0.06X, df=/13, $p<0.05$, adj. $R^2 = 0.37$), and G) pollen counts of Cuppressaceae (as Juniper) (Y=-18.1-0.04X, df=/13, $p>0.1$, adj. $R^2 = 0$).

$\delta^{13}C$ was significantly correlated with changes in vegetation. *Neotoma* had a larger proportion of C_4/CAM in their diet with increasing amounts of *Opuntia* (linear model F-statistic = 9.06, df=1/13, $p<0.05$) and decreasing C_3 grasses (linear model F-statistic=10.58, df=1/13, $p<0.01$) on the landscape (Figure 3.6F). We found no correlation between changes in diet and presence of juniper (linear model F-statistic=0.71, df=1/13, $p>0.1$) (Figure 3.6G).

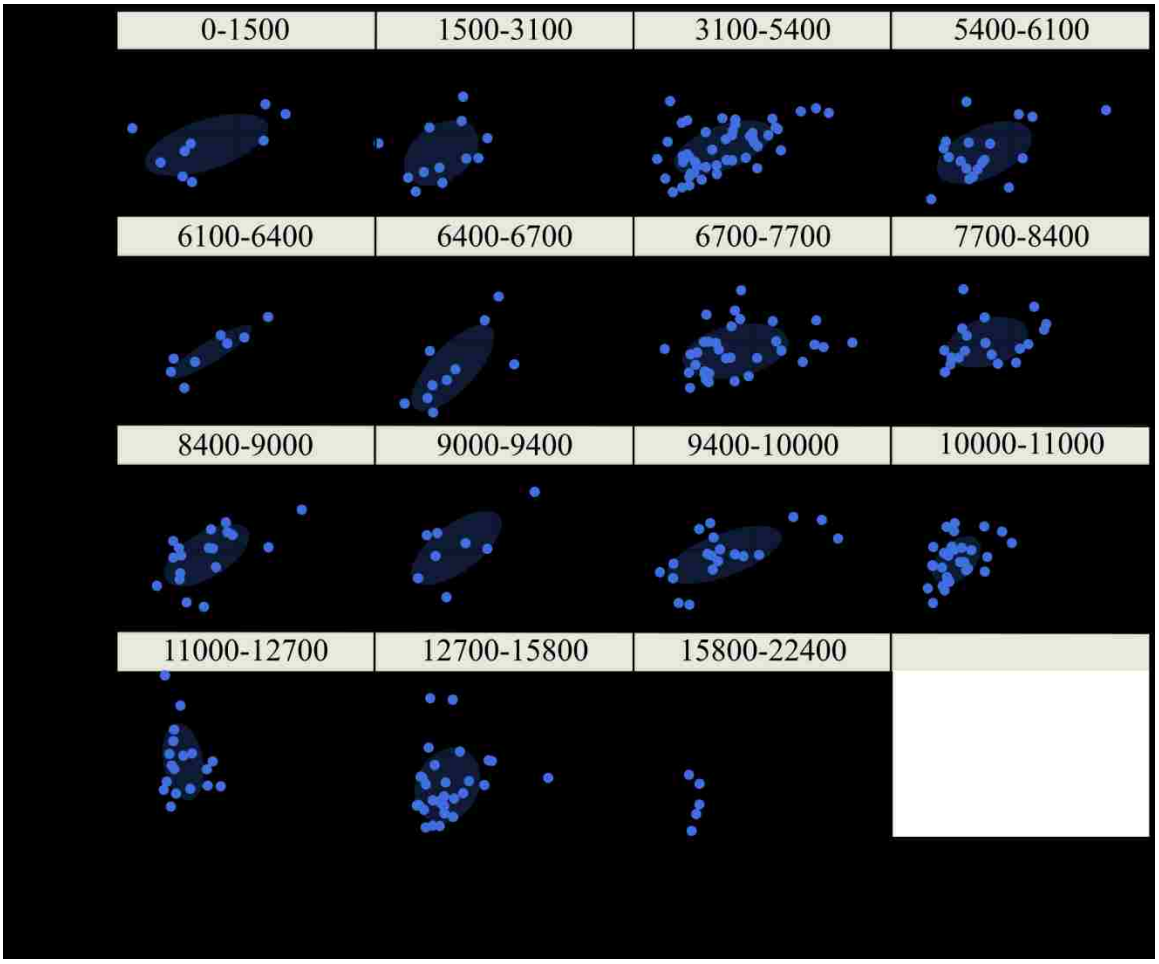

Figure 3.7. Isotopic niche of *Neotoma* by time interval. Standard ellipse areas (SEAs) represent 50% coverage of where *Neotoma* populations for each time interval (cal BP) lie in $\delta^{13}C$ and $\delta^{15}N$ space. Each interval is divided by intersecting lines at $\delta^{13}C$ = -16‰ and $\delta^{15}N$ = 6‰. SEA was not calculated for oldest time interval due to low sample size (n=5).

Discussion

Our results clearly show that *Neotoma* responded to the climate and biodiversity changes of the terminal Pleistocene. As the glacial ice sheets retreated and the climate warmed, *Neotoma* became smaller (Figure 3.4A) and made use of a more mixed diet by increasing their use of C_4/CAM resources over time (Figure 3.7). Decreased size and greater mixed resource use were also associated with the loss and turnover in biodiversity (Table 3.3, Figure 3.4C,

6E). Whether these changes resulted from adaptation within a single species, as has been shown elsewhere (Brown and Lee 1969, Smith et al. 1995, 1998, Smith and Betancourt 1998, 2003), or resulted from the partial or full replacement of species within the genus is unclear, but overall we find a large change in the ecology of *Neotoma* as it responds to a combination of abiotic and biotic stressors.

Neotoma underwent significant decreases in body size across the end Pleistocene megafaunal extinction and throughout the Holocene (Figure 3.3A). Decreased maximum body size in *Neotoma* over time was predominantly associated with community turnover and increasing regional temperatures (Figure 3.3E, Table 3.1 & 3.5). With the warming climate of the Holocene, thermal intolerance likely led to reduced body size in the largest individuals of *Neotoma* across time intervals following Bergmann's rule, as has commonly been found within the genus (Brown and Lee 1969, Smith et al. 1995, 1998, Smith and Betancourt 1998, 2003). The influence of community turnover on both maximum and median body mass suggest that the genus becomes smaller overall as the community composition becomes more similar to modern (Table 3.3). Community restructuring following the megafauna extinction may have led to changes in biotic interactions and competition for resource availability. Decreased size may be advantageous for predator avoidance in small mammals (Stanley 1973). At the same time, smaller size may have altered *Neotoma's* ability to compete for resources or habitat, as larger size in modern *Neotoma* can act as a competitive advantage (Finley 1958, Cameron 1971, Dial 1988).

Separately from changes in body size, the dietary niche of *Neotoma* also shifted across the past 22,000 years with changes in climate, biodiversity loss and vegetation. The mean $\delta^{13}C$ value of *Neotoma* across the entire temporal record at Hall's Cave were generally reflective of

browsers, and ranged between -17.1 to -19.5‰ (SD: 0.3-3.1) (Table 3.1). However, *Neotoma* shift between consuming a greater proportion of C_3 plants prior to the extinction to higher mixed C_3-C_4/CAM use. Prior to 14,000 cal BP, the Edwards Plateau was covered in deciduous forest (Bryant and Holloway 1985). A regional shift to warmer and drier conditions led to the expansion of grassland and oak savanna ecosystems by ~11,600 cal BP (Bryant and Holloway 1985). C_4 vegetation continued to increase across Texas over the Holocene, leading to a more open landscape on the Edwards Plateau (Nordt et al. 1994, Fox and Koch 2003, Cotton et al. 2016, Cordova and Johnson 2019). We find an increase in the dietary niche space of *Neotoma* beginning 10,000 years ago. Following an increase in *Opuntia* at about 9000 cal BP (Cordova and Johnson 2019, Figure 3.3D), we find an increase the consumption of C_4/CAM at 6700-7700 cal BP. A sudden decrease in isotopic niche between 6400-6700 cal BP (Figure 3.2D, 6C, 7) mirrors the disappearance of *Opuntia* from the Hall's Cave fossil record, and a shift away from a more mixed C_3-C_4/CAM diet to greater use of C_3 resources. As *Opuntia* reappears, the breadth of $\delta^{13}C$ values of *Neotoma* increase as well (Figure 3.2D, 6C, 7). These patterns suggest a strong influence by vegetation shifts and resource availability on the diet of *Neotoma.*

The changes in the $\delta^{15}N$ values of *Neotoma* (Figure 6B, 7) potentially reflect changes in trophic level or baseline shifts in the nitrogen isotope composition of consumed plants. Modern *Neotoma* are essentially herbivorous, with occasional and very limited consumption of insects (Vorhies and Taylor 1940, Rainey 1956). However, if increased $\delta^{15}N$ values were due to a trophic level shift, it would suggest Neotoma were more omnivorous than believed. Alternatively, the correlation between increased C_4 consumption and higher $\delta^{15}N$ values (Figure 4C) could result from changing environmental conditions (DeNiro and Epstein 1981, Amundson et al. 2003). In general, plant $\delta^{15}N$ values are higher in more arid relative to mesic

environments (Ambrose 1991, Austin and Vitousek 1998, Amundson et al. 2003). We found $\delta^{15}N$ in *Neotoma* to be positively correlated with increasing minimum temperature, suggesting plant $\delta^{15}N$ increased as the environment warmed. However, we also found $\delta^{15}N$ decreased with increasing maximum temperature, and we found no correlation between $\delta^{15}N$ and precipitation (Table 3.3), as may have been expected from modern patterns. Thus, whether changes in the proportion of nitrogen isotopes in bone collagen are due to changes in the vegetation or to trophic level remains unclear.

Changes in both the body size and diet of *Neotoma* may also be related to temporal changes in the composition of *Neotoma* species present in the record. Prior to the extinction, the larger *N. floridana* is most likely the only species of *Neotoma* present according to aDNA work on fossils from the oldest strata (Stafford, *pers. comm.*). At this time, the environment of the Edwards Plateau was still a deciduous forest, a typical habitat of *N. floridana* (Rainey 1956, Bryant and Holloway 1985). After 17,000 cal BP, the region shifts towards a more open grassland/savanna landscape (Bryant and Holloway 1985, Cordova and Johnson 2019), conditions shifted from habitats favorable for *N. floridana* to those more typical of *N. micropus* and/or *Neotoma albigula* (Finley 1958, Macêdo and Mares 1988, Braun and Mares 1989). Thus, the immigration of these smaller species onto the Edwards Plateau could have been driven by regional vegetation and resource shifts due to changing climate and the loss of the megafauna from the landscape. At around 6700-7700 cal BP, we find that mass in *Neotoma* has become significantly smaller compared to the oldest time interval. The dramatic decrease in body size of *Neotoma*, may then be a consequence of not only a genus level adaptation to increasing temperatures, but also due to increased populations of these smaller species.

Changes in diet of *Neotoma* over time may also be related to differences in resource use among the species. Today, both *N. albigula* and *N. micropus* consume high proportions of cacti, such as *Opuntia* (Finley 1958, Dial 1988, Macêdo and Mares 1988, Braun and Mares 1989). Drought adapted CAM plants such as cacti typically have carbon isotope values that are similar to C_4 plants; mean (±SE) $\delta^{13}C$ values for *Opuntia* collected in Texas south of the Edwards Plateau is -15.6 (±0.2) ‰ (Mooney et al. 1974, Sutton 1976, Mooney et al. 1989, Boutton et al. 1998). Thus, shifts to higher $\delta^{13}C$ values in *Neotoma* may reflect a greater proportion of CAM in the diet. Indeed, we find a significant and positive correlation between the increase in the amount of the *Opuntia* cactus in the region and the use of C_4/CAM resources by *Neotoma* (Figure 3.6F). An increase in species abundances of *N. micropus* or *N. albigula* may be causing a shift to a more C_3-C_4/CAM diet. These regional vegetation shifts are also likely decreasing the habitat and resources *N. floridana* relies on for den building, and increasing those used by *N. micropus* and/or *N. albigula* (i.e. shrubs and cacti) (Rainey 1956, Finley 1958, Brown et al. 1972, Thies and Caire 1990). In modern populations, reduced appropriate habitat/materials for dens can lead to declines in *Neotoma* populations, generally related to reduced thermal and predator protection (Raun 1966, Brown 1968, Brown et al. 1972, Smith 1995, Ford et al. 2006). We find that while presence of cacti is significantly correlated changes in diet, juniper is not. Of the three species, *N. albigula* makes the most use of juniper, with it making up as much as 35% of the diet within some populations (Dial 1988). The lack of correlation with changes in juniper and diet (Figure 3.6G) may suggest *N. albigula* is present in lower abundances than *N. micropus* in the Hall's Cave record, potentially because the larger *N. micropus* is outcompeting the smaller species for space and resources (Finley 1958, Cameron 1971, Dial 1988). We also found no overall correlation between mass and diet

(Table 3.4), despite shifts towards smaller size and higher C_3-C_4/CAM consumption over time. If *N. micropus* abundances were higher than those *N. albigula*, the larger overlap in mass with co-occurring *N. floridana* may mask changes at the species level versus wider resource use at the genus level.

Overall, *Neotoma's* responses suggest a strong abiotic influence from climate at the terminal Pleistocene and a likely change in species abundances from *N. floridana* to *N. micropus* and/or *N. albigula* in the Holocene with changing resource availability. Interestingly, the response of *Neotoma* to the dramatic climate and community changes of the late Quaternary are considerably different from that of *Sigmodon* (cotton rat). Smaller than *Neotoma*, *Sigmodon* (80-150g in Texas today) is generally found in grassland habitats, where it forages mostly on grass leaves and seeds (Cameron and Spencer 1981, Kincaid and Cameron 1985, Randolph et al. 1991, Toomey 1993, Schmidly and Bradley 2016). Present in the Halls Cave record beginning 16,000 years ago, *Sigmodon* was heavily influenced by shifts in community composition and resource availability over temperature, with overall less variation in mass and diet than compared to *Neotoma* (Tomé et al., *in review*). Climatic fluctuations and ecosystem remodeling due to the megafauna extinction may both have played roles in vegetation shifts that led to changes in the mass and diet of both *Neotoma* and *Sigmodon* (Owen-Smith 1992). The differences in how *Neotoma* and *Sigmodon* responded to the late Pleistocene megafauna extinction and the cooccurring climatic changes of the Holocene in North America show important variation in the changes to individual species niches. Characterization of these niches through time provides insight into the regional vegetational and community shifts produced as a consequence of large-scale abiotic and biotic changes, which can inform how modern communities may respond to modern anthropogenic climate change and biodiversity loss.

APPENDIX 1

Table 1. Locality and accession information for *Neotoma* specimens used in analysis. Museum IDs correspond to the Smithsonian National Museum of Natural History (USNM) in Washington D.C., the Bell Museum of Natural History (MMNH) at the University of Minnesota (St. Paul, MN).

Species	Locality Name	State (Country)	Latitude	Longitude	N	Museum IDs
Neotoma albigula	Grants	New Mexico (USA)	35.15	-107.85	10	USNM: 137714, 137716, 137718, 137719, 137739, 138159, 138160, 138161, 138164, 138167
	Pima	Arizona (USA)	31.86	-110.71	10	USNM: 251307, 251312, 251313, 251314, 251315, 251318, 251319, 251320, 251321, 251326
Neotoma cinerea	Bennett City	British Columbia (Canada)	59.84	-134.99	10	USNM: 128218, 128588, 128589, 128590, 130204, 130205, 130206, 130207, 130208, 130209
	Jaspar House	Alberta (Canada)	52.95	-118.14	10	USNM: 75899, 75900, 75901, 75902, 75905, 75906, 75907, 75910, 75915, 75917
	Spokane	Washington (USA)	47.26	-117.71	10	USNM: 24188, 24189, 24190, 24191, 74775, 74778, 74779, 74780, 230075, 230462
	Klickitat	Washington (USA)	45.70	-120.76	10	USNM: 57139, 89738, 89742, 89743, 226192, 226193, 226194, 226196, 226198, 230460
	Big Horn	Montana (USA)	45.60	-107.46	10	USNM: 214708, 214709, 214710, 214711, 214723, 214724, 214725, 214726, 214727, 214728
	Harney	Oregon (USA)	42.98	-119.00	10	USNM: 79349, 79375, 79382, 80177, 80179, 80180, 205246, 216030, 216035, 222339
	Sweetwater	Wyoming (USA)	42.08	-110.04	10	USNM: 88297, 176909, 177489, 179306, 179307, 179308, 179477, 179478, 179479, 179480
	Bear Lake	Utah & Idaho (USA)	41.67	-111.79	10	USNM: 55181, 55381, 55382, 158533, 167507, 190335, 190336, 263987, 264308, 264309
	Donner	California (USA)	39.21	-120.01	10	USNM: 55547, 55780, 55783, 88327, 88328, 88329, 88330, 88331, 88332, 100661
Neotoma floridana	Wakarusa	Kansas (USA)	38.89	-95.31	10	MMNH: 12621, 12622, 12623, 12627, 12628, 12629, 12630, 12631, 12632, 12633
	Osage	Oklahoma (USA)	36.96	-96.57	10	MMNH: 10254, 11399, 11400, 11401, 11403, 11404, 12642, 12643, 12644, 12646
Neotoma lepida	Secret Valley	Nevada (USA)	40.72	-119.48	10	USNM: 67896, 67897, 78280, 78283, 78284, 78285, 78286, 78288, 94255, 94258
	Coso	California (USA)	36.18	-117.65	10	USNM: 28039, 28042, 28044, 28045, 28049, 28292, 28293, 28302, 28303, 28305
	Lees Ferry	Arizona (USA)	36.06	-112.13	10	USNM: 161167, 161169, 161171, 161173, 161175, 215542, 215543, 215544, 215638, 243126
	Panamint Valley	California (USA)	35.33	-116.10	10	USNM: 25343, 25344, 25345, 25346, 25347, 25348, 25349, 25350, 25351, 25356

Species	Locality Name	State (Country)	Latitude	Longitude	N	Museum IDs
	Oro Grande	California (USA)	34.60	-117.34	10	USNM: 136141, 136143, 136145, 136146, 136149, 136150, 136153, 136154, 136155, 136157
Neotoma mexicana	Loveland	Colorado (USA)	40.41	-105.10	10	USNM: 87674, 87677, 87678, 87679, 87680, 87681, 87682, 87921, 87922, 87923
	Manzano Mountains	New Mexico (USA)	34.71	-106.41	10	USNM: 131665, 131672, 131677, 131855, 131860, 131861, 131863, 131866, 131872, 131873
	Omiltemi	Guerrero (Mexico)	17.54	-99.52	10	USNM: 126892, 126920, 126923, 127498, 127499, 340638, 340641, 340642, 340643, 340645
Neotoma micropus	Fort Supply	Oklahoma (USA)	36.57	-99.57	10	USNM: 273225, 273227, 273232, 273322, 273323, 273325, 273326, 273327, 273328, 273699
	Major	Oklahoma (USA)	36.17	-98.92	10	MMNH: 12704, 12705, 12706, 12709, 12710, 12711, 12712, 12714, 12717, 12718

APPENDIX 2

1. Sensitivity Analyses

To test whether our selection and standardization of molars elements for mass estimation led to biases in our analysis, we ran several sensitivity analyses. First, we included all data, without the exclusion of potential duplicates or subadults, processed as described within the methods of the main text. Second, we reran analyses on all data but excluded potential subadults. Finally, we ran analyses on single elements, either upper or lower molars.

We conducted the analyses across both our pre- (12700-15800 cal BP) versus post- (0-12700 cal BP) extinction bins, and then across our 14-time intervals to test whether the inclusion of only lower or only upper molars changed the results we obtained from using minimum number of individuals (MNI) and a standardization of upper molars to estimate body size. This analysis therefore contained all 399 specimens for which we obtained molar length measurements, and were divided into 230 lower molar measurements and 169 upper molar measurements, including both left and right orientations. We analyzed variation across our pre- and post-extinction bins using the F-test and Two-sample T-test, and considered changes across our 14-time intervals using ANOVAs and Tukey Multiple Comparisons.

Analyses using all 399 mass estimates gave the same results as those given by data analyzed after applying our MNI, independent of whether subadults were maintained or removed. Analysis of all data, including potential duplicate individuals and subadults, found no significant change in the variation or distribution of mass across our pre- and post-extinction time intervals (F-test $P>0.05$, df=12/385, Two Sample T-test $P>0.1$, df=397) or across our 14-time intervals (ANOVA $P>0.1$, df=13/385). Similar results were obtained when subadults

were removed both for the pre- and post-extinction bins (F-test $P>0.05$, df=12/368, Two Sample T-test $P>0.1$, df=380) and 14-time intervals (ANOVA $P>0.1$, df=13/368).

Our results were consistent across lower and upper molars and those obtained using our MNI selection criteria, even with the inclusion of subadults. Analysis for pre- and post-extinction time intervals found no significant change in variation or distribution of mass as given by lower molar length (F-test $P>0.1$, df=5/223, Two Sample T-test $P>0.1$, df=228) or upper molar length (F-test $P>0.1$, df=6/161, Two Sample T-test $P>0.1$, df=167).

No significant differences were found across adjacent or non-adjacent 14-time intervals when only lower molar lengths were used (ANOVA $P>0.1$, df = 13/216). No significant differences were found across adjacent time intervals, but a single significant change in body size was found between non-adjacent time intervals for upper molars (ANOVA df=13/155, p-value<0.05, Tukey p-value<0.05 for time intervals 1500-3100 and 8400-9000 cal BP). This difference was found to be driven by a single outlier. Thus, the use of a single element did not alter our overall results, but because temporal bins were lost or low, it would compromise our ability to do other analyses, such as with our state space models.

Table 1. *Sigmodon* elements present within each time interval as given by stratigraphic depth (cm) and age range (cal BP). Elements included mandibles, maxilla or loose molars designated as follows: lower left first molar (LLM1), lower right first molar (LRM1), upper left first molar (ULM1) and upper right first molar (URM1). Mandibles or maxilla without first molars are designated as "other". "Total" are all molar measurements taken (N=399) across all time intervals. "Used in Analysis" is the number of molar measurements included after removal of potential duplicates using minimum number of individuals and removal of potential subadults. The age range comes from the age model presented in Appendix 2 Figure 1, Table 2.

		Sigmodon Elements Present					Molar Lengths	
Stratigraphic Depth (cm)	Age Range (cal BP)	LLM1	LRM1	ULM1	URM1	Other	Total	Used in Analysis
0 - 10	0 - 1500	2	8	5	2	4	17	14
10 - 35	1500 - 3100	6	5	6	8	8	25	18
35 - 70	3100 - 5400	6	3	5	3	5	17	13
70 - 80	5400 - 6100	4	8	5	3	8	20	13
80 - 85	6100 - 6400	6	6	2	7	14	21	13
85 - 90	6400 - 6700	12	7	6	3	1	28	19
90 - 105	6700 - 7700	8	9	3	1	15	21	16
105 - 115	7700 - 8400	12	11	9	3	7	35	25
115 - 125	8375 - 9033	19	11	12	15	16	57	34
125 - 130	9033 - 9363	3	2	9	8	4	22	15
130 - 140	9363 - 10021	10	18	11	5	5	44	26
140 - 155	10021 - 11010	22	23	14	11	5	70	45
155 - 180	11010 - 12656	0	3	4	2	0	9	7
180 - 230	12656 - 15095	5	1	4	3	22	13	12

2. Age Model

Table 2. Stratigraphic depth and radiocarbon and calibrated ages (cal BP).

Stratigraphic Depth (cm)	Calibrated Age (cal BP)
15-20	1207
15-20	1381
25-30	2182
25-30	2344
25-30	2372
40-45	2987
50-55	3522
50-55	5015
60-65	4462
65-70	5921
70-75	5284
80-85	5445
85-90	6200
90-95	6102
90-95	5005
100-105	7036
105-110	8480
120-125	9572
130-135	9810
130-135	9945
140-145	13271
145-150	11851
145-150	12033
145-150	12100
145-150	12172
145-150	12440
145-150	13059
155-160	13081
155-160	13146
160-165	13150
160-165	12100
160-165	13361
163	13339

Stratigraphic Depth (cm)	Calibrated Age (cal BP)
164	13225
164	13225
165-170	13260
175-180	13415
179	13702
185-190	13414
185-190	13435
190-195	13803
195-200	13903
210-215	16961
215-220	13977
215-220	15349
215-220	16913
220-225	14156
220-225	14608
220-225	14637
220-225	14698
220-225	14890
220-225	14994
230-235	14767
230-235	14804
235-240	17506
270-275	16253
295-300	19363
300-305	19743
305-310	19603
305-310	20017
315-320	19625
345-350	19918

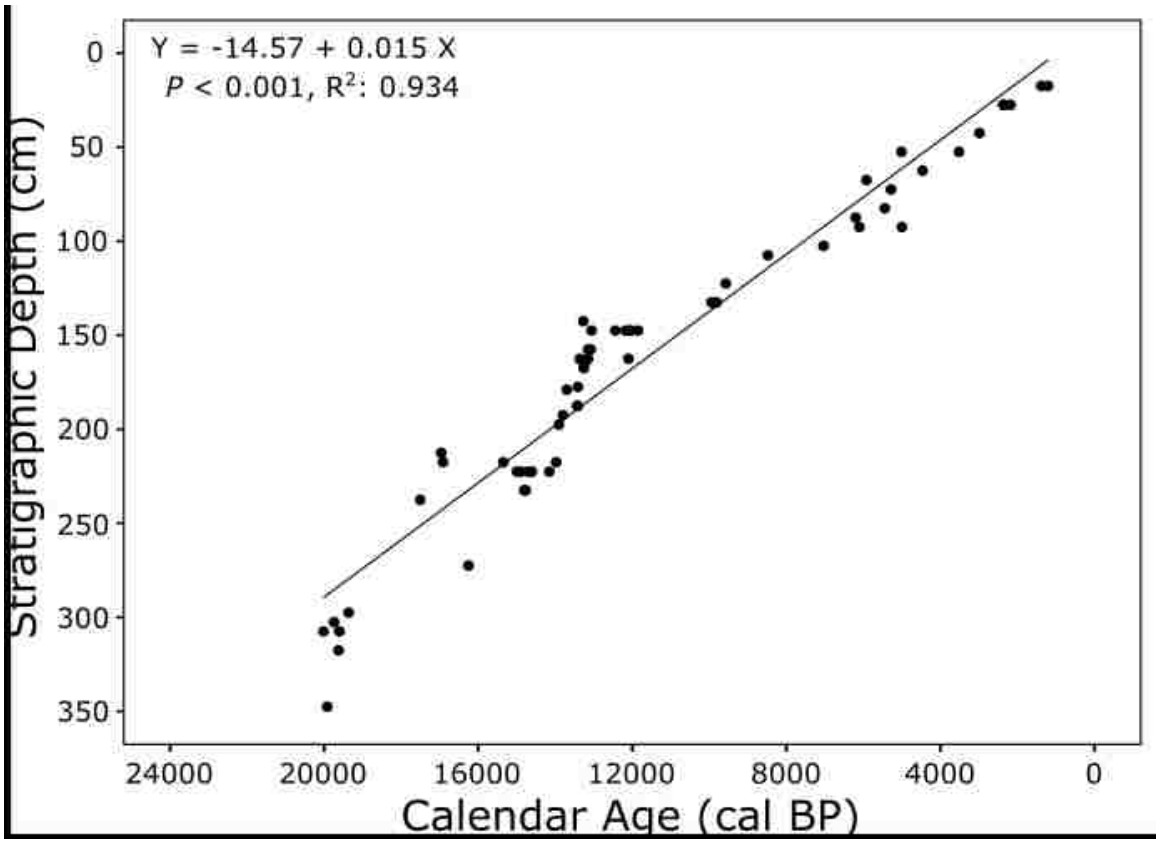

Figure 1. Age Model of Hall's Cave. Regression of calibrated radiocarbon ages (cal BP) and Stratigraphic Depth (cm) of the Hall's Cave fossil record. Because elements were binned into 5-15cm units, the midpoint of the stratigraphic depth was employed in the regression. A linear regression yielded an equation of Y = -14.57 + 0.015 X (df=61, P<0.001, R^2=0.934).

3. Additional Data

Table 3. First molars (M1) measurements of *Sigmodon hispidus* from the Museum of Southwestern Biology (MSB), University of New Mexico. Mean lengths of upper left (ULM1), upper right (URM1), lower left (LLM1) and lower right (LRM1) first molars are given with standard error (SE), as well as weight as it was recorded on the specimen tag are given. Measurements were taken using a AM4515ZT Dino-Lite Edge.

MSB ID	Weight (g)	ULM1 ± SE	URM1 ± SE	LLM1 ± SE	LRM1 ± SE
57610	157.0	2.26 ± 0.00	2.17 ± 0.01	2.47 ± 0.01	2.49 ± 0.00
57611	156.0	2.33 ± 0.01	2.22 ± 0.01	2.43 ± 0.02	2.54 ± 0.00
57612	150.0	2.31 ± 0.01	2.27 ± 0.00	2.53 ± 0.01	2.56 ± 0.01
57613	134.0	2.22 ± 0.00	2.3 ± 0.00	2.34 ± 0.01	2.34 ± 0.01
57615	187.0	2.16 ± 0.00	2.22 ± 0.01	2.4 ± 0.01	2.45 ± 0.01
57616	206.0	2.22 ± 0.02	2.21 ± 0.01	2.64 ± 0.01	2.61 ± 0.01
57617	142.5	2.25 ± 0.00	2.32 ± 0.00	2.52 ± 0.01	2.52 ± 0.01
57618	125.0	2.25 ± 0.01	2.22 ± 0.02	2.56 ± 0.00	2.56 ± 0.01
57619	118.0	2.32 ± 0.01	2.24 ± 0.01	2.44 ± 0.00	2.44 ± 0.01
57622	44.1	2.11 ± 0.01	2.14 ± 0.01	2.28 ± 0.01	2.33 ± 0.01
57624	160.0	2.23 ± 0.01	2.28 ± 0.01	2.55 ± 0.00	2.65 ± 0.00
88977	59.7	1.92 ± 0.00	1.96 ± 0.00	2.16 ± 0.01	2.22 ± 0.01
104054	99.7	2.18 ± 0.01	2.14 ± 0.01	2.41 ± 0.00	2.39 ± 0.00
104055	87.8	2.4 ± 0.01	2.48 ± 0.01	2.65 ± 0.00	2.69 ± 0.01
104056	96.5	2.00 ± 0.00	2.08 ± 0.01	2.35 ± 0.00	2.35 ± 0.00
140853	106.0	1.98 ± 0.02	1.89 ± 0.00	2.08 ± 0.01	2.13 ± 0.01
180617	73.5	2.29 ± 0.00	2.18 ± 0.01	2.45 ± 0.00	2.41 ± 0.00
180618	81.0	2.15 ± 0.00	2.14 ± 0.01	2.31 ± 0.01	2.34 ± 0.00
180619	47.0	2.17 ± 0.01	2.16 ± 0.01	2.25 ± 0.01	2.30 ± 0.01
180895	88.9	2.18 ± 0.01	2.23 ± 0.01	2.51 ± 0.01	2.60 ± 0.01

Table 4. Results of Tukey Honest Significant Differences on ANOVA (P<0.001, df=13/252) of δ^{15}N across all time interval. Only significant differences shown. Significance given as follow: *=p<0.05, **=p<0.01, ***=p<0.001.

Upper Age Range (cal BP)	Lower Age Range (cal BP)	Difference of Means	p-value
12656 - 15095	1458 - 3104	1.23	**
11010 - 12656	5410 - 6069	1.57	*
11010 - 12656	1458 - 3104	1.85	**
10021 - 11010	5410 - 6069	1.14	**
10021 - 11010	1458 - 3104	1.42	***
9363 - 10021	1458 - 3104	1.37	**
8375 - 9033	6069 - 6398	1.02	**
8375 - 9033	5410 - 6069	1.22	**
8375 - 9033	1458 - 3104	1.50	***
8375 - 9033	0 - 1458	1.24	*
7716 - 8375	6728 - 7716	1.16	**
7716 - 8375	6069 - 6398	1.42	***
7716 - 8375	5410 - 6069	1.62	***
7716 - 8375	1458 - 3104	1.90	***
7716 - 8375	0 - 1458	1.65	**

Table 5. Fit Linear Model results for $\delta^{13}C$ and $\delta^{15}N$ for each age interval. Significance denoted under p-value as follows: ns=not significant, *=p<0.05, **=p<0.01, ***=p<0.001.

Age Range (cal BP)	Adjusted R^2	p-value
0 - 1458	0.04	*ns*
1458 - 3104	-0.04	*ns*
3104 - 5410	0.28	*
5410 - 6069	0.08	*ns*
6069 - 6398	0.27	**
6398 - 6728	-0.14	*ns*
6728 - 7716	0.23	*
7716 - 8375	-0.05	*ns*
8375 - 9033	0.38	***
9033 - 9363	0.04	*ns*
9363 - 10021	0.21	*
10021 - 11010	0.40	***
11010 - 12656	-0.11	*ns*
12656 - 15095	0.11	*

Table 6. Outputs for 3 state-space model outputs for mass (Y_{mass}), $\delta^{13}C$ (Y_{carbon}) and $\delta^{15}N$ ($Y_{nitrogen}$) showing regression weight (β) values, with corresponding standard deviations (SD). All standard errors were < 0.05.

		Y_{mass}	SD_{mass}	Y_{carbon}	SD_{carbon}	$Y_{nitrogen}$	$SD_{nitrogen}$
Main Variables							
body size	β_1	~	~	0.0	0.0	0.0	0.00
$\delta^{13}C$	β_2	1.7	0.5	~	~	0.2	0.00
$\delta^{15}N$	β_3	1.0	1.2	1.2	0.2	~	~
Climate Variables							
mean precipitation	β_4	0.0	0.1	0.0	0.0	0.0	0.0
maximum temperature	β_5	0.9	1.9	-0.1	1.1	-0.8	0.8
minimum temperature	β_6	0.6	2.0	0.2	1.7	0.6	1.4
Community Variables							
α-diversity	β_7	-0.3	1.1	-0.3	1.0	0.0	0.9
β-diversity	β_8	0.1	1.9	0.4	2.0	-0.6	2.0
% browsers	β_9	-0.4	1.8	0.2	1.0	0.0	0.8
% carnivores	β_{10}	0.3	1.3	-0.2	0.8	0.0	0.7
% frugivores/granivores	β_{11}	0.4	1.8	0.5	0.9	-0.4	0.8
% grazers	β_{12}	-0.9	1.7	0.5	1.0	-0.1	0.8
% insectivores	β_{13}	-0.6	1.9	-0.8	1.1	0.3	0.8
% omnivores	β_{14}	0.7	1.9	-0.3	1.1	0.2	0.8

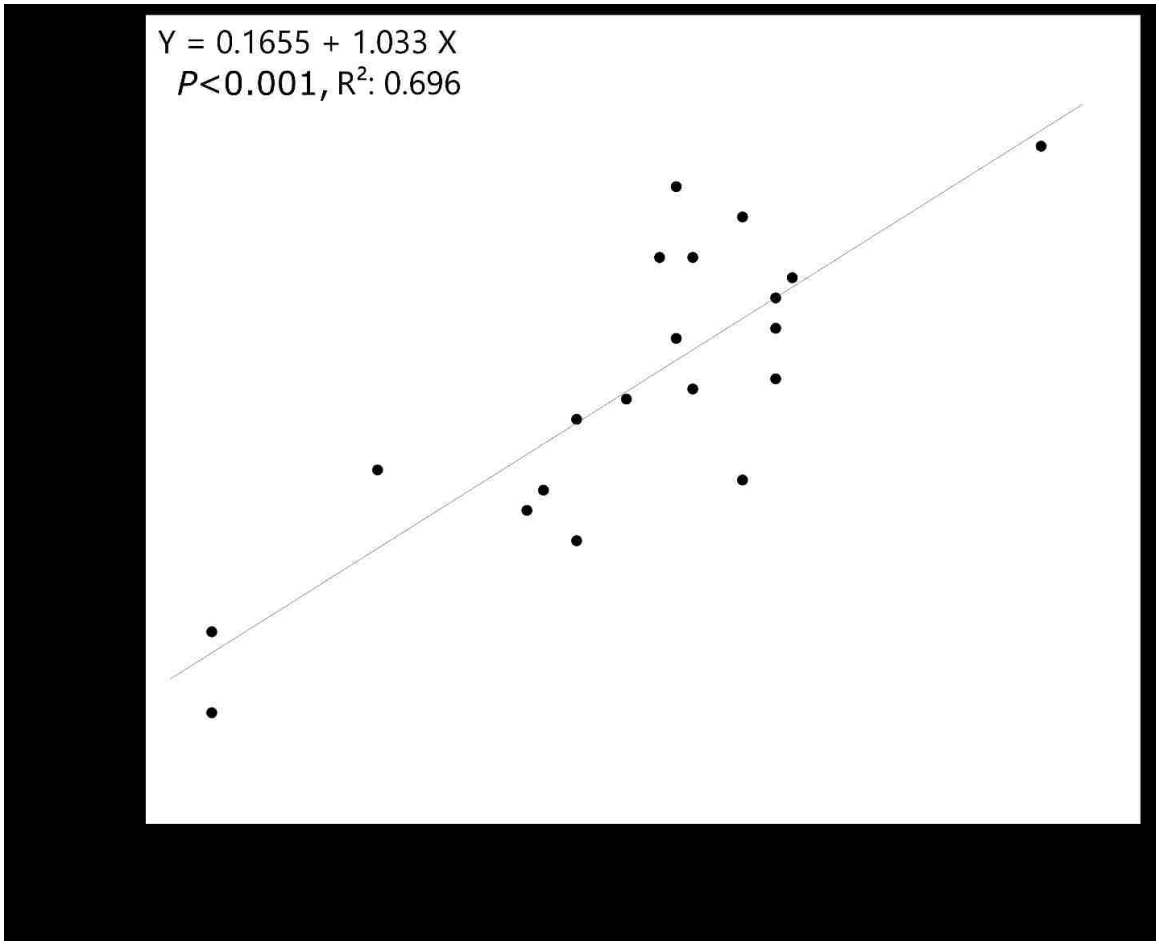

Figure 2. Upper and Lower First Molar Relationship. Linear fit of upper and lower first molar length (mm) of *Sigmodon hispidus.* Note: sample size is low (N=20), with $R^2 = 0.7$ and adjusted $R^2 = 0.68$.

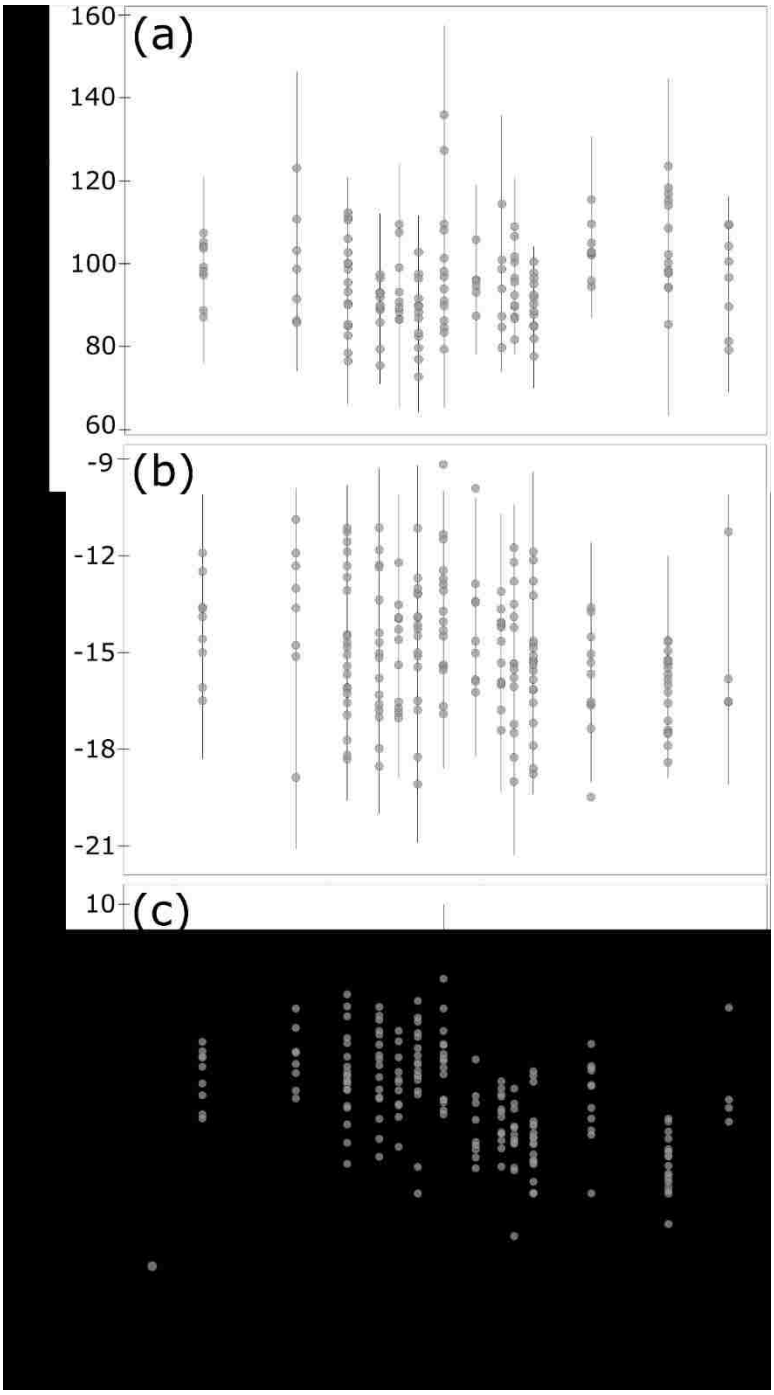

Figure 3: State-Space Models. Results of state space models showing the fit of modelled responses for a) mass, b) $\delta^{13}C$, c) $\delta^{15}N$. Black lines represent the range of raw data values. Grey circles are the output data from each model.

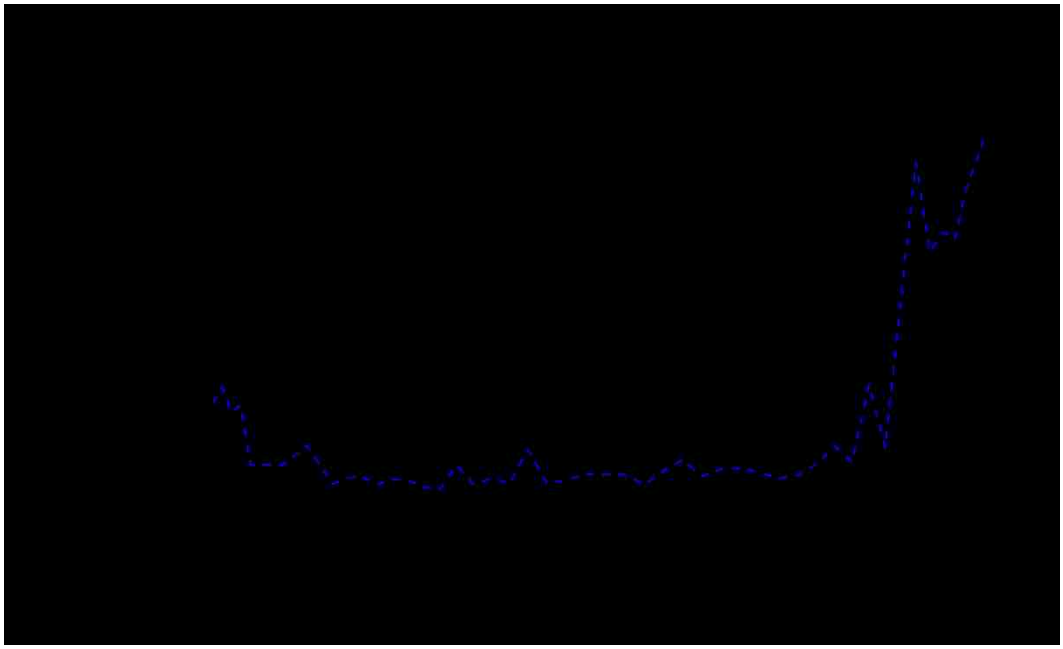

Figure 4: C_3 versus C_4 grasses at Hall's Cave over time. Plant fossil data from Cordova and Johnson 2019 showing the ratio of C_3 to C_4 grasses as a percent (solid line) and the proportion of grass out of all phytolith fossils (dashed blue line) present in the Hall's Cave record over 17000 years (cal BP).

APPENDIX 3

Table 1. Measurements of first upper and lower molars of modern *Neotoma* from the Bell Museum of Natural History (MMNH) and the Museum of Southwestern Biology (MSB). Mean lengths of upper left (ULM1) and right (URM1), lower left (LLM1) and right (LRM1) first molars are given with standard error (SE).

Museum ID	Specimen ID	ULM1 ± SE	URM1 ± SE	LLM1 ± SE	LRM1 ± SE
MMNH	10254	3.42 ± 0.02	3.41 ± 0.01	3.19 ± 0	3.16 ± 0
MMNH	11399	3.29 ± 0.01	3.17 ± 0	3.05 ± 0.01	3.11 ± 0.01
MMNH	11400	3.57 ± 0.01	3.55 ± 0.02	3.4 ± 0.02	3.32 ± 0
MMNH	11401	3.64 ± 0.03	3.68 ± 0	3.24 ± 0.01	3.26 ± 0.01
MMNH	11403	3.47 ± 0.01	3.6 ± 0	3.38 ± 0.01	3.3 ± 0
MMNH	11404	3.34 ± 0.03	3.36 ± 0.03	3.09 ± 0.01	3.12 ± 0
MMNH	12621	3.41 ± 0.03	3.39 ± 0.02	3.19 ± 0.04	3.18 ± 0.01
MMNH	12622	3.21 ± 0.01	3.26 ± 0.01	3.37 ± 0.04	3.41 ± 0.02
MMNH	12623	3.28 ± 0.02	3.26 ± 0.01	3.19 ± 0	3.28 ± 0.02
MMNH	12627	3.28 ± 0.02	3.25 ± 0.01	3.07 ± 0.01	3.07 ± 0
MMNH	12628	3.45 ± 0.01	3.39 ± 0.01	3.48 ± 0	3.42 ± 0.01
MMNH	12629	3.69 ± 0.01	3.52 ± 0.03	3.81 ± 0.01	3.63 ± 0.03
MSB	109867	3.12 ± 0.02	3.13 ± 0.01	2.86 ± 0.01	2.77 ± 0.02
MSB	109868	3.25 ± 0	3.17 ± 0	2.82 ± 0.02	2.82 ± 0
MSB	109963	2.88 ± 0	2.88 ± 0	2.62 ± 0.01	2.66 ± 0.01
MSB	109964	3.02 ± 0	2.94 ± 0.01	2.75 ± 0.02	2.74 ± 0.01
MSB	109998	3.28 ± 0.01	3.19 ± 0	3.07 ± 0.01	3.11 ± 0.01
MSB	109999	2.86 ± 0	2.89 ± 0.01	2.88 ± 0.01	2.85 ± 0
MSB	121289	3.04 ± 0	3.01 ± 0.01	2.92 ± 0.01	2.87 ± 0
MSB	121308	3.23 ± 0	3.17 ± 0.03	3.15 ± 0.01	3.15 ± 0.01
MSB	121332	3.05 ± 0.01	3.03 ± 0	2.92 ± 0.01	2.92 ± 0
MSB	121401	3.21 ± 0.01	3.11 ± 0.02	3.05 ± 0.01	3.08 ± 0.02

Table 2. Tukey Honest Significant Differences on ANOVA of mass ($p<0.001$, $df=14/381$), $\delta^{13}C$ ($p<0.001$, $df=14/270$), and $\delta^{15}N$ ($p<0.001$, $df=14/270$) across all time interval. Significant p-values are bolded.

		Mass (g)		$\delta^{13}C$ (‰)		$\delta^{15}N$ (‰)	
Upper Mid-age (cal BP)	Lower Mid-age (cal BP)	Diff.	p-value	Diff.	p-value	Diff.	p-value
2280	730	11.5	1.000	-1.4	0.977	-0.4	1.000
4260	730	33.8	0.591	-0.1	1.000	-0.1	1.000
5740	730	30.2	0.877	0.1	1.000	-0.4	1.000
6230	730	29.6	0.938	0.2	1.000	0.0	1.000
6560	730	19.6	1.000	-0.8	1.000	-0.7	0.995
7220	730	16.7	0.999	0.6	1.000	0.1	1.000
8050	730	32.6	0.877	0.3	1.000	0.5	1.000
8700	730	36.6	0.672	0.0	1.000	0.3	1.000
9200	730	58.9	0.117	-0.5	1.000	0.6	1.000
9690	730	52.5	0.119	0.0	1.000	0.2	1.000
10520	730	33.2	0.743	-1.5	0.874	0.0	1.000
11830	730	40.6	0.316	-1.3	0.973	0.2	1.000
14230	730	42.2	0.245	-1.1	0.994	-0.9	0.884
19100	730	59.7	**0.025**	-1.7	0.985	-1.7	0.533
4260	2280	22.3	0.517	1.3	0.855	0.3	1.000
5740	2280	18.7	0.959	1.5	0.857	0.0	1.000
6230	2280	18.1	0.991	1.7	0.937	0.4	1.000
6560	2280	8.1	1.000	0.7	1.000	-0.3	1.000
7220	2280	5.1	1.000	2.1	0.238	0.5	0.999
8050	2280	21.0	0.965	1.7	0.738	0.9	0.845
8700	2280	25.1	0.767	1.4	0.898	0.7	0.986
9200	2280	47.3	0.108	0.9	1.000	1.0	0.934
9690	2280	41.0	0.072	1.4	0.917	0.6	0.988
10520	2280	21.7	0.825	-0.1	1.000	0.4	1.000
11830	2280	29.1	0.185	0.1	1.000	0.6	0.989
14230	2280	30.7	0.110	0.4	1.000	-0.5	0.999
19100	2280	48.2	0.005	-0.3	1.000	-1.3	0.852
5740	4260	-3.6	1.000	0.2	1.000	-0.2	1.000
6230	4260	-4.2	1.000	0.3	1.000	0.2	1.000
6560	4260	-14.2	1.000	-0.7	1.000	-0.6	0.990
7220	4260	-17.2	0.860	0.7	0.975	0.2	1.000
8050	4260	-1.2	1.000	0.3	1.000	0.6	0.873
8700	4260	2.8	1.000	0.1	1.000	0.4	0.998
9200	4260	25.1	0.907	-0.5	1.000	0.7	0.976
9690	4260	18.7	0.945	0.1	1.000	0.4	0.998
10520	4260	-0.6	1.000	-1.4	0.241	0.1	1.000

		Mass (g)		$\delta^{13}C$ (‰)		$\delta^{15}N$ (‰)	
Upper Mid-age (cal BP)	Lower Mid-age (cal BP)	Diff.	p-value	Diff.	p-value	Diff.	p-value
11830	4260	6.8	1.000	-1.2	0.748	0.4	0.999
14230	4260	8.4	1.000	-1.0	0.854	-0.7	0.464
19100	4260	25.9	0.500	-1.6	0.959	-1.5	0.391
6230	5740	-0.6	1.000	0.2	1.000	0.4	1.000
6560	5740	-10.6	1.000	-0.9	1.000	-0.4	1.000
7220	5740	-13.6	0.998	0.5	1.000	0.5	0.995
8050	5740	2.3	1.000	0.2	1.000	0.9	0.697
8700	5740	6.4	1.000	-0.1	1.000	0.7	0.963
9200	5740	28.6	0.894	-0.6	1.000	1.0	0.890
9690	5740	22.3	0.943	-0.1	1.000	0.6	0.965
10520	5740	3.0	1.000	-1.6	0.416	0.4	1.000
11830	5740	10.4	1.000	-1.4	0.792	0.6	0.971
14230	5740	12.0	0.999	-1.1	0.896	-0.5	0.993
19100	5740	29.5	0.599	-1.8	0.943	-1.3	0.782
6560	6230	-10.0	1.000	-1.0	1.000	-0.8	0.992
7220	6230	-13.0	1.000	0.4	1.000	0.0	1.000
8050	6230	2.9	1.000	0.0	1.000	0.4	1.000
8700	6230	7.0	1.000	-0.2	1.000	0.2	1.000
9200	6230	29.2	0.931	-0.8	1.000	0.5	1.000
9690	6230	22.9	0.971	-0.3	1.000	0.2	1.000
10520	6230	3.6	1.000	-1.8	0.766	-0.1	1.000
11830	6230	11.0	1.000	-1.6	0.925	0.2	1.000
14230	6230	12.6	1.000	-1.3	0.974	-0.9	0.877
19100	6230	30.1	0.747	-2.0	0.960	-1.7	0.521
7220	6560	-2.9	1.000	1.4	0.897	0.8	0.906
8050	6560	13.0	1.000	1.0	0.997	1.2	0.444
8700	6560	17.0	1.000	0.8	1.000	1.0	0.788
9200	6560	39.3	0.784	0.2	1.000	1.3	0.665
9690	6560	32.9	0.861	0.7	1.000	1.0	0.792
10520	6560	13.6	1.000	-0.8	1.000	0.7	0.964
11830	6560	21.0	0.992	-0.6	1.000	1.0	0.807
14230	6560	22.6	0.983	-0.3	1.000	-0.1	1.000
19100	6560	40.1	0.556	-0.9	1.000	-0.9	0.991
8050	7220	15.9	0.997	-0.4	1.000	0.4	0.998
8700	7220	20.0	0.946	-0.6	1.000	0.2	1.000
9200	7220	42.2	0.237	-1.2	0.988	0.5	0.999
9690	7220	35.8	0.196	-0.7	0.999	0.2	1.000
10520	7220	16.5	0.974	-2.2	**0.007**	-0.1	1.000
11830	7220	23.9	0.473	-2.0	0.114	0.2	1.000

		Mass (g)		$\delta^{13}C$ (‰)		$\delta^{15}N$ (‰)	
Upper Mid-age (cal BP)	Lower Mid-age (cal BP)	Diff.	p-value	Diff.	p-value	Diff.	p-value
14230	7220	25.6	0.333	-1.7	0.123	-0.9	0.175
19100	7220	43.1	**0.022**	-2.3	0.614	-1.7	0.214
8700	8050	4.1	1.000	-0.2	1.000	-0.2	1.000
9200	8050	26.3	0.971	-0.8	1.000	0.1	1.000
9690	8050	19.9	0.992	-0.3	1.000	-0.2	1.000
10520	8050	0.6	1.000	-1.8	0.255	-0.5	0.988
11830	8050	8.0	1.000	-1.6	0.637	-0.2	1.000
14230	8050	9.7	1.000	-1.3	0.761	-1.4	**0.021**
19100	8050	27.2	0.863	-2.0	0.892	-2.2	0.051
9200	8700	22.2	0.989	-0.6	1.000	0.3	1.000
9690	8700	15.9	0.998	-0.1	1.000	0.0	1.000
10520	8700	-3.4	1.000	-1.5	0.514	-0.3	1.000
11830	8700	4.0	1.000	-1.4	0.852	0.0	1.000
14230	8700	5.6	1.000	-1.1	0.937	-1.1	0.153
19100	8700	23.1	0.923	-1.7	0.959	-1.9	0.147
9690	9200	-6.4	1.000	0.5	1.000	-0.3	1.000
10520	9200	-25.7	0.941	-1.0	0.998	-0.6	0.998
11830	9200	-18.3	0.995	-0.8	1.000	-0.3	1.000
14230	9200	-16.6	0.998	-0.5	1.000	-1.5	0.208
19100	9200	0.9	1.000	-1.2	1.000	-2.2	0.116
10520	9690	-19.3	0.975	-1.5	0.550	-0.3	1.000
11830	9690	-11.9	1.000	-1.3	0.877	0.0	1.000
14230	9690	-10.3	1.000	-1.0	0.953	-1.1	0.147
19100	9690	7.2	1.000	-1.7	0.967	-1.9	0.148
11830	10520	7.4	1.000	0.2	1.000	0.3	1.000
14230	10520	9.0	1.000	0.5	1.000	-0.9	0.359
19100	10520	26.5	0.697	-0.2	1.000	-1.7	0.301
14230	11830	1.6	1.000	0.3	1.000	-1.1	0.170
19100	11830	19.1	0.932	-0.4	1.000	-1.9	0.157
19100	14230	17.5	0.963	-0.7	1.000	-0.8	0.994

Table 3. Tukey Honest Significant Differences on ANOVA $\delta^{13}C$ ($p<0.05$, df=3/106) across aggregate mass groups.

Mass Group 1	Mass Group 2	Diff.	p-value
180-225g	<180g	1.3	0.072
225-280g	<180g	0.8	0.420
>280g	<180g	-0.6	0.884
225-280g	180-225g	-0.4	0.814
>280g	180-225g	-1.9	0.076
>280g	225-280g	-1.4	0.267

REFERENCES

Adams, D. C. 1999. Methods for shape analysis of landmark data from articulated structures. Evolutionary Ecology Research 1: 959–970.

Adams, D. C., F. J. Rohlf, and D. E. Slice. 2004. Geometric morphometrics: Ten years of progress following the 'revolution.' Italian Journal of Zoology 71: 5–16. doi: 10.1080/11250000409356545

Adams, D. C., M. L. Collyer, and A. Kaliontzopoulou. 2018. Geomorph: Software for geometric morphometric analyses. R package version 3.0.6. https://cran.r-project.org/package=geomorph.

Adebowale, A., A. Nicholas, J. Lamb, and Y. Naidoo. 2012. Elliptic Fourier analysis of leaf shape in southern African Strychnos section Densiflorae (Loganiaceae). Botanical Journal of the Linnean Society 170: 542-553. doi: 10.1111/j.1095-8339.2012.01308.x

Alley, R. B. 2000. The Younger Dryas cold interval as viewed from central Greenland. Quaternary Science Reviews 19: 213–226. doi: 10.1016/S0277-3791(99)00062-1

Alroy, J. 1999. Putting North America's end-Pleistocene megafaunal extinction into context. - In: MacPhee, R. D. E. (ed), Extinctions in near time. Springer US, pp. 105–143. doi: 10.1007/978-1-4757-5202-1_6

Ambrose, S. H. 1990. Preparation and characterization of bone and tooth collagen for isotopic analysis. Journal of Archaeological Science 17: 431–451. doi: 10.1016/0305-4403(90)90007-R

Ambrose, S. H. 1991. Effects of Diet, Climate and Physiology on Nitrogen Isotope Abundances in Terrestrial Foodwebs. Journal of Archaeological Science 18: 293–317. doi: 10.1016/0305-4403(91)90067-Y

Amundson, R. et al. 2003. Global patterns of the isotopic composition of soil and plant nitrogen. Global Biogeochemical Cycles. 17: 1031-1062. doi: 10.1029/2002GB001903

Andrewartha, H. G. and L. C. Birch. 1986. The ecological web: more on the distribution and abundance of animals. University of Chicago Press.

Ashton, K. G. et al. 2000. Is Bergmann's Rule Valid for Mammals? The American Naturalist 156: 390–415. doi: 10.2307/3079173

Asner, G. P. et al. 2009. Large-scale impacts of herbivores on the structural diversity of African savannas. Proceedings of the National Academy of Sciences 106: 4947–4952. doi: 10.1073/pnas.0810637106

Auffray, J. C., S. Renaud, and J. Claude. 2009. Rodent biodiversity in changing environments. Kasetsart Journal, Natural Sciences. 43: 83-93.

Austin, A. T. and P. M. Vitousek. 1998. Nutrient dynamics on a precipitation gradient in Hawai'i. Oecologia 113: 519–529. doi: 10.1007/s004420050405

Baker, R. H. and K. A. Shump Jr. 1978. *Sigmodon ochrognathus*. Mammalian Species 97: 1-2. doi: 10.2307/3503861

Bakker, E. S. et al. 2006. Herbivore impact on grassland plant diversity depends on habitat productivity and herbivore size. Ecology Letters 9: 780–788. doi: 10.1111/j.1461-0248.2006.00925.x

Bakker, E. S. et al. 2016. Combining paleo-data and modern exclosure experiments to assess the impact of megafauna extinctions on woody vegetation. Proceedings of the National Academy of Sciences. 113: 847-855. doi: 10.1073/pnas.1502545112

Barnosky, A. D. 2004. Biodiversity response to climate change in the Middle Pleistocene: the Porcupine Cave fauna of Colorado. University of California Press. doi: 10.1525/california/9780520240827.001.0001

Barnosky, A. D. et al. 2003. Mammalian Response to Global Warming on Varied Temporal Scales. Journal of Mammalogy 84: 354–368. doi: 10.1644/1545-1542(2003)084<0354:MRTGWO>2.0.CO;2

Barron-Ortiz, C. R. and J. Theodor. 2011. A geometric morphometric study of North American late Pleistocene equid upper premolars and its potential significance for equid systematics. Current Research in the Pleistocene 28: 147-149.

Batzli, G. O. and F. R. Cole. 1979. Nutritional ecology of microtine rodents: digestibility of forage. Journal of Mammalogy 60: 740-750. doi: 10.2307/1380189

Bender, M. M. 1971. Variations in the $^{13}C/^{12}C$ ratios of plants in relation to the pathway of photosynthetic carbon dioxide fixation. Phytochemistry 10: 1239-1244. doi: 10.1016/S0031-9422(00)84324-1

Bergmann, C. 1847. Über die Verhältnisse der Wärmeökonomie der Thiere zu ihrer Größe. Göttinger Stud. 3: 595-708.

Bergstrom, B. J. 2013. Would East African savanna rodents inhibit woody encroachment? Evidence from stable isotopes and microhistological analysis of feces. Journal of Mammalogy 94: 436-447. doi: 10.1644/12-MAMM-A-146.1

Betancourt, J. L., T. R. Van Devender, and P. S. Martin. (ed.). 1990. Packrat middens: the last 40,000 years of biotic change. University of Arizona Press.

Birney, E. C. et al. 1975. Eye Lens Proteins as Criteria of Age in Cotton Rats. The Journal of Wildlife Management 39: 718-728. doi: 10.2307/3800233

Blackburn, T. M. et al. 1999. Geographic gradients in body size: a clarification of Bergmann's rule. Diversity and Distributions 5: 165-174. doi: 10.1046/j.1472-4642.1999.00046.x

Blois, J. L. et al. 2010 Small mammal diversity loss in response to late-Pleistocene climatic change. Nature 465: 771. doi: 10.1038/nature09077

Blois, J. L. et al. 2013. Climate change and the past, present, and future of biotic interactions. Science 341: 499–504. doi: 10.1126/science.1237184

Bonhomme, V. et al. 2012. Momocs package. http://cran.r-project.org/web/packages/Momocs/index.html

Bonhomme, V. et al. 2014. Momocs: Outline Analysis Using R. Journal of Statistical Software 56: 1-24. doi: 10.18637/jss.v056.i13

Bonhomme, V. et al. 2013. Interspecific variability of pollen morphology as revealed by elliptic Fourier analysis. Plant Systematics and Evolution 299: 811-816. doi: 10.1007/s00606-013-0762-5

Bookstein, F. L. 1997. Morphometric tools for landmark data: geometry and biology. Cambridge University Press. doi: 10.2307/2534038

Bourne, M. D. et al. 2016. High-intensity geomagnetic field 'spike' observed at ca. 3000 cal BP in Texas, USA. Earth and Planetary Science Letters 442: 80-92. doi: 10.1016/j.epsl.2016.02.051

Boutton, T. W. et al. 1993. Stable carbon isotope ratios of soil organic matter and their potential use as indicators of palaeoclimate. (pp. 445-459) In Proceedings of the International Symposium on Applications of Isotope Techniques in Studying Past and Current Environmental Changes in the Hydrosphere and the Atmosphere. IAEA.

Boutton, T. W. et al. 1998. $\delta^{13}C$ values of soil organic carbon and their use in documenting vegetation change in a subtropical savanna ecosystem. Geoderma 82: 5-41. doi: 10.1016/S0016-7061(97)00095-5

Bowers, M. A. and J. H. Brown. 1982. Body size and coexistence in desert rodents: chance or community structure? Ecology 63: 391-400. doi: 10.2307/1938957

Brown, J. H. 1968. Adaptation to environmental temperature in two species of woodrats, *Neotoma cinerea* and *N. albigula*. Miscellaneous Publications, Museum of Zoology, University of Michigan. 135: 1-48.

Brown, J. H. 1973. Species diversity of seed-eating desert rodents in sand dune habitats. Ecology 54: 775-787. doi: 10.2307/1935672

Brown, J. H. and A. K. Lee. 1969. Bergmann's rule and climatic adaptation in woodrats (*Neotoma*). Evolution 23: 329-338. doi: 10.2307/2406795

Brown, J. H. and J. C. Munger. 1985. Experimental manipulation of a desert rodent community: food addition and species removal. Ecology 66: 1545–1563. doi: 10.2307/1938017

Brown, J. H. and E. J. Heske. 1990. Temporal changes in a Chihuahuan Desert rodent community. Oikos 59: 290-302. doi: 10.2307/3545139

Brown, J. H. and P. F. Nicoletto. 1991. Spatial scaling of species composition: body masses of North American land mammals. The American Naturalist 138: 1478-1512. doi: 10.1086/285297

Brown, J. H. et al. 1972. Woodrats and cholla: dependence of a small mammal population on the density of cacti. Ecology 53: 310-313. doi: 10.2307/1934087

Brown, J. H. et al. 1997. Reorganization of an arid ecosystem in response to recent climate change. Proceedings of the National Academy of Sciences 94: 9729–9733. doi: 10.1073/pnas.94.18.9729

Brown, J. H. et al. 2001. Complex species interactions and the dynamics of ecological systems: Long-term experiments. Science 293: 643–650. doi: 10.1126/science.293.5530.643

Braun, J. K. and M. A. Mares. 1989. *Neotoma micropus*. Mammalian Species 330: 1-9. doi: 10.2307/3504233

Brown, J. S. 1996. Coevolution and community organization in three habitats. Oikos 75: 193-206. doi: 10.2307/3546243

Bryant Jr, V. M. and R. G. Holloway. 1985. A late-Quaternary paleoenvironmental record of Texas: an overview of the pollen evidence. Pollen records of late-Quaternary North American sediments, pp.39-70.

Calder, W. A. 1984. Size, function, and life history. Courier Corporation.

Cameron, G. N. 1971. Niche overlap and competition in woodrats. Journal of Mammalogy 52: 288-296. doi: 10.2307/1378673

Cameron, G. N. 1977. Experimental Species Removal: Demographic Responses by *Sigmodon hispidus* and *Reithrodontomys fulvescens*. Journal of Mammalogy 58: 488-506. doi: 10.2307/1379997

Cameron, G. N. and D. G. Rainey. 1972. Habitat utilization by *Neotoma lepida* in the Mohave desert. Journal of Mammalogy 53: 251-266. doi: 10.2307/1379160

Cameron, G. N. and B. D. Eshelman. 1996. Growth and reproduction of hispid cotton rats (*Sigmodon hispidus*) in response to naturally occurring levels of dietary protein. Journal of Mammalogy 77: 220-231. doi: 10.2307/1382723

Cameron, G. N. and S. R. Spencer. 1981. *Sigmodon hispidus*. Mammalian Species 158: 1–9. doi: 10.2307/3504057

Carey, A. B. 1991. The biology of arboreal rodents in Douglas-fir forests. Gen. Tech. Rep. PNW-GTR-276. Portland, OR: US Department of Agriculture, Forest Service, Pacific Northwest Research Station. 46: 276. doi: 10.2737/PNW-GTR-276

Carrasco, M. A. 2000. Species discrimination and morphological relationships of kangaroo rats (*Dipodomys*) based on their dentition. Journal of Mammalogy 81:107-122. doi: 10.1644/1545-1542(2000)081<0107:SDAMRO>2.0.CO;2

Carraway, L. N. and B. J. Verts. 1991. *Neotoma fuscipes*. Mammalian Species 386: 1–10. doi: 10.2307/3504130

Cerling, T. E. et al. 1997. Global vegetation change through the Miocene/Pliocene boundary. Nature 389: 153-158. doi: 10.1038/38229

Claude, J. 2008. Morphometrics with R. Springer Science & Business Media.

Cole, K.L. and S.T. Arundel. 2005. Carbon isotopes from fossil packrat pellets and elevational movements of Utah agave plants reveal the Younger Dryas cold period in Grand Canyon, Arizona. Geology 33: 713-716. doi: 10.1130/G21769.1

Commandeur J. J. and S. J. Koopman. 2007. Practical Econometrics: an introduction to state space time series analysis.

Cooke, M. J. et al. 2003. Precise timing and rate of massive late Quaternary soil denudation. Geology 31: 853–856. doi: 10.1130/G19749.1

Cornely, J. E. and R. J. Baker. 1986. *Neotoma mexicana*. Mammalian Species 262: 1-7. doi: 10.2307/3504054

Cotton, J. M. et al. 2016. Climate, CO_2, and the history of North American grasses since the Last Glacial Maximum. Science Advances 2: e1501346. doi: 10.1126/sciadv.1501346

Dalquest, W. W. et al. 1969. The mammal fauna of Schulze Cave, Edwards County, Texas. Bulletin of the Florida State Museum 13: 205-276.

Daly, C. et al. 1994. A statistical topographic model for mapping climatological precipitation over mountainous terrain. Journal of Applied Meteorology 33: 140-158. doi: 10.1175/1520-0450(1994)033<0140:ASTMFM>2.0.CO;2

Dammhahn, M. et al. 2013. Trophic Niche Differentiation and Microhabitat Utilization in a Species-rich Montane Forest Small Mammal Community of Eastern Madagascar. Biotropica 45: 111-118. doi: 10.1111/j.1744-7429.2012.00893.x

Damuth, J. 1981. Population density and body size in mammals. Nature 290: 699–700. doi: 10.1038/290699a0

Damuth, J. and B. J. MacFadden. 1990. Body size in mammalian paleobiology: estimation and biological implications. Cambridge University Press.

Dansgaard, W., J. W. C. White and S. J. Johnsen. 1989. The abrupt termination of the Younger Dryas climate event. Nature 339: 532. doi: 10.1038/339532a0

Davidson, A. D. et al. 2009. Multiple ecological pathways to extinction in mammals. Proceedings of the National Academy of Sciences 106: 10702-10705. doi: 10.1073/pnas.0901956106

Dawson, T. E. et al. 2002. Stable Isotopes in Plant Ecology. Annual Review of Ecology and Systematics 33: 507-559. doi: 10.1146/annurev.ecolsys.33.020602.095451

Dearing, M. D et al. 2005. Woodrat (*Neotoma*) herbivores maintain nitrogen balance on a low-nitrogen, high-phenolic forage, *Juniperus monosperma*. Journal of Comparative Physiology B 175: 349-355. doi: 10.1007/s00360-005-0491-3

DeNiro, M. J. and S. Epstein. 1978. Influence of diet on the distribution of carbon isotopes in animals. Geochimica et Cosmochimica Acta 42: 495-506. doi: 10.1016/0016-7037(78)90199-0

DeNiro, M. J. and S. Epstein. 1981. Influence of diet on the distribution of nitrogen isotopes in animals. Geochimica et Cosmochimica Acta 45: 341-351. doi: 10.1016/0016-7037(81)90244-1

Derner, J. D. et al. 2006. Grazing and ecosystem carbon storage in the North American Great Plains. Plant and Soil 280: 77-90. doi: 10.1007/s11104-005-2554-3

DeVisser, S. N. et al. 2008. Trophic interactions among invertebrates in termitaria in the African savanna: a stable isotope approach. Ecological Entomology 33: 758-764. doi: 10.1111/j.1365-2311.2008.01029.x

Dial, K. P. 1988. Three sympatric species of *Neotoma*: dietary specialization and coexistence. Oecologia 76: 531-537. doi: 10.1007/BF00397865

Didan, K. 2015. MOD13C1 MODIS/Terra Vegetation Indices 16-Day L3 Global 0.05Deg CMG V006 [Data set]. NASA EOSDIS Land Processes DAAC. doi:10.5067/MODIS/MOD13C1.006

Dirzo, R. et al. 2014. Defaunation in the Anthropocene. Science 345: 401-406. doi: 10.1126/science.1251817

Doughty, C. E., et al. 2013. The legacy of the Pleistocene megafauna extinctions on nutrient availability in Amazonia. Nature Geoscience 6: 761-764. doi: 10.1038/ngeo1895

Dublin, H. T. et al. 1990. Elephants and fire as causes of multiple stable states in the Serengeti-Mara woodlands. The Journal of Animal Ecology 59: 1147-1164. doi: 10.2307/5037

Dunaway, P. B. and S. V. Kaye. 1961. Cotton rat mortality during severe winter. Journal of Mammalogy 42: 265-268. doi: 10.2307/1376850

Durbin, J. and S. J. Koopman. 2001. Time series analysis by state space models. Oxford University Press.

Edgar, R. C. 2004 MUSCLE: multiple sequence alignment with high accuracy and high throughput. Nucleic Acids Research 32:1792-1797. doi: 10.1093/nar/gkh340

Eifler, M. A. and N. A. Slade. 1998. Activity patterns in relation to body mass and ambient temperature among overwintering cotton rats (*Sigmodon hispidus*). Canadian Journal of Zoology 76: 668-672. doi: 10.1139/z97-241

Ellwood, B. B. and W. A. Gose. 2006. Heinrich H1 and 8200 yr B.P. climate events recorded in Hall's Cave, Texas. Geology 34: 753-756. doi: 10.1130/G22549.1

Ernest, S. K. M. et al. 2000. Rodents, plants, and precipitation: Spatial and temporal dynamics of consumers and resources. Oikos 88: 470-482. doi: 10.1034/j.1600-0706.2000.880302.x

Estes, J. A. et al. 1998. Killer whale predation on sea otters linking oceanic and nearshore ecosystems. Science 282: 473-476. doi: 10.1126/science.282.5388.473

Estes, J. A. et al. 2011. Trophic downgrading of planet earth. Science 333: 301-306. doi: 10.1126/science.1205106

Evans, A. R et al. 2007. High-level similarity of dentitions in carnivorans and rodents. Nature 445: 78-81. doi: 10.1038/nature05433

Evans, A. R. and G. D. Sanson. 2003. The tooth of perfection: Functional and spatial constraints on mammalian tooth shape. Biological Journal of the Linnean Society 78:173-191. doi: 10.1046/j.1095-8312.2003.00146.x

Farquhar, G. D et al. 1989. Carbon isotope discrimination and photosynthesis. Annual Review of Plant Biology 40: 503-537. doi: 10.1146/annurev.arplant.40.1.503

Finley, R. B. 1958. The Wood Rats of Colorado, Distribution and Ecology. University of Kansas Publications, Museum of Natural History. 10: 213-552.

Fleharty, E. D. and M. A. Mares. 1972. Fluctuation in Population Density of the Hispid Cotton Rat: Factors Influencing a" Crash". Bulletin of the Southern California Academy of Sciences 71: 132-138.

Flowerdew, J. R. et al. 2017. Strong "bottom-up" influences on small mammal populations: State-space model analyses from long-term studies. Ecology and Evolution 7: 1699–1711. doi: 10.1002/ece3.2725

Ford, W. M. et al. 2006. Persistence of Allegheny woodrats Neotoma magister across the mid-Atlantic Appalachian Highlands landscape, USA. Ecography 29: 745-754. doi: 10.1111/j.0906-7590.2006.04703.x

Fortelius, M. 1985. Ungulate cheek teeth: developmental, functional, and evolutionary interrelations. Acta Zoologica Fennica 180:1-76.

Fox, D. L. and P. L. Koch. 2003. Tertiary history of C_4 biomass in the Great Plains, USA. Geology 31: 809–812. doi: 10.1130/G19580.1

Freckleton, R. P. et al. 2003. Bergmann's rule and body size in mammals. The American Naturalist 161: 821-825. doi: 10.1086/374346

Frieß and Baylac. 2003. Exploring artificial cranial deformation using ellipitical Fourier analysis of Procrustes aligned outlines. American Journal of Physical Anthropology: The Official Publication of the American Association of Physical Anthropologists 122:11-22. doi: 10.1002/ajpa.10286

Fry, B. 2006. Stable Isotope Ecology. Springer New York. doi: 10.1007/0-387-33745-8

Galetti, M. et al. 2015. Defaunation affect population and diet of rodents in Neotropical rainforests. Biological Conservation 190: 2-7. doi: 10.1016/j.biocon.2015.04.032

Galetti, M. et al. 2016. Trophic niche differentiation in rodents and marsupials revealed by stable isotopes. PLoS One 11: 1-15. doi: 10.1371/journal.pone.0152494

Gillooly, J. F. et al. 2001. Effects of size and temperature on metabolic rate. Science 293: 2248–2251. doi: 10.1126/science.1061967

Glass, G. E. and N. A. Slade. 1980. The Effect of *Sigmodon hispidus* on Spatial and Temporal Activity of *Microtus ochrogaster*: Evidence for Competition. Ecology 61: 358–370. doi: 10.2307/1935194

Glynn, P.W. 1993. Coral reef bleaching: ecological perspectives. Coral reefs 12: 1-17. doi: 10.1007/BF00303779

Goheen, J. R. et al. 2004. Net effects of large mammals on Acacia seedling survival in an African savanna. Ecology 85: 1555-1561. doi: 10.1890/03-3060

Goheen, J. R. et al. 2010. Large herbivores facilitate savanna tree establishment via diverse and indirect pathways. Journal of Animal Ecology 79: 372-382. doi: 10.1111/j.1365-2656.2009.01644.x

Goheen, J. R. et al. 2018. Conservation lessons from large-mammal manipulations in East African savannas: the KLEE, UHURU, and GLADE experiments. Annals of the New York Academy of Sciences 1429: 31-49. doi: 10.1111/nyas.13848

Gottfried, M. et al. 2012. Continent-wide response of mountain vegetation to climate change. Nature Climate Change 2: 111-115.

Gould, S. J. 1975. On the scaling of tooth size in mammals. Integrative and Comparative Biology 15:351–362. doi: 10.1093/icb/15.2.353

Graham, R. W. 1987. Late Quaternary mammalian faunas and paleoenvironments of the southwestern Plains of the United States. Pages 24-86 in Late Quaternary mammalian biogeography and environments of the Great Plains and prairies (R. W. Graham, H. A. Semken, Jr., and M. A. Graham, editors), Illinois State Museum Scientific Papers 22.

Graham, R. W. et al. 1996. Spatial response of mammals to late Quaternary environmental fluctuations. Science 5208: 1601-1606. doi: 10.1126/science.272.5268.1601

Grayson, D. K. 2000. Mammalian responses to Middle Holocene climatic change in the Great Basin of the western United States. Journal of Biogeography 27: 181-192. doi: 10.1046/j.1365-2699.2000.00383.x

Grayson, D. K. 2007. Deciphering North American Pleistocene extinctions. Journal of Anthropological Research 63: 185–213. doi: 10.3998/jar.0521004.0063.205

Gross, J. E. et al. 1985. Effects of food quality and energy needs: changes in gut morphology and capacity of *Microtus ochrogaster*. Journal of Mammalogy 66: 661-667. doi: 10.2307/1380792

Guérécheau A., et al. 2010. Seasonal variation in molar outline of bank voles: An effect of wear? Mammalian Biology 75:311–319. doi: 10.1016/j.mambio.2009.03.013

Hadly, E. A. 1996. Influence of Late-Holocene Climate on Northern Rocky Mountain Mammals. Quaternary Research 310: 298-310. doi: 10.1006/qres.1996.0068

Hall, E. R. 1981. The mammals of North America. 2nd ed. John Wiley & Sons, Inc. New York 1: 1-600+90

Hammond, K. A. and B. A. Wunder. 1991. The role of diet quality and energy need in the nutritional ecology of a small herbivore, *Microtus ochrogaster*. Physiological and Biochemical Zoology 64: 541–567. doi: 10.1086/physzool.64.2.30158190

Harris, A. H. 1984. Neotoma in the late Pleistocene of New Mexico and Chihuahua. Special Publications, Carnegie Museum of Natural History 8:164-178.

Harvey, A. C. 1990. Forecasting, structural time series models and the Kalman filter. Cambridge University Press. doi: 10.1017/CBO9781107049994

Hay, E. L. et al. 2010. Morphology and metrics, isotopes and dates: determining the validity of *Equus laurentius* Hay, 1913. Journal of Vertebrate Paleontology 30: 1840-1847. doi: 10.1080/02724634.2010.520780

Hickling, G. J. 1987. Seasonal reproduction and group dynamics of bushy-tailed woodrats, *Neotoma cinerea*. Ph.D. dissertation, The University of Western Ontario, London, Ontario, Canada.

Hillson, S. 2005. Teeth. Cambridge University Press. doi: 10.1017/CBO9780511614477

Hobson, K. A. and R. G. Clark. 1992. Assessing avian diets using stable isotopes I: Turnover of 13C in tissues. Condor 94: 181-188. doi: 10.2307/1368807

IPCC 2014. Climate Change 2014: Synthesis Report. Contribution of Working Groups I, II and III to the Fifth Assessment Report of the Intergovernmental Panel on Climate Change.

IUCN. 2018. The IUCN Red List of Threatened Species. Ver. 2018.2. http://www.iucnredlist.org. Accessed 15 March 2018.

Jackson, A. L. et al. 2011. Comparing isotopic niche widths among and within communities: SIBER - Stable Isotope Bayesian Ellipses in R. Journal of Animal Ecology 80: 595-602. doi: 10.1111/j.1365-2656.2011.01806.x

Janis, C. M. 1995. Correlation between craniofacial morphology and feeding behavior in ungulates: reciprocal illumination between living and fossil taxa. pp. 76–98 in Functional morphology in vertebrate paleontology (J. J. Thomason, ed.). Cambridge University Press.

Janis, C. M. and M. Fortelius. 1988. On the means whereby mammals acieve increased functional durability of their dentitions, with special reference to limiting factors. Biological Reviews 63: 197–230. doi: 10.1111/j.1469-185X.1988.tb00630.x

Jardine, P. E. et al. 2012. Grit not grass: Concordant patterns of early origin of hypsodonty in Great Plains ungulates and Glires. Palaeogeography, Palaeoclimatology, Palaeoecology 365-366: 1-10. doi: 10.1016/j.palaeo.2012.09.001

JMP Pro 13.1.0. SAS Institute Inc, Cary, NC, 1989-2016.

Johnson, C. N. 2009. Ecological consequences of Late Quaternary extinctions of megafauna. Proceedings of the Royal Society B: Biological Sciences 276: 2509-2519. doi: 10.1098/rspb.2008.1921

Joines, J. P. 2011. 17,000 years of climate change: the phytolith record from Hall's Cave, Texas.

Jones, C., and N. J. Hildreth. 1989. *Neotoma stephensi*. Mammalian Species 328:1-3. doi: 10.2307/3504134

Justice, K. E. and F. A. Smith. 1992. A model of dietary fiber utilization by small mammalian herbivores with empirical results for *Neotoma*. The American Naturalist 139: 398-416. doi: 10.1086/285333

Kay, R. F. and K. M. Hiiemae. 1974. Jaw movement and tooth use in recent and fossil primates. American Journal of Physical Anthropology 40: 227-256. doi: 10.1002/ajpa.1330400210

Keesing, F. 1998. Impacts of ungulates on the demography and diversity of small mammals in central Kenya. Oecologia 116: 381-389. doi: 10.1007/s004420050601

Keesing, F. and T. P. Young. 2014. Cascading consequences of the loss of large mammals in an African savanna. Bioscience 64: 487-495. doi: 10.1093/biosci/biu059

Kefena, E. et al. 2012. Discordances between morphological systematics and molecular taxonomy in the stem line of equids: A review of the case of taxonomy of genus Equus. Livestock Science 143: 105–115. doi: 10.1016/j.livsci.2011.09.017

Kim, C. J. and Nelson, C. R. 1999. State-space models with regime switching: classical and Gibbs-sampling approaches with applications. MIT Press Books.

Kincaid, W. B. and G. N. Cameron. 1982. Dietary Variation in Three Sympatric Rodents on the Texas Coastal Prairie. Journal of Mammalogy 63: 668-672. doi: 10.2307/1380277

Kincaid, W. B. and G. N. Cameron. 1985. Interactions of cotton rats with a patchy environment: dietary responses and habitat selection. Ecology 66: 1769-1783. doi: 10.2307/2937373

Kincaid, W. B. et al. 1983. Patterns of Habitat Utilization in Sympatric Rodents on the Texas Coastal Prairie. Ecology 64: 1471-1480. doi: 10.2307/1937502

Koch, P. L. 2007. Isotopic study of the biology of modern and fossil vertebrates. – In: Michener, R. and Lajtha, K. (eds), Stable isotopes in ecology and environmental science. Blackwell Publishing, pp.99-154. doi: 10.1002/9780470691854.ch5

Koch, P. L. et al. 2009. The isotopic ecology of fossil vertebrates and conservation paleobiology. - In: Conservation Paleobiology: Using the past to manage for the future. Paleontological Society Papers, pp. 96–112.

Koerner, S.E. et al. 2014. Plant community response to loss of large herbivores differs between North American and South African savanna grasslands. Ecology 95: 808-816. doi: 10.1890/13-1828.1

Kotler, B. P. and J. S. Brown. 1988. Environmental heterogeneity and the coexistence of desert rodents. Annual review of ecology and systematics 19: 281-307. doi: 10.1146/annurev.ecolsys.19.1.281

Kuhl, F. P. and C. R. Giardina. 1982. Elliptic Fourier features of a closed contour. Computer Graphics and Image Processing 18:236-258. doi: 10.1016/0146-664X(82)90034-X

Laws, R. M. et al. 1975. Elephants and their habitats. Clarendon Press.

Ledevin, R. J. Quére, and S. Renaud. 2010. Morphometrics as an insight into processes beyond tooth shape variation in a bank vole population. 5:e15470. doi: 10.1371/journal.pone.0015470

Leung, B. et al. 2017. Trends in mean growth and stability in temperate vertebrate populations. Diversity and Distributions 23: 1372-1380. doi: 10.1111/ddi.12636

Li, Y. X. et al. 2012. Synchronizing a sea-level jump, final Lake Agassiz drainage, and abrupt cooling 8200 years ago. Earth and Planetary Science Letters 315: 41-50. doi: 10.1016/j.epsl.2011.05.034

Lorenz, D. J. et al. 2016a. Downscaled and debiased climate simulations for North America from 21,000 years ago to 2100 AD. Scientific Data 3: 1-19. doi: 10.1038/sdata.2016.48

Lorenz, D. J. et al. 2016b. Data from: Downscaled and debiased climate simulations for North America from 21,000 years ago to 2100AD. Dryad Digital Repository. doi: 10.1038/sdata.2016.48

Lucas, P. W., et al. 2014. The role of dust, grit and phytoliths in tooth wear. Annales Zoologici Fennici 2450:143-152. doi: 10.5735/086.051.0215

Lundelius, E. L., Jr. 1967. Late Pleistocene and Holocene faunal history of central Texas. Pages 287-319 in Pleistocene extinctions: a search for a cause (P. S. Martin and H. E. Wright, Jr., editors), Yale University Press, New Haven.

Lyons, S. K. 2003. A quantitative assessment of the range shifts of Pleistocene mammals. Journal of Mammalogy 84: 385–402. doi: 10.1644/1545-1542(2003)084<0385:AQAOTR>2.0.CO;2

Lyons, S. K. 2005. A quantitative model for assessing community dynamics of Pleistocene mammals. The American Naturalist 165: E168-E185. doi: 10.1086/429699

Lyons, S. K. et al. 2004. Of mice, mastodons and men: Human-mediated extinctions on four continents. Evolutionary Ecology Research 6: 339-358.

Macêdo, R. H. and M. A. Mares. 1988. *Neotoma albigula*. Mammalian species 310:1-7. doi: 10.2307/3504165

Malhi, Y. et al. 2016. Megafauna and ecosystem function from the Pleistocene to the Anthropocene. Proceedings of the National Academy of Sciences 113: 838–846. doi: 10.1073/pnas.1502540113

Martin, P. S. 1967. Prehistoric overkill. In *Pleistocene Extinctions, the Search for a Cause*. (PS Martin and HE Wright, Eds.).

Martin, P. S. and R. G. Klein. 1989. Quaternary extinctions: a prehistoric revolution. University of Arizona Press.

Martin, P. S. and D. W. Steadman. 1999. Prehistoric extinctions on islands and continents. In *Extinctions in near time* (pp. 17-55). Springer, Boston, MA. doi: 10.1007/978-1-4757-5202-1_2

Martin, R. A. 1986. Energy, ecology, and cotton rat evolution. Paleobiology 12: 370–382. doi: 10.1017/S0094837300003110

Martin, R. A. 1990. Estimating body mass and correlated variables in extinct mammals: travels in the fourth dimension. - In: Damuth, J. and MacFadden, B. J. (eds), Body size in mammalian paleobiology. pp. 49–68.

Matocq, M. D. and P. J. Murphy. 2007. Fine-scale phenotypic change across a species transition zone in the genus *Neotoma*: distangling independent evolution from phylogenetic history. Evolution 61:2544-2557. doi: 10.1111/j.1558-5646.2007.00215.x

Matocq, M. D et al. 2007. Phylogenetics of the woodrat genus *Neotoma* (Rodentia: Muridae) implications for the evolution of phenotypic variation in male external genitalia. Molecular Phylogenetics and Evolution 42: 637-652. doi: 10.1016/j.ympev.2006.08.011

Mayr, E. 1956. Geographical Character Gradients and Climatic Adaptation. Evolution 10: 105-108. doi: 10.1111/j.1558-5646.1956.tb02836.x

M'Closkey, R. T. 1976. Community structure in sympatric rodents. Ecology 57: 728-739. doi: 10.2307/1936186

McCauley, D. J. et al. 2006. Indirect effects of large herbivores on snakes in an African savanna. Ecology 87: 2657–2663. doi: 10.1890/0012-9658(2006)87[2657:IEOLHO]2.0.CO;2

McLister, J. D. et al. 2004. Effects of consumption of juniper (*Juniperus monosperma*) on cost of thermoregulation in the woodrats *Neotoma albigula* and *Neotoma stephensi* at different acclimation temperatures. Physiological and Biochemical Zoology 77: 305-312. doi: 10.1086/380211

McNab, B. K. 1971. On the ecological significance of Bergmann's Rule. Ecology 52: 845-854. doi: 10.2307/1936032

McNab, B. K. 1980. Food habits, energetics, and the population biology of mammals. The American Naturalist 116: 106–124. doi: 10.1086/283614

Meiri, S. and T. Dayan. 2003. On the validity of Bergmann's rule. Journal of biogeography 20: 331-351. doi: 10.1046/j.1365-2699.2003.00837.x

Meiri, S. et al. 2005. Variability and correlations in carnivore crania and dentition. Functional Ecology 19: 337-343. doi: 10.1111/j.1365-2435.2005.00964.x

Meserve, P. L. 1974. Ecological relationships of two sympatric woodrats in a California coastal sage scrub community. Journal of Mammalogy 55: 442-447. doi: 10.2307/1379012

Millien, V. et al. 2006. Ecotypic variation in the context of global climate change: Revisiting the rules. Ecology Letters. 9: 853-869. doi: 10.1111/j.1461-0248.2006.00928.x

Mitchell J. 2016. Application of micro-CT and Elliptic Fourier analysis on molar outline shape for group discrimination of notoungulates. Ph.D. dissertation, University of California, Santa Barbara, California.

Mooney, H. et al. 1974. Arid climates and photosynthetic systems. Annu Rep Dep Plant Biol Carnegie Inst.

Mooney, H. A. et al. 1989. Carbon isotope ratios of plants of a tropical dry forest in Mexico. *Functional Ecology*. 3: 137-142. doi: 10.2307/2389294

Moritz, C. et al. 2008. Impact of a century of climate change on small-mammal communities in Yosemite National Park, USA. - Science. 322: 261-264. doi: 10.1126/science.1163428

Munday, P. L. 2004. Habitat loss, resources specialization, and extinction on coral reefs. - Glob. Chang. Biol. 10: 1642-1647. doi: 10.1111/j.1365-2486.2004.00839.x

Murphy, B. P. and D. M. J. S. Bowman. 2006. Kangaroo metabolism does not cause the relationship between bone collagen $\delta^{15}N$ and water availability. Functional Ecology 20: 1062-1069. doi: 10.1111/j.1365-2435.2006.01186.x

Murphy, M. F. 1952. Ecology and helminths of the Osage wood rat, *Neotoma floridana osagensis*, including the description of *Longistriata neotoma* n. sp. (Trichostrongylidae). American Midland Naturalist 48: 204-218. doi: 10.2307/2422143

Murray, I.W. and Smith, F.A., 2012. Estimating the influence of the thermal environment on activity patterns of the desert woodrat (*Neotoma lepida*) using temperature chronologies. Canadian Journal of Zoology 90: 1171-1180. doi: 10.1139/z2012-084

Nagy, K. A. 2005. Field metabolic rate and body size. Journal of Experimental Biology 208: 1621-1625. doi: 10.1242/jeb.01553

Neotoma Paleoecology Database. 2015. http://www.neotomadb.org/

Newsome, S. D. et al. 2007. A Niche for Isotope Ecology. Frontiers in Ecology and the Environment 5: 429-436. doi: 10.1890/060150.1

Nordt, L. C. et al. 1994. Late quaternary vegetation and climate changes in central Texas based on the isotopic composition of organic carbon. Quaternary Research 41: 109-120. doi: 10.1006/qres.1994.1012

Okullo, P. et al. 2013. Termites, Large Herbivores, and Herbaceous Plant Dominance Structure Small Mammal Communities in Savannahs. Ecosystems 16: 1002-1012. doi: 10.1007/s10021-013-9663-2

Olsen, R. W. 1973. Shelter-site selection in the white-throated woodrat, *Neotoma albigula*. Journal of Mammalogy 54: 594-610. doi: 10.2307/1378961

Olsen, R. W. 1976. Water: a limiting factor for a population of wood rats. The Southwestern Naturalist 21: 391-398. doi: 10.2307/3669724

Orr, T. J. et al. 2015. Cacti supply limited nutrients to a desert rodent community. Oecologia 178: 1045-1062. doi: 10.1007/s00442-015-3304-8

Owen-Smith, R. N. 1992. Megaherbivores: the influence of very large body size on ecology. Cambridge University Press.

Parmesan, C. and Yohe, G. 2003. A globally coherent fingerprint of climate change impacts across natural systems. Nature 421: 37-42. doi: 10.1038/nature01286

Parnell, A. and A. Jackson. 2013. siar: Stable Isotope Analysis in R. R package version 4.2.2. https://CRAN.R-project.org/package=siar

Parsons, E. W. R., et al. 2013. Elk herbivory alters small mammal assemblages in high-elevation drainages. Journal of Animal Ecology 82: 459-467. doi: 10.1111/1365-2656.12009

Patton, J. L., D. G. Huckaby, and S. T. Alvarez-Castaneda. 2007. The evolutionary history and a systematic revision of woodrats of the *Neotoma lepida* group. University of California Press. doi: 10.1525/california/9780520098664.001.0001

Peters, R. H. 1983. The ecological implications of body size. Cambridge University Press. doi: 10.1017/CBO9780511608551

Petersen, M. K. 1973. Interactions between the cotton rats, *Sigmodon fulviventer* and *S. hispidus*. The American Midland Naturalist 90: 319-333. doi: 10.2307/2424456

Peterson, B. J. and B. Fry. 1987. Stable Isotopes in Ecosystem Studies. Annual Review of Ecology and Systematics 18: 293-320. doi: 10.1146/annurev.es.18.110187.001453

Prentice, I. C. et al. 1991. Vegetation and Climate Change in Eastern North America Since the Last Glacial Maximum. Ecology 72: 2038-2056. doi: 10.2307/1941558

R Development Core Team. 2016. R: a language and environment for statistical computing. R Foundation for Statistical Computing. Vienna, Austria. www.R-project.org/.

Rainey, D.G., 1956. Eastern woodrat, *Neotoma floridana*: life history and ecology. University of Kansas Publications, Museum of Natural History. 8: 536-646.

Randolph, J. C. et al. 1991. Dietary choice of a generalist grassland herbivore, *Sigmodon hispidus*. Journal of Mammalogy 72: 300-313. doi: 10.2307/1382100

Raun, G.G. 1966. A population of woodrats (*Neotoma micropus*) in southern Texas. Texas Memorial Museum. doi: 10.2307/3668859

Raun, G. G. and B. J. Wilks. 1964. Natural history of *Baiomys taylori* in southern Texas and competition with *Sigmodon hispidus* in mixed population. Texas Journal of Science 16: 28-49.

Renaud, S. and V. Millien. 2001. Intra-and interspecific morphological variation in the field mouse species *Apodemus argenteus* and *A. speciosus* in the Japanese archipelago: the role of insular isolation and biogeographic gradients. Biological Journal of the Linnean Society 74: 557-569. doi: 10.1111/j.1095-8312.2001.tb01413.x

Renaud, S. et al. 1996. Fourier analysis applied to *Stephanomys* (Rodentia, Muridae) molars: nonprogressive evolutionary pattern in a gradual lineage. Paleobiology 22: 255-265. doi: 10.1017/S0094837300016201

Repenning, C. A. 2004. Fossil wood rats of Porcupine Cave: tectonic or climatic controls. Pp. 193-206 in Biodiversity Response to Climate Change in the Middle Pleistocene: The Porcupine Cave fauna from Colorado (A. D. Barnosky, ed.). University of California Press, Berkeley, California. doi: 10.1525/california/9780520240827.003.0018

Ripple, W. J. et al. 2014. Status and ecological effects of the world's largest carnivores. Science. 1241484. doi: 10.1126/science.1241484

Ripple, W. J. et al. 2015. Collapse of the world's largest herbivores. Science Advances 1: e1400103. doi: 10.1126/sciadv.1400103

Rodrigues, H. G. et al. 2013. Roles of dental development and adaptation in rodent evolution. Nature Communications 4: 3504. doi: 10.1038/ncomms3504

Rogers, L. A. et al. 2017. Fine-scale population dynamics in a marine fish species inferred from dynamic state-space models. Journal of Animal Ecology 86: 888–898. doi: 10.1111/1365-2656.12678

Rohlf, F. J. 1990. Morphometrics. Annual Review of Ecology and Systematics 21: 299-316. doi: 10.1146/annurev.ecolsys.21.1.299

Rohlf, F. J., and D. Slice. 1990. Extensions of the Procrustes method for the optimal superimposition of landmarks. Systematic Biology 39: 40-59. doi: 10.2307/2992207

Rohling, E. J. and H. Pälike. 2005. Centennial-scale climate cooling with a sudden cold event around 8,200 years ago. Nature 434: 975. doi: 10.1038/nature03421

Rose, R. K. and H. G. Salamone. 2017. Population Dynamics of the Cotton Rat in Southeastern Virginia. Virginia Journal of Science 68: 1.

RStudio Team 2016. RStudio: Integrated Development for R. RStudio Inc. Boston, MA

Rule, S. 2012. The aftermath of megafaunal extinction: Ecosystem transformation in Pleistocene Australia. *Science*. 335: 1483-1486. doi: 10.1126/science.1214261

Sagebiel, J. C. 1998. Late Pleistocene fauna and environment at Zesch Cave, Mason County, Texas. Master's thesis. University of Texas, Austin, Texas, USA.

Samuels, J. X. 2009. Cranial morphology and dietary habits of rodents. Zoological Journal of the Linnean Society 156:864-888. doi: 10.1111/j.1096-3642.2009.00502.x

Samuels, J. X. and S. S. B. Hopkins. 2017. The impacts of Cenozoic climate and habitat changes on small mammal diversity of North America. Global and Planetary Change, 149: 36-52. doi: 10.1016/j.gloplacha.2016.12.014

Sauer, J. R. 1985. Mortality associated with severe weather in a northern population of cotton rats. American Midland Naturalist. 113: 188-189. doi: 10.2307/2425360

Schetter, T. A. et al. 1998. Examination of the nitrogen limitation hypothesis in non-cyclic populations of cotton rats (*Sigmodon hispidus*). Journal of Animal Ecology 67: 705-721. doi: 10.1046/j.1365-2656.1998.00240.x

Schlager, S. 2017. Morpho and Rvcg - Shape Analysis in R. Pp. 217-256 in Statistical Shape and Deformation Analysis (Zheng G., S. Li and G. Szekely, ed.). Academic Press. ISBN 9780128104934. doi: 10.1016/B978-0-12-810493-4.00011-0

Schmidly, D. J. and R. D. Bradley. 2016. The mammals of Texas. University of Texas Press.

Schmidt-Kittler, N. 2002. Feeding specializations in rodents. Senckenbergiana Lethaea 82:141–152. doi: 10.1007/BF03043780

Schmitz, O. J. et al. 2000. Trophic Cascades in Terrestrial Systems: A Review of the Effects of Carnivore Removals on Plants. The American Naturalist 155: 141-153. doi: 10.1086/303311

Schwartz-Narbonne, R. et al. 2015. Solving the woolly mammoth conundrum: amino acid ^{15}N-enrichment suggests a distinct forage or habitat. Scientific Reports. 5: 9791. doi: 10.1038/srep09791

Sharp, Z. 2017. Principles of Stable Isotope Geochemistry.

Shurin, J. B. et al. 2002. A cross-ecosystem comparison of the strength of trophic cascades. - Ecol. Lett. 5: 785-791. doi: 10.1046/j.1461-0248.2002.00381.x

Slade, N. A. et al. 1984. Seasonal variation in field-determined growth rates of the hispid cotton rat (*Sigmodon hispidus*). Journal of Mammalogy 65: 263-270. doi: 10.2307/1381165

Smith, F. A. 1995a. Den characteristics and survivorship of woodrats (*Neotoma lepida*) in the eastern Mojave Desert. Southwestern Naturalist 41: 366-372.

Smith, F. A. 1995b. Scaling of digestive efficiency with body mass in *Neotoma*. Functional Ecology 9: 299-305. doi: 10.2307/2390577

Smith, F. A. 1997. *Neotoma cinerea*. Mammalian Species 564: 1-8. doi: 10.2307/3504384

Smith, F. A. 2008. Body size, energetics, and evolution. - In: Jorgensen, S. E. and Fath, B. D. (eds), Encyclopedia of Ecology. pp. 477-482. doi: 10.1016/B978-008045405-4.00776-X

Smith, F. A. and J. L. Betancourt. 1998. Response of bushy-tailed woodrats (*Neotoma cinerea*) to late Quaternary climatic change in the Colorado Plateau. Quaternary Research 50: 1-11. doi: 10.1006/qres.1998.1982

Smith, F. A. and J. L. Betancourt. 2003. The effect of Holocene temperature fluctuations on the evolution and ecology of *Neotoma* (woodrats) in Idaho and northwestern Utah. Quaternary Research 59: 160-171. doi: 10.1016/S0033-5894(03)00004-8

Smith, F. A. and J. L. Betancourt. 2006. Predicting woodrat (*Neotoma*) responses to anthropogenic warming from studies of the palaeomidden record. Journal of Biogeography 33: 2061-2076. doi: 10.1111/j.1365-2699.2006.01631.x

Smith, F. A. et al. 1995. Evolution of body size in the woodrat over the past 25,000 years of climate change. Science 270: 2012–2014. doi: 10.1126/science.270.5244.2012

Smith, F. A. et al. 1997. Path analysis: a critical evaluation using long-term experimental data. The American Naturalist 149: 29-42. doi: 10.1086/285977

Smith, F. A. et al. 1998. The influence of climate change on the body mass of woodrats Neotoma in an arid region of New Mexico, USA. Ecography 21:140-148. doi: 10.1111/j.1600-0587.1998.tb00668.x

Smith, F. A. et al. 2009. A tale of two species: extirpation and range expansion during the late Quaternary in an extreme environment. Global and Planetary Change 65: 122-133. doi: 10.1016/j.gloplacha.2008.10.015

Smith, F. A. et al. 2010. The evolution of maximum body size of terrestrial mammals. Science. 330: 1216-1219. doi: 10.1126/science.1194830

Smith, F. A. et al. 2016a. Megafauna in the Earth system. Ecography 39: 99-108. doi: 10.1111/ecog.02156

Smith, F. A. et al. 2016b. Unraveling the consequences of the terminal Pleistocene megafauna extinction on mammal community assembly. Ecography 39: 223-239. doi: 10.1111/ecog.01779

Smith, F. A. et al. 2018. Body size downgrading of mammals over the late Quaternary. Science. 360: 310-313. doi: 10.1126/science.aao5987

Spencer, D. A. and A. L. Spencer. 1941. Food habits of the white-throated wood rat in Arizona. *Journal of Mammalogy*. 22: 280-284. doi: 10.2307/1374953

Stamatakis, A. 2014. RAxML Version 8: A tool for phylogenetic analysis and post-analysis of large phylogenies. Bioinformatics 30: 1312-1313. doi: 10.1093/bioinformatics/btu033

Stan Development Team 2018. RStan: the R interface to Stan. in press.

Stanley, S. M. 1973. An explanation for Cope's rule. Evolution 27: 1-26. doi: 10.1111/j.1558-5646.1973.tb05912.x

Stenseth, N. C. et al. 2002. Ecological effects of climate fluctuations. Science 297: 1292-1296. doi: 10.1126/science.1071281

Strait, S. G. 1993a. Differences in occlusal morphology and molar size in frugivores and faunivores. Journal of Human Evolution 25: 471-484. doi: 10.1006/jhev.1993.1062

Strait, S. G. 1993b. Molar morphology and food texture among small-bodied insectivorous mammals. Journal of Mammalogy 74: 391-402. doi: 10.2307/1382395

Sutton, B. G. et al. 1976. Seasonal effects on carbon isotope composition of cactus in a desert environment. Nature 26: 42-43. doi: 10.1038/261042a0

Swihart, R. K. and N. A. Slade. 1984. Road crossing in *Sigmodon hispidus* and *Microtus ochrogaster*. Journal of Mammalogy 65: 357-360. doi: 10.2307/1381184

Thies, M. and W. Caire. 1990. Association of *Neotoma micropus* nests with various plant species in southwestern Oklahoma. The Southwestern Naturalist 35: 80-82. doi: 10.2307/3671988

Thomason, J. (ed.)., 1997. Functional morphology in vertebrate paleontology. Cambridge University Press.

Toomey, R. S. III. 1993. Late Pleistocene and Holocene faunal and environmental changes at Hall’s Cave, Kerr County, Texas.

Toomey, R. S. III. et al. 1993. Late Quaternary climates and environments of the Edwards Plateau, Texas. Global Planetary Change 7: 299-320. doi: 10.1016/0921-8181(93)90003-7

Travis 1994. Evaluating the adaptive role of morphological plasticity. Pp. 99-122 in Ecological morphology: integrative organismal biology (P. C. Wainwright and S. M. Reilly, ed.). The University of Chicago Press, Chicago and London.

Ungar, P. S. 2010. Mammal teeth: origin, evolution, and diversity. Johns Hopkins University Press.

Ungar, P. S., and M. Sponheimer. 2011. The diets of early hominins. Science 334: 190-193. doi: 10.1126/science.1207701

Ungar, P., and M. Williamson. 2000. Exploring the effects of tooth wear on functional morphology: a preliminary study using dental topographic analysis. Palaeontologia electronica 3: 1-18.

Van Devender, T. R. et al. 1977. Late Pleistocene reptiles and small mammals from the lower Grand Canyon of Arizona. Southwestern Association of Naturalists 22: 49-66. doi: 10.2307/3670463

Van Valkenburgh B. 1989. Carnivore dental adaptations and diet: a study of trophic diversity within guilds. Pp. 410-436 in Carnivore Behavior, Ecology and Evolution (J. L. Gittleman, ed.). Springer, Boston, MA. doi: 10.1007/978-1-4757-4716-4_16

Van Valkenburgh, B. 1994. Ecomorphological analysis of fossil vertebrates and their paleocommunities. Pp. 140-166 in Ecological morphology: integrative organismal biology (P. C. Wainwright and S. M. Reilly, ed.). The University of Chicago Press, Chicago and London.

Veloso, C. and F. Bozinovic. 1993. Dietary and digestive constraints on basal energy metabolism in a small herbivorous rodent. Ecology 74: 2003-2010. doi: 10.2307/1940843

Verts, B. J., and L. N. Carraway. 2002. *Neotoma lepida*. Mammalian Species 699: 1-12. doi: 10.1644/1545-1410(2002)699<0001:NL>2.0.CO;2

Vorhies, C. T. and W. P. Taylor. 1940. Life history and ecology of the white-throated wood rat, *Neotoma albigula* Hartley, in relation to grazing in Arizona. College of Agriculture, University of Arizona, Tucson, Arizona.

Walsh, R. E. et al. 2016. Morphological and dietary responses of chipmunks to a century of climate change. Global change biology 22: 3233-3252. doi: 10.1111/gcb.13216

Walther, G. R. et al. 2002. Ecological responses to recent climate change. Nature 416: 389. doi: 10.1038/416389a

Wang, D.H et al. 2003. Digestive tract morphology and food habits in six species of rodents. Folia Zoologica-Praha 52: 51-56.

Wang, T et al. 2012. ClimateWNA—high-resolution spatial climate data for western North America. Journal of Applied Meteorology and Climatology 51: 16-29. doi: 10.1175/JAMC-D-11-043.1

West, J.B. et al. 2006. Stable isotopes as one of nature's ecological recorders. Trends in Ecology & Evolution 21: 408-414. doi: 10.1016/j.tree.2006.04.002

Whitlock, C. and Bartlein, P. J. 1997. Vegetation and climate change in northwest America during the past 125 kyr. Nature 388: 57-61. doi: 10.1038/40380

Wiley, R. W. 1980. *Neotoma floridana*. Mammalian Species 139: 1-7. doi: 10.2307/3503989

Williams, S. H., and R. F. Kay. 2001. A comparative test of adaptive explanations for hypsodonty in ungulates and rodents. Journal of Mammalian Evolution 8: 207-229. doi: 10.1023/A:1012231829141

Winans, M. C. 1989. A quantitative study of North American fossil species of the genus Equus. - In: Prothero, D. R. and Schoch, R. M. (eds), The Evolution of Perissodactyls. Oxford University Press, pp. 262-297.

Windberg, L. A. 1998. Population trends and habitat associations of rodents in southern Texas. American Midland Naturalist. 140: 153-160. doi: 10.1674/0003-0031(1998)140[0153:PTAHAO]2.0.CO;2

Zawkrzewski, R. J. 1993. Morphological change in woodrat (Rodentia: Cricetidae) molars. Pp. 392-409 in Morphological change in Quaternary mammals of North America (R. A. Martin, and A.D. Barnosky, ed). Cambridge University Press, Cambridge, United Kingdom. doi: 10.1017/CBO9780511565052.016

Zelditch, M., D. L. Swiderski, and H. D. Sheets. 2012. Geometric morphometrics for biologists: a primer. 2nd ed. Academic Press.